# WIRELESS COMMUNICATION OVER FADING CHANNELS WITH IMPERFECT CHANNEL ESTIMATES

BY

AMIR ALI BASRI

A THESIS SUBMITTED IN CONFORMITY WITH THE REQUIREMENTS
FOR THE DEGREE OF DOCTOR OF PHILOSOPHY,
GRADUATE DEPARTMENT OF ELECTRICAL AND COMPUTER ENGINEERING,
IN THE UNIVERSITY OF TORONTO.

*Your file Votre référence*
ISBN: 978-0-494-57956-5
*Our file Notre référence*
ISBN: 978-0-494-57956-5

# Wireless Communication over Fading Channels with Imperfect Channel Estimates

Doctor of Philosophy Thesis
Edward S. Rogers Sr. Department of Electrical and Computer Engineering
University of Toronto

*by Amir Ali Basri*
*July 2008*

# Abstract

In wireless communication systems, transmitted signals are corrupted by fading as well as noise. The receiver can benefit from the estimates of fading channels to detect the transmitted symbols. However, in practical wireless systems channel information cannot be estimated perfectly at the receiver. Therefore, it is crucial to examine the effect of channel estimation error on the structure and performance of the receivers. In the first part of the thesis, we study single-user systems with single-antenna reception over fading channels in the presence of Gaussian-distributed channel estimation error. By using the statistical information of the channel estimation error, we will derive the structure of maximum-likelihood receivers for a number of different modulation formats and then analyze their performance over fading channels. In the second part of the thesis, we consider the uplink of multi-user wireless systems with multi-antenna reception. For conventional diversity combining techniques such as maximal ratio combining and optimum combining we analyze the performance degradation due to imperfect channel estimates in the presence of multiple interfering users for several fading channels. By investigating the probability density function of the output signal-to-interference ratio, we will derive analytical expressions for several performance measures such as the average signal-to-interference ratio, outage probability and average bit-error probability. These expressions quantify performance degradation due to channel estimation error.

# Acknowledgements

I would like to express my deep and sincere gratitude towards my supervisor Professor Teng Joon Lim. His wide knowledge and logical way of thinking have been of great value for me. His understanding, encouraging and personal guidance have provided a good basis for the present thesis. I would like to thank him for his invaluable guidance, patience and constructive feedback and for freedom he gave me to conduct my research. I owe him lots of gratitude for showing me integral view on research and for being always available when I needed his advises.

I warmly thank the members of my Ph.D. committee who monitored my work and took effort in reading and providing me with valuable comments: Professor Frank Kschischang, Professor Wei Yu, and Professor Raviraj Adve.

Special thanks for my colleagues and friends for their support and friendship and for insightful discussions that eventually helped shaping my thesis into its present form. Especially, I would like to thank Roya Doostnejad, Darryl Lin, Yi Zhao, Mahdi Lotfinezhad, Mahdi Shabany, Amir Ghasemi, Ali Khachan, Hanli Wang, Weixiong Lin, Hayssam Dahrouj, Keivan Navaie, Peyman Razzaghi, Adam Tenenbaum, Reza Safian, Hassan Shojania, Elzbieta Beres, Dhammika Bokolamulla, Jonathan Lam, Hadi Bannazadeh, Amin Farbod, Ali Naji, Ali Saadatpoor, Amir Aghaei, Hassen Karaa, Earnest Lock, Josephine Chu and Lok Ho.

I would like to thank my parents for their enduring caring and support and for all the help and encouragement, and my grandmother for her endless love.

# Contents

# List of Tables

# List of Figures

# Chapter 1

# Introduction

Digital wireless systems have been growing in popularity, complexity and capabilities over the last decade, and there are now mobile as well as fixed wireless networks, proprietary as well as standardized systems, personal area networks as well as metropolitan area networks. Each of these systems has unique requirements and constraints, but they share at least one key feature: Digital signals should be transmitted over physical channels, which are usually subject to fading.

Multi-path fading is one of the most common phenomena in wireless systems. It is due to the constructive and destructive combination a number of multi-paths received at the receiver with random attenuations and delays. This type of fading affects the signals transmitted through wireless channels and causes the short-term signal variations. There are various models to describe statistical behavior of this phenomenon. Two common models are Rayleigh and Rice fading channels. The Rayleigh distribution models multi-path fading with no line-of-sight (LOS) while Rice distribution models fading channel in the presence of LOS.

The fading channels that information is transmitted over may change over time, or the bandwidth occupied by these channels may be large enough that the frequency response of the channel varies over that range. We call the former class of channels time-selective fading channels, while the latter is called frequency-selective or inter-symbol-interference (ISI) channels. Channels can be both time- and frequency-selective. In this thesis, we consider flat (non-frequency-selective)

fading channels, also known as multiplicative fading, and hence ISI is not present.

There has been great interest in the structure of optimum receivers for detection of digital signals transmitted over a flat fading in the presence of additive white Gaussian noise (AWGN) for last decades. To detect transmitted symbols, two types of receivers, coherent and noncoherent, are conventionally considered in the literature [1], [2]:

**Coherent Receiver** It attempts to estimate the channel and use this estimate as if it is the true channel. In other words, the design of coherent receivers is based on the assumption that the channel estimate is error-free.

**Non-Coherent Receiver** For this type of receiver no attempt is made to estimate the channel, and hence, the receiver does not use any channel estimate.

The structure of the mentioned conventional receivers in communication systems has been investigated in the literature [1], [2]. For coherent reception, when the channel information is precisely known at the receiver, maximum-likelihood (ML) detection in AWGN channels is achieved by passing the received signals through a matched filter in the case of binary antipodal signalling or through a pair of matched filters in the case of binary orthogonal signalling. For non-coherent reception, when it is not possible for the receiver to perform channel estimation, and thus no channel estimate is available at the receiver, the ML detector in AWGN channels is the envelope detector or square-law detector. The performance of these detectors has been studied in both non-faded and fading channels [1]-[6].

In practical wireless systems, the channels cannot be estimated exactly. Several channel estimation techniques such as minimum mean-square error (MMSE) estimation [9]-[10] or pilot-symbol-assisted modulation (PSAM) [11] are considered in the literature. In the presence of complex Gaussian fading channels (Rayleigh and Rician fading channels), these channel estimation techniques have been shown to result in complex Gaussian channel estimate and channel estimation error. In PSAM, pilot symbols are inserted periodically into the data sequence at the transmitter.

Then, the receiver extract the received signals due to pilot symbols and interpolates them to estimate the channel state. Several interpolation filters have been studied in the literature. In MMSE estimation, the channel estimate is derived from the received signal due to pilot symbols such that the mean square of estimation error is minimized.

In general, Gaussian-distributed channel estimation error emerges mainly when an MMSE estimator is used for channel estimation in the Bayesian linear model [8]. A Gaussian estimation error was also assumed in [46], [48] for the case when pilot and data channels are separated in frequency or time such that the magnitude of the correlation coefficient between them is not unity. In this thesis, channel estimation errors are assumed to be circularly symmetric Gaussian distributed and independent from the channel estimates. We will see that these assumptions result in channel estimates which are correlated with the true channels to an extent measured by the correlation coefficient $\rho$. This type of channel estimate is referred to in the literature as noisy channel estimates or noisy side information as well [89].

In the presence of channel estimation error, coherent receiver may not be optimum anymore. If the statics of error are available at the receiver, then these statistics can be used to design a new structure for the receiver to get a better performance than conventional receivers. As explained in Section 1.1, in this thesis, for Gaussian channel estimation error, we use statical information of channel estimation error to design new types of receiver for single-user systems with single-antenna reception in fading channel.

In wireless communication systems, in addition to fading, interference from other users is another major reason for performance degradation. In urban area, interference is more severe due the large number of base stations and mobile users. Co-channel interference (CCI) is one of the major types of interference which is generated in a cellular system due to frequency re-use, i.e. from the cells that use the same frequencies. Number of receive antennas is usually only two or at most four, so in a wireless system the number of interferers most probably exceeds the number of antennas, as assumed in the most parts of this thesis.

In this thesis, we study several performance measures of wireless systems in fading channels in

the presence of multiple interfering users. Some key measures of performance related to practical communication system design are as follows:

**Average Signal-to-interference-plus noise Ratio (SINR)** It is a vital performance measure of a communication system. This performance measure is usually measured at the output of the receiver and indicates the overall quality of the system. For wireless communication system due to the presence of fading, the instantaneous SINR is a random variable. Therefore, a more suitable metric to assess the system performance is the average SINR which can be obtained by averaging the SINR over the probability density function (PDF) of fading, or equivalently over the PDF of SINR.

**Outage Probability** It is another important measure of performance to calculate the quality of service provided by wireless systems over fading channels and is defined as the probability that SINR falls below a certain threshold.

**Average Bit Error Probability (BEP)** It is one of the most informative indicators about the performance of the system. This measure can be obtained by averaging the conditional (on the fading) BEP over fading statistics.

Spatial diversity, as provided by multiple antennas, is one of the best-known methods to combat fading. Multiple antennas at the receiver provide the receiver with replicas of the same information bearing signals over independently fading channels [1], [26], [27], [28], which is known as receive diversity. Diversity combining is a very effective method to overcome the problem of fading, in which the received signals at each antenna are combined and weighted appropriately to improve the performance of the system. In the uplink (mobile to base station) of wireless communication systems, multi-antenna receivers can also combat CCI as well as fading by combining the received signals appropriately [28]. In this thesis, we study two conventional diversity combining methods: maximal-ratio combining (MRC) and optimum combining (OC).

**MRC** It is a well-known diversity combining technique to combat the effect of fading [26]. The maximal ratio combiner applies weights which are proportional to the signal-to-noise ratio

(SNR) of each branch and then combines the weighted signals. Therefore, the reduction in fading is obtained by increasing the signal level at each antenna branch based on the level of SNR at that branch. For fading channels with AWGN, in the absence of interference MRC realizes an ML receiver [27], [6]. MRC is also optimal from the standpoint of maximizing the SNR at the output of the combiner in noise-limited systems [26], [6]. When the power of noise at different antennas are the same, the MRC weight vector is the desired user's channel vector. In this case, MRC is also called channel-matched combining [29]. In this thesis, for the systems with noise it is assumed that the power of noise at different branches are the same, and hence, the MRC vector is the desired user's channel vector. For interference-limited systems, where the power of the interference is much greater than the thermal noise power so that the effect of the noise can be neglected, we also use the desired user's channel vector as the MRC vector.

**OC** As mentioned above, in cellular wireless systems, interfering users are a major limiting factor. MRC ignores interference and just combats fading by maximizing the desired signal power. In other words, MRC treats interference from other users as Gaussian noise. Therefore, MRC is optimal in systems with no interference. However, a multiple-antenna receiver can be used to combat interference as well. In the presence of interference, a multi-antenna receiver can apply OC technique. This combining technique is a well-known method in space diversity reception that combines and weights the received signals to combat both fading and interference [61], [62], [6, Ch. 11]. This method maximizes the SINR at the output of the combiner [61], [62]. It is shown in [30] that a significant increase in the capacity of the system can be achieved by using OC. The OC vector is actually an MMSE vector, i.e., it is equal to the inverse of the interference covariance matrix multiplied by the desired user's channel. The OC is the ML receiver when the transmitted signals of interfering users as well as the additive noise are Gaussian-distributed. To implement OC, the receiver needs knowledge of both the desired user's channel as well as the interference covariance matrix, which is a function of the interfering users' channels. So, OC needs the knowledge of the

desired user's channel as well as interfering users' channels. However, MRC requires only the desired user's channel information at the receiver. Therefore, OC is a more complex diversity combining technique compared with MRC.

The above mentioned combining techniques are based on the assumption that channel estimates at the receivers are perfect. Therefore, it is crucial to examine the effect of channel estimation error on these diversity combining techniques. As explained in Section 1.2, in this thesis, we analyze the performance degradation due to imperfect channel estimates in the presence of multiple interfering users for multi-antenna reception in the uplink of interference-limited systems. By investigating the PDF of the output signal-to-interference ratio (SIR), we will derive analytical expressions for different performance measures such as the average SIR, outage probability and average BEP. These expressions quantify performance degradation due to channel estimation error.

In this thesis, we present several theoretical results to assess the performance of wireless systems. These analytical results give insight into the system performance and guide the researchers and engineers to design their systems and to evaluate the performance of such systems. We use several mathematical results such as quadratic forms of Gaussian random variables and hypergeometric functions to facilitate performance analysis.

The structure of thesis is as follows:

## 1.1 Single-User Single-Antenna Reception

In Chapter 2, we study single-user systems with single-antenna reception over fading channels in the presence of Gaussian-distributed channel estimation error. We propose the structure of ML receivers for several modulation formats. Then, we analyze the performance of derived receivers over fading channels.

In AMGN channels, the matched filter is the ML receiver front-end when the channel is precisely estimated at the receiver. However, in the presence of channel error the matched filter may not be the ML receiver. If the statistical information of the channel estimation error is available at

the receiver, this information can be used to design new types of receivers.

This new ML receiver can result in better performance compared with the matched filter since the latter is optimal only if the channel estimate is perfect. The receiver that models estimation error probabilistically can outperform the optimum non-coherent receiver, the square-law detector, as well, since the square-law detector does not use any channel estimate at all. Fig. 1.1 shows the central role played by channel state information in receiver design.

In [7], Viterbi studied the case when a phased-locked loop is used to estimate the phase of the channel resulting in a Tikhonov-distributed phase error. It was shown that the optimum detector for binary signals over an AWGN channel is a linear combination of the optimum coherent detector and optimum noncoherent detector. The derived optimum detector is known as the partially coherent detector in the literature, and its average BEP in AWGN channels was obtained in [7] in integral forms. An overview of partially coherent communication is presented in [2].

For MMSE channel estimators, the performance of M-ary phase-shift keying (M-PSK) signals as well as M-ary quadrature amplitude modulated (M-QAM) signals are studied in [9] for Rayleigh fading channels and in [10] for Rician fading channels. In these two papers, a key assumption is the orthogonality between the channel estimate and the channel estimation error. Their work has been extended in [12] to remove the orthogonality condition. The PDFs of the receiver decision variables for Rayleigh and Rician fading channels were derived. These PDF's were used to evaluate error probabilities of 16-QAM with channel estimation errors. In [13], the average BEP of M-QAM signals are examined in Rayleigh fading channels with PSAM channel estimation. The exact average BEP of 16-QAM signals with PSAM has been derived in [14] for Rayleigh fading channels. The average symbol error probability of arbitrary two-dimensional signalling with MMSE channel estimators and PSAM are derived in [15] for Rayleigh fading channels and in [16] for Rician fading channels.

The ML detection of binary antipodal signals with Gaussian channel estimation error is studied in [17] when the receiver is equipped with multiple antennas. The ML receiver for single-antenna reception in AWGN channels is a matched filter that is matched to the channel estimate.

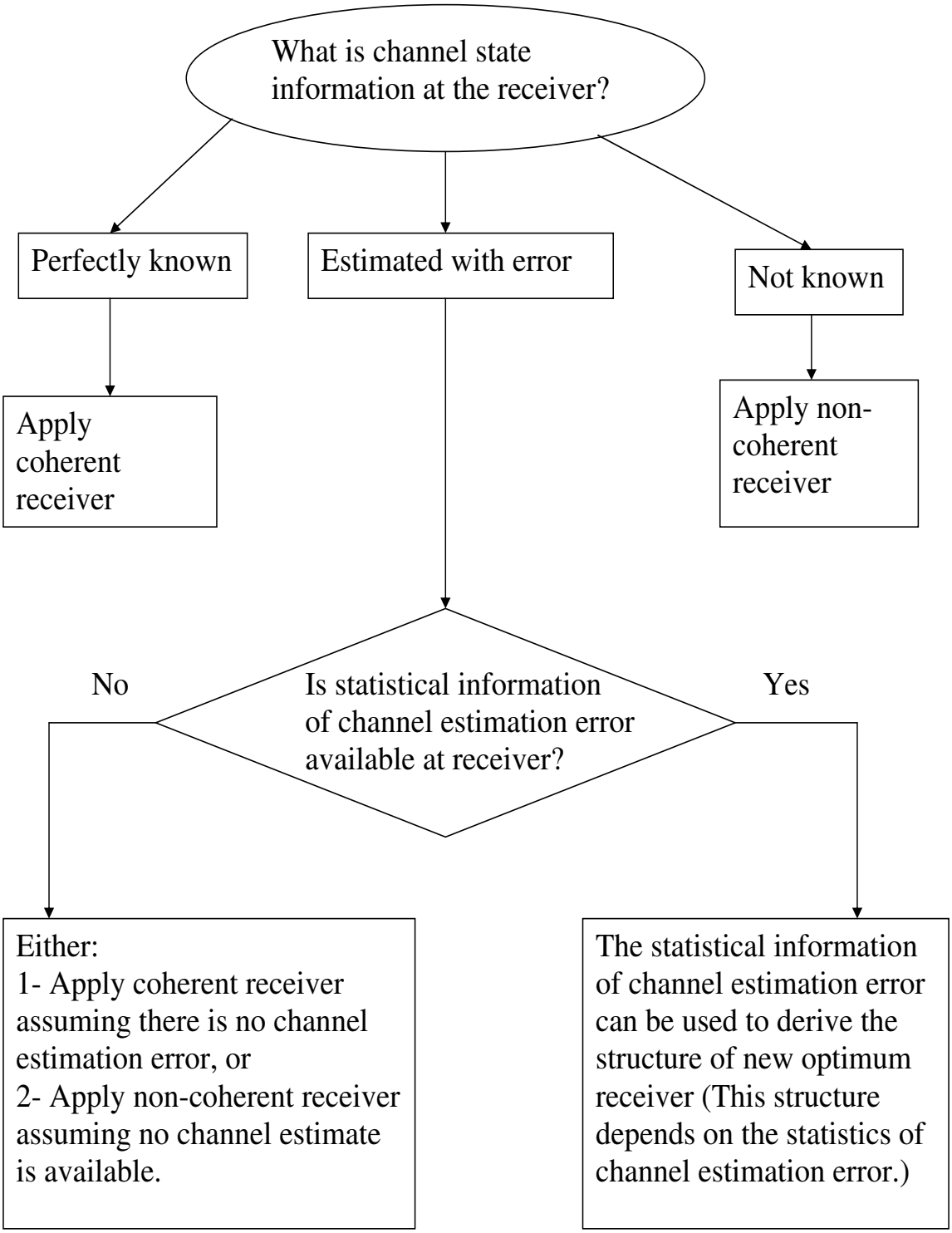


Figure 1.1: Structure of optimum receiver versus channel state information

Orthogonal modulation, such as orthogonal frequency-shift keying, is another important type of modulation. In Section 2.1, we derive the structure of the ML receiver for orthogonal binary signals in the presence of Gaussian-distributed channel estimation error and AWGN for single-antenna reception. We will see that the ML receiver is a linear combination of the matched filter and square-law detector, i.e., optimum coherent and noncoherent receivers, respectively. We will derive an exact theoretical expression for the average BEP of the proposed ML detector in Rayleigh fading channels. It is known that when the channels are perfectly estimated at the receiver, antipodal modulation outperforms orthogonal signalling. However, we show that in the presence of channel estimation error, orthogonal signalling may have a better performance than antipodal modulation under a certain condition and we express this condition precisely.

We then study two special applications where Gaussian-distributed channel estimation error arises: first quasi-static Rayleigh fading channels with pilot symbols and the MMSE channel estimator, and second, time-varying Rayleigh fading channels modeled with an autoregressive (AR) process of order one. In both cases, we will show that the channel estimation error is Gaussian, and hence, the receiver derived for the general case of Gaussian estimation error can be applied. We analyze the performance of the proposed receiver for these special cases by using the results derived for the general case of Gaussian estimation error.

In [20]-[21], the time-varying channel is also modeled by an AR process of order one, and it is shown that the ML receiver for orthogonal signals is a linear combination of the matched filter and square-law detector. An upper bound for the average BEP of this ML receiver is calculated in [20]-[21] by using this fact that the average BEP of the mentioned receiver is less than the minimum of average BEPs of coherent and non-coherent receivers. The main difference between that work and this thesis is that the results of this thesis, including the structure of the proposed receiver and the average BEP expressions, are derived for the general case of Gaussian-distributed channel estimation error and not only for time-varying fading channels. Moreover, we present an exact closed-form expression of the average BEP of the ML receiver for orthogonal modulation in time-varying fading channels.

In Section 2.2, we will derive the structure of the ML receiver for quadrature phase-shift keying (QPSK) signals in the presence of Gaussian channel estimation error and AWGN for single-antenna reception. We will see that the ML receiver is a matched filter matched to the channel estimate. We will derive an exact expression for the average BEP of this receiver in Rayleigh fading channels. Then, the performance of the receiver is analyzed for a special case where Gaussian channel estimation error arises: MMSE channel estimation with pilot symbols in quasi-static Rayleigh fading channels.

## 1.2 Multi-User Multiple-Antenna Reception

### 1.2.1 Maximal Ratio Combining

The performance of MRC in the presence of multiple interferers is analyzed in Chapter 3 for both cases of perfect and imperfect channel estimates.

#### Perfect Channel Estimates

In Section 3.1, we will derive the exact average BEP expression of binary phase-shift keying (BPSK) signals in Rayleigh fading channels for MRC in the presence of multiple interfering users and AWGN.

The performance of MRC in the presence of multiple interferers is studied in [31]–[45] for different types of fading channels when the desired user's channel is estimated perfectly at the receiver. The summary of those papers is shown in Table 1.1. As explained in this table, in [31]-[35] and [41]-[42], the PDF of the output SINR and the outage probability are studied for MRC when the desired user and interfering users experience independent fading channels. In the case of correlated fading channels, the outage probability of MRC is studied in [36]–[38]. The details of these references are described in Table 1.2.

The PDF of the output SINR can also be used to find the average BEP for MRC by using the conventional PDF-based method [39]–[43]. The main idea behind this method is to find the

| References | Main Derivations |
|---|---|
| [31]–[35] and [41]-[42] | The PDF of the output SINR and the outage probability for several types of independent fading channels |
| [36]–[38] | Outage probability for several types of correlated fading channels |
| [39]–[43] | Average bit-error probability by using the conventional PDF-based method |

Table 1.1: Summary of literature review of MRC with perfect channel estimates and multiple interferers.

BEP conditioned on channel realizations of both the desired user and interfering users and then averaging the conditional BEP over the joint distribution of fading channels of all users in order to obtain the average BEP. However, both finding the BEP conditioned on the fading channels of all users as well as integrating that conditional BEP over the joint PDF of fading channels of all users are complicated processes. Therefore, to simplify the procedure of deriving the average BEP expression, in the PDF-based method it is assumed that the interference-plus-noise term at the output of the combiner conditioned on fading channels of all users is circularly symmetric Gaussian distributed. We will see that based on this assumption, the BEP conditioned on the fading channels of all users can be obtained in a straightforward manner, as a function of just the output SINR. Therefore, in the PDF-based method deriving the expression for the average BEP starts with deriving the PDF of the output SINR, and then, the average BEP is derived by averaging the mentioned conditional BEP, which is a function of just SINR, over the PDF of SINR.

The conventional PDF-based method suffers from two issues: First, finding the PDF of SINR is a complicated process since SINR is a function of fading channels of the desired user and all interfering users. The second issue is that the average BEP derived by this method is only exact when the interference-plus-noise term conditioned on fading channels of all users can be assumed to be circularly symmetric Gaussian distributed. As we will see, this assumption is only valid either when the transmitted symbols of interfering users are circularly symmetric Gaussian distributed or when the number of interfering users is infinite. However, in practice we deal with cases where the number of interfering users is finite and transmitted symbols are not Gaussian distributed. Therefore, the average BEP derived by the conventional method can be seen only as an approximation.

| References | Main Derivations |
|---|---|
| [31] | First the authors derive the PDF of the output SINR for MRC in the presence of arbitrary number of equal-power co-channel interference as well as noise when users fade independently with Rayleigh statistic. Then, they obtain the outage probability of MRC for a dual antenna system in the presence of at most three unequal-power co-channel interferers. |
| [32] | The results of [31] are extended and closed-from expressions are derived for the outage probability of MRC in the presence of an arbitrary number of interferers with equal or distinct powers. |
| [41] | The PDF of the output SIR is derived for an interference-limited system with equal-power interferers for independent Rician/Rayleigh channels, where the desired user is subject to Rician fading while the interfering users experience Rayleigh fading. Then, the PDF expression is used to derive an expression for the average BEP of BPSK signals for Rayleigh fading channels . |
| [33] | The PDF expression in [41] is used to obtain expressions of the outage probability. |
| [34] | In the presence of co-channel interferers with arbitrary powers, the outage probability expressions are derived for an interference-limited system in Rician/Rayleigh environment as well as Nakagami/Rayleigh environment. |
| [35] | The results of [42] are generalized and the outage probability of MRC is derived for Nakagami/Nakagami model when co-channel interferers have arbitrary powers and fading parameters. |
| [36] | In the case of correlated Rayleigh fading channels for both desired user and interfering users, the outage probability of MRC is studied in [36] for equal-power co-channel interferers. |
| [37] | In the case of correlated Rayleigh fading channels for both desired user and interfering users, the outage probability of MRC is studied in [36] for unequal-power co-channel interferers. |
| [38] | The outage probability expression of MRC is derived in an interference-limited system when the desired user's channel vector has a general fading distribution with arbitrary spatial correlation and interfering users have equal powers with i.i.d Rayleigh fading. |
| [42] | The outage probability of MRC is derived in the presence of noise and equal-power and independent interferers when both the desired user and interfering users are subject to Nakagami fading (Nakagami/Nakagami model). The conventional PDF-based method has also been used to derive expressions for the average BEP. |
| [43] | The conventional PDF-based method has been used to derive expressions for the average BEP for Rician/Rayleigh fading model where the desired user is subject to Rician fading while the interferers experience Rayleigh fading. |

Table 1.2: Detailed literature review of MRC with perfect channel estimates and multiple interferers.

In this thesis, for deriving the average BEP we propose a new method which is different from the PDF-based approach. We use the decision variable at the output of the maximal ratio combiner conditioned on the fading channel of the desired user only rather than the channels of all users. We derive an exact expression for the average BEP of MRC when the transmitted signals have BPSK modulation and the desired signal and interferers fade independently with Rayleigh statistics. We will see that this approach helps us find an exact expression for the BEP conditioned on channel realization of the desired user. Then, an exact closed-from expression for the average BEP can be derived by averaging the conditional BEP.

We will see that the exact expression of the average BEP in the presence of interference can be obtained from the expression for the average BEP of MRC in single-user systems (with AWGN and no interference) by replacing the average SNR per channel with the ratio of the desired signal's power to the total power of the interfering users plus noise. We will study the difference between the results of the PDF-based method and exact results and will find that this difference is considerable for a smaller number of interfering users. The results of the proposed exact method can be easily generalized to M-PSK modulation.

The performance of MRC is studied in [44] by using the moment generating functions of the decision variables at the output of the combiner. In that paper, a closed-form expression is derived for the average BEP of MRC in the presence of multiple interferers where the channels are subject to Rician fading and the transmitted signals have BPSK modulation. However, the complexity of the derived expression increases exponentially with the number of users, and hence, that expression is overwhelmingly complicated in the presence of a large number of interferers. Therefore, approximate expressions, which are much simpler for performance evaluation, have been provided. In [45], Zhang and Beaulieu have derived explicit expressions for the outage probability and average BEP of MRC for BPSK signals when the channel vector of the desired user as well as the channel vectors of interfering users are modeled by correlated Rayleigh fading. However, the analysis of that paper is performed when the correlation coefficient between different branches is neither equal to zero nor one. In other words, [45] has not considered the case of independent

fading channels, the case that we will study in this thesis.

**Imperfect Channel Estimates**

In Section 3.2, we analyze the performance of MRC by deriving exact closed-from expressions of the average SINR and the average BEP for binary differential phase-shift keying (DPSK) and binary non-coherent frequency-shift keying (NCFSK) signals.

When there are no interfering users in the system, the effect of weighting errors on the performance of MRC is studied in [46]–[58]. The details of these references are described in Table 1.3.

In the presence of interfering users, performance analysis of MRC with channel estimation error is more demanding. In the presence of multiple equal-power interferers, the PDF and the outage probability of the output SINR are calculated in [59] for MRC in flat Rayleigh fading channels with Gaussian channel estimation errors and AWGN. The results of [59] are extended in [60] to the case of unequal-power interferers.

In this thesis, we use the PDF expression in [59] for performance analysis of MRC in an interference-limited system with equal-power interferers. First, for the case when the AWGN can be ignored, i.e., an interference-limited system, we simplify the PDF in [59], which was derived in the presence of AWGN. Then, we use the simplified PDF to derive simplified expression for the outage probability in interference-limited systems. The simplified PDF is also used to derive analytical expressions for the average BEP of different modulation formats in interference-limited systems. We will quantify the performance improvement of MRC as the correlation between the exact and estimated channels increases and will show that this improvement is more substantial when there is a larger number of antennas at the receiver.

### 1.2.2 Optimum Combining

Performance analysis of OC in the presence of channel estimation errors with multiple interferers is lacking in the literature. In Chapter 4, we analyze the impact of channel estimation errors on

| References | Main Derivations |
|---|---|
| [46] | The effect of channel estimation error on the performance of MRC is studied by Bello and Nelin. They showed that in frequency selective Rayleigh fading channels, a pilot tone which is separated in frequency from data results in a Gaussian-distributed channel estimation error. They derived closed-form expressions for the PDF of the output SNR and the average BEP of both coherent and non-coherent binary orthogonal detections. |
| [47] | Proakis has studied the performance of MRC when channels are estimated by using pilot tones. He has derived closed form expressions for the average BEP of MRC for M-PSK signals in Rayleigh fading channels with AWGN. |
| [48] | For Gaussian channel estimation errors, the PDF of the SNR at the output of maximal ratio combiner is derived as a function of correlation between the actual channel and its estimate in Rayleigh fading channels. |
| [49] | Tomiuk et al. have used the PDF expression in [48] to obtain the average BEP for DPSK signals. Their analysis is based on the concept that the average BEP can be obtained by averaging the conditional BEP for an AWGN channel (conditioned on the SNR) over the PDF of SNR. |
| [50] | The authors have used the same concept of averaging the conditional symbol error probability over the distribution of SNR to find the average symbol error probability of hybrid selection/maximal ratio combining for both differential and coherent demodulations in the presence of Gaussian channel estimation error. |
| [51] | The authors have shown that in the presence of channel estimation error coherent demodulation of certain modulation formats, e.g. BPSK, yields conditional error probabilities that are not functions of the output SNR, and hence, averaging the conditional probability over the distribution of the SNR at the output of the combiner does not result in the exact average probability of error. They have shown that for coherent demodulations with imperfect channel estimates averaging the conditional probability over the distribution of the output SNR results in a lower bound of true average probability of error. They have also derived the exact expression of the average BEP for BPSK signals on independent and identically distributed fading channels with Gaussian weighting errors. |
| [52] | Ma et al. have shown that in the presence of weighting errors the PDF expression in [48] cannot be used to derive exact expressions of the average BEP for coherent demodulations such as M-PSK. |
| [53]-[58] | The performance of MRC is studied for several types of fading channel and modulation in the presence of channel estimation errors. |

Table 1.3: Literature review of MRC with imperfect channel estimates and no interfering users.

| References | Main Derivations |
|---|---|
| [65] | Shah and Haimovich have derived closed-form expressions for the PDF and the mean of the SIR, as well as the outage probability and the average bit-error probability for binary phase-shift keying, in terms of hypergeometric functions over a flat Rayleigh-fading environment. |
| [41] | The PDF and the mean of the output SIR are derived for Rician/Rayleigh fading. |
| [66] | The authors give the expressions for the moments of SIR and the outage probability for interference-limited systems and Rician/Rayleigh fading environment. |
| [67] | By simplifying the hypergeometric functions in the PDF expression of [41], simplified expressions are found for the outage probability. |
| [68] | The outage probability of optimum combining in the presence of correlated Rayleigh interferers and arbitrarily faded desired signal is studied for interference-limited systems. |

Table 1.4: Literature review of OC with perfect channel estimates and multiple interferers in interference-limited systems.

the performance of OC with multiple interferers when channel estimation errors are assumed to be circularly symmetric Gaussian distributed and independent from the channel estimates.

The performance of OC with a single interferer is studied in [61]-[64] for Rayleigh fading environments. The performance analysis of OC in the presence of multiple interferers is more demanding and has been investigated extensively when the channel is known perfectly at the receiver. As described in Table 1.4, the performance of the optimum combiner in interference-limited systems is studied in [41], [65]-[68] for several types of fading.

OC performance in the presence of thermal noise and multiple interferers has also been studied when the receiver knows the channel exactly. Monte Carlo simulations [62], upper bounds [69]-[71], exact expressions [72]-[78], and approximate expressions [79]-[84] have been presented for several performance measures of OC. As explained in Table 1.5, performance analysis in [78]-[82] is done by finding the distribution of the output SINR for flat Rayleigh fading channels.

In all the above-mentioned papers, channel information is assumed to be estimated perfectly at the receiver. The impact of estimation error of the interference covariance matrix on the performance of OC is studied in [87] for sample matrix inversion method and reduced-rank array processing when the desired user's channel is perfectly estimated. In [88], the authors have investigated the effect of imperfect estimation of the desired user's channel on the BEP of OC for

| References | Main Derivations |
|---|---|
| [78] | By using statistical analysis, an exact closed-form expression is derived for the link reliability, i.e., the probability that the output SINR is greater than a given threshold. |
| [79] | Approximate expressions for the PDF of the SINR and then for the outage probability are derived in the presence of multiple equal-power interferers when the number of interferers is less than the number of antenna elements. |
| [80] | An approximate cumulative distribution function of the output SINR, in the case of multiple equal-power interferers, is presented. |
| [81]–[82] | The authors have investigated the distribution of the output SINR with an arbitrary number of interferers. They have found an approximate PDF expression for the SINR of a system with more antenna elements than interferers with unequal-power interferers. When the number of interferers is larger than the number of antennas, upper and lower bounds on the PDF of SINR are derived for equal-power interferers. |
| [85] | The authors have derived exact expressions for the PDF of the output SINR and outage probability with a Rayleigh faded desired signal in the presence of correlated equal-power Rayleigh interferers and noise. |
| [86] | The performance of OC in a Rician/Rayleigh environment in the presence of interference and noise is investigated. |

Table 1.5: Literature review of OC with perfect channel estimates in the presence of multiple interferers and thermal noise.

binary phase-shift keying signals when perfect knowledge of the interference covariance matrix is available at the receiver. In this thesis, we study the impact of channel estimation error on the performance of OC when both the desired user's channel estimate as well as interfering users' channel estimates are imperfect.

The distribution of the output SIR is a crucial discovery which makes it possible to obtain some other important measures of performance such as the average SIR and outage probability. As we will see, Gaussian distributed channel estimation errors would result in jointly Gaussian true and estimated channels which is an important outcome that makes it possible to perform statistical analysis of the output SIR. To facilitate the statistical analysis of the output SIR and derive closed-form expressions, we assume that our system is interference-limited. Our next assumption is that the interfering users have equal received signal powers, which is valid for instance when these users are at the same distance from the receiver or when power control is used.

In Section 4.2, first we use multivariate statistical analysis [90]-[92] to derive the PDF of SIR at

the output of the optimum combiner over flat Rayleigh fading channels. Then, in Section 4.3, we will use that PDF expression to obtain analytical expressions for various measures of performance such as the moments of SIR, the outage probability, and the average BEP for binary DPSK or binary NCFSK modulations. These expressions are useful tools for studying the performance of the system instead of using time-consuming Monte Carlo simulations. We will study the performance improvement of OC as the correlation between the true and estimated channels increases and will find that this improvement becomes more significant as the number of antennas at the receiver increases.

The statistical analysis of the output SIR of Section 4.2 is performed when both the desired user and interfering users are subject to Rayleigh fading. In Section 4.4, we generalize those results and derive the PDF expression of the output SIR for a Rician/Rayleigh fading environment. In the Rician/Rayleigh fading model, the desired user is subject to Rician fading while the interferers experience Rayleigh fading. In other words, it is assumed that there is a LOS between the desired user and its base station while for interfering users there is no LOS. Using multivariate statistical analysis, an exact closed-form expression is derived for the PDF of the output SIR. The theoretical result is verified by Monte Carlo simulations as well. The analysis in Section 4.4 is valid for the same conditions stated in Section 4.2, i.e. for interference-limited systems with Gaussian distributed channel estimation errors. We assume that the interferers have equal power and the number of interferers exceeds or is equal to the number of antennas.

### 1.2.3 Maximal Ratio Combi ning versus Optimum Combining

Given error-free channel information, the relative performance of MRC and OC in the presence of multiple interferers has been extensively studied in [62], [41], [67], [6]; not surprisingly, it was found that OC outperforms MRC for all considered modulation formats and fading distributions.

In Section 4.5, we compare the performance of MRC with OC in the presence of channel estimation error. For this performance comparison, we use the expressions derived in Sections 3.2 and 4.3. Fig. 1.2 shows the approach we will use for performance comparison. We will discover

that in the presence of channel estimation errors MRC can outperform OC, especially for small values of the correlation coefficient between true and estimated channels. Moreover, we will also observe that as the number of antennas increases there is a larger range of correlation coefficients over which MRC performs better than OC. These results allow researchers to execute tradeoff studies among MRC and OC to determine the better choice in the presence of channel estimation error.

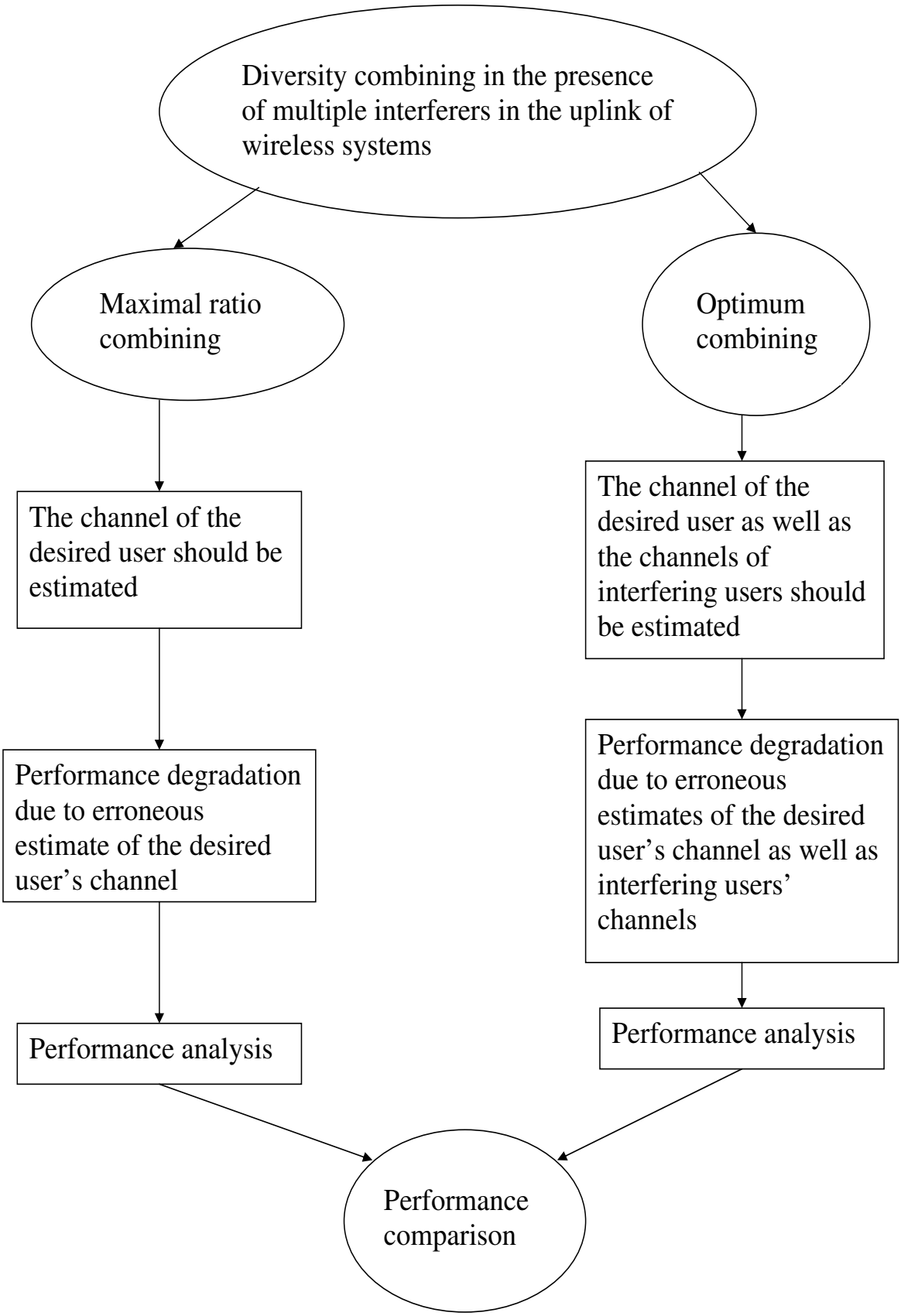


Figure 1.2: Diversity combining with imperfect channel estimates

# Chapter 2

# Detection with Imperfect Channel Estimates

This chapter contains two main sections. The analysis of this chapter is for single-antenna transmitters and receivers. In the first section, we present the ML receiver structure for binary orthogonal signals in the presence of Gaussian-distributed channel estimation error and additive white Gaussian noise. We find that the ML receiver for binary orthogonal signals is a linear combination of a matched filter and envelope detector, which are ML receivers for ideal coherent reception and non-coherent reception, respectively. The exact average bit error probability of the proposed receiver is derived for flat Rayleigh fading channels. We compare the performance of the ML receiver for orthogonal modulation with the one for antipodal signalling in the presence of channel estimation error and find the conditions under which orthogonal modulation results in better performance. The performance of the proposed receiver is analyzed in both quasi-static fading and time-varying fading channels.

In the second section, we derive the structure of the ML receiver for QPSK signals in the presence of Gaussian-distributed channel estimation error and additive white Gaussian noise. We find that the ML receiver is a matched filter which is matched to the channel estimate. In other words, for Gaussian-distributed channel estimation error whether we use channel estimation statistics or not, the structure of ML receiver is the same. We derive the exact expression of the average bit error probability of this receiver in flat Rayleigh fading channels. The performance of the receiver

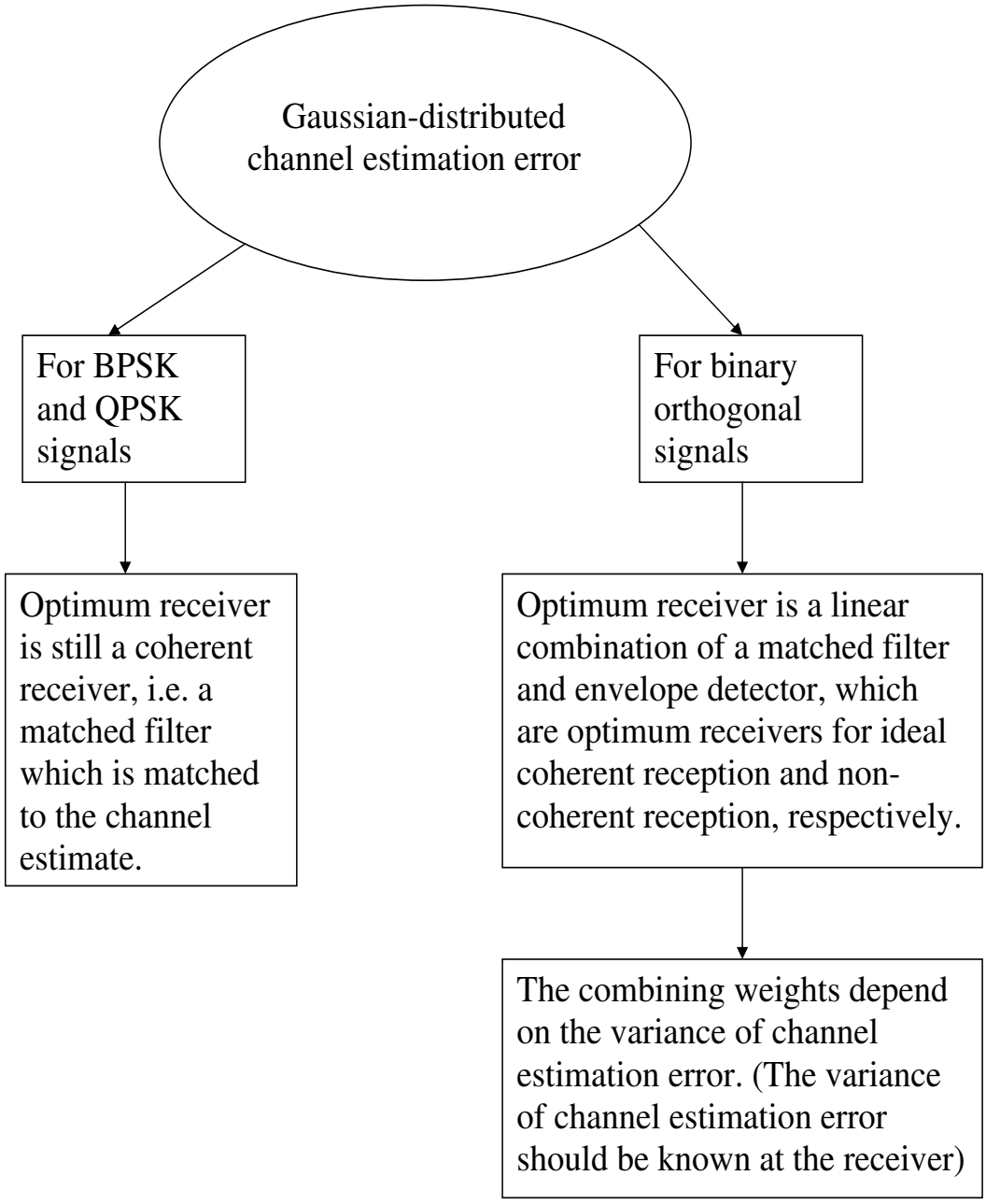


Figure 2.1: Structure of ML receivers with Gaussian channel estimation error

is analyzed in quasi-static channels with pilot symbols and an MMSE channel estimator. We also compare the performance of QPSK signalling with BPSK in the presence of channel estimation error.

The above-mentioned discussion about the structure of ML receivers in the presence of Gaussian channel estimation error is summarized in Fig. 2.1.

## 2.1 Maximum-likelihood Detection of Binary Signals

In this section, we derive the structure of the ML receiver for *orthogonal* binary signals in the presence of Gaussian-distributed channel estimation error and AWGN for single-antenna reception. We derive an exact expression for the average BEP of the proposed ML detector in Rayleigh fading channels.

We then study two special cases where Gaussian-distributed channel estimation error arises: first quasi-static Rayleigh fading channels with pilot symbols and the MMSE channel estimator, and second, time-varying Rayleigh fading channels modeled with an AR process of order one.

### 2.1.1 System Model

We consider transmitting binary signals over flat fading channels. For binary antipodal signalling, the received baseband signal $r$ can be written as

$$r = hs + n \tag{2.1}$$

where $s$ is the transmitted signal which is either $s_1 = \sqrt{E_b}$ or $s_2 = -\sqrt{E_b}$, and $E_b$ is the energy per bit. The fading channel is denoted by $h$, and complex AWGN $n$ is distributed as $n \sim CN(0, 2\sigma_n^2)$ where $CN(m, 2\sigma^2)$ denotes a circularly symmetric Gaussian distribution for a complex random variable with mean $m$ and variance $2\sigma^2$.

For binary orthogonal signalling, e.g. orthogonal frequency-shift keying, the baseband received

vector $\boldsymbol{r}$ is

$$\boldsymbol{r} = h\boldsymbol{s} + \boldsymbol{n} \tag{2.2}$$

where the transmitted signal vector $\boldsymbol{s}$ is either $\boldsymbol{s}_1 = \left(\sqrt{E_b}, 0\right)$ or $\boldsymbol{s}_2 = \left(0, \sqrt{E_b}\right)$, and $h$ denotes the fading channel. We assume that the same channel coefficient applies to both dimensions, which is valid for flat fading channels. The vector $\boldsymbol{n} = (n_1, n_2)$ is the complex AWGN vector, where independently distributed $n_1$ and $n_2$ are the first and second elements of vector $\boldsymbol{n}$, respectively, and $n_1, n_2 \sim CN(0, 2\sigma_n^2)$.

The analysis in this chapter is valid for all orthogonal modulations where each symbol has the same energy $E_b$. Therefore, the analysis does not include on-off keying (OOK) modulation since in OOK one symbol has zero energy while the other has $2E_b$. In other words, for OOK it is not possible to have $\boldsymbol{s}_1$ and $\boldsymbol{s}_2$ as described above.

Throughout this section, channel $h$ is assumed to be Rayleigh with variance $2\sigma_h^2$, i.e. $h \sim CN(0, 2\sigma_h^2)$. The received SNR per bit $\gamma_b$ for both antipodal and orthogonal modulations is defined as $\gamma_b = \frac{E_b|h|^2}{2\sigma_n^2}$, and thus, the average SNR per bit $\bar{\gamma}_b$ is equal to

$$\bar{\gamma}_b = E\left(\gamma_b\right) = \frac{E_b}{2\sigma_n^2} E\left(|h|^2\right) = \frac{E_b\sigma_h^2}{\sigma_n^2} \tag{2.3}$$

where $E(.)$ denotes the statistical expectation.

To detect the transmitted bits, the channel $h$ must be estimated at the receiver. The channel estimation error is defined as

$$e = h - \hat{h} \tag{2.4}$$

where $\hat{h}$ is the channel estimate. The channel estimation error $e$ is assumed to be circularly symmetric Gaussian with variance $2\sigma_e^2$, i.e. $e \sim CN\left(0, 2\sigma_e^2\right)$. The channel estimate $\hat{h}$ is also circularly

symmetric Gaussian distributed with variance $2\sigma_{\hat{h}}^2$, i.e. $\hat{h} \sim CN(0, 2\sigma_{\hat{h}}^2)$. Channel estimation error $e$ and channel estimate $\hat{h}$ are assumed to be mutually independent which is valid for MMSE estimation in which the estimate and the error are orthogonal [8]. Note that since $\hat{h}$ and $e$ are independent, from (2.4) we have $\sigma_e^2 = \sigma_h^2 - \sigma_{\hat{h}}^2$, and $\hat{h}$ and $h$ are jointly circularly symmetric Gaussian distributed with the correlation coefficient $\rho$ which can be written as

$$\rho = \frac{E\left(h^*\hat{h}\right)}{\left(\sqrt{2}\sigma_h\right)\left(\sqrt{2}\sigma_{\hat{h}}\right)} = \frac{\sigma_{\hat{h}}}{\sigma_h} = \frac{1}{\sigma_h}\sqrt{\sigma_h^2 - \sigma_e^2} \tag{2.5}$$

For ideal coherent reception we have $\hat{h} = h$, and thus from (2.4) $e = 0$ and $\sigma_e^2 = 0$, and from (2.5) we get $\rho = 1$. On the other hand, if the channel estimation is so poor that $\rho \to 0$, the reception will be non-coherent, and from (2.5) $\sigma_e^2 = \sigma_h^2$.

Throughout this section it is assumed that channel estimation error $e$ is independent of the thermal noise during transmission of data symbols, i.e. error $e$ is independent of noise $n$ in antipodal signalling and of noise $\boldsymbol{n}$ in orthogonal signalling. We will show in Subsection 2.1.5 that this assumption is valid for both quasi-static and time-varying channels.

### 2.1.2 Maximum-likelihood Receiver Structure

In this subsection, first we review the ML detection of binary antipodal signals in the presence of Gaussian channel estimation error, which is described in [17]. Then, we propose the structure of the ML receiver for binary orthogonal modulation with Gaussian channel estimation error.

#### Antipodal Signalling

In this part, we review the structure of ML receiver for binary antipodal signals with single-antenna reception, which is derived by You et al. in [17].

In antipodal signalling, if $s_1 = \sqrt{E_b}$ is transmitted the received signal $r$ from (2.1) and (2.4) is

$$r = hs_1 + n = \hat{h}s_1 + es_1 + n = \sqrt{E_b}\hat{h} + \sqrt{E_b}e + n = \sqrt{E_b}\hat{h} + n' \tag{2.6}$$

where $n'$ is defined as

$$n' = \sqrt{E_b}e + n \tag{2.7}$$

Since independent random variables $e$ and $n$ are circularly symmetric Gaussian distributed, $n'$ in (2.7) is also circularly symmetric Gaussian distributed and we have

$$n' \sim CN\left(0, 2\left(E_b\sigma_e^2 + \sigma_n^2\right)\right) \tag{2.8}$$

Similarly, if $s_2 = -\sqrt{E_b}$ is transmitted, from (2.1) and (2.4) the received signal $r$ can be written as

$$r = hs_2 + n = \hat{h}s_2 + es_2 + n = -\sqrt{E_b}\hat{h} - \sqrt{E_b}e + n = -\sqrt{E_b}\hat{h} + n'' \tag{2.9}$$

where $n''$ is defined as

$$n'' = -\sqrt{E_b}e + n \tag{2.10}$$

and since independent random variables $e$ and $n$ are circularly symmetric Gaussian distributed we get

$$n'' \sim CN\left(0, 2\left(E_b\sigma_e^2 + \sigma_n^2\right)\right) \tag{2.11}$$

Based on the ML criterion, the decision rule is

$$p_r\left(r|\hat{h}, s_1\right) \underset{\hat{s}=s_2}{\overset{\hat{s}=s_1}{\gtrless}} p_r\left(r|\hat{h}, s_2\right) \tag{2.12}$$

From (2.6), the left-hand side of (2.12) can be written as

$$p_r\left(r|\hat{h}, s_1\right) = p_{n'}\left(r - \sqrt{E_b}\hat{h}\right) = \frac{1}{2\pi\left(E_b\sigma_e^2 + \sigma_n^2\right)}\exp\left(-\frac{\left|r - \sqrt{E_b}\hat{h}\right|^2}{2\left(E_b\sigma_e^2 + \sigma_n^2\right)}\right) \tag{2.13}$$

in which we have used the fact that, from (2.8), $n' \sim CN\left(0, 2\left(E_b\sigma_e^2 + \sigma_n^2\right)\right)$.

Similarly, from (2.9), the right-hand side of (2.12) can be written as

$$p_r\left(r|\hat{h}, s_2\right) = p_{n''}\left(r + \sqrt{E_b}\hat{h}\right) = \frac{1}{2\pi\left(E_b\sigma_e^2 + \sigma_n^2\right)}\exp\left(-\frac{\left|r + \sqrt{E_b}\hat{h}\right|^2}{2\left(E_b\sigma_e^2 + \sigma_n^2\right)}\right) \tag{2.14}$$

in which we have used the fact that, from (2.11), $n'' \sim CN\left(0, 2\left(E_b\sigma_e^2 + \sigma_n^2\right)\right)$.

Therefore, from (2.13) and (2.14), the decision rule in (2.12) can be expressed as

$$\left|r - \sqrt{E_b}\hat{h}\right|^2 \underset{\hat{s}=s_2}{\overset{\hat{s}=s_1}{\lessgtr}} \left|r + \sqrt{E_b}\hat{h}\right|^2 \tag{2.15}$$

which reduces to

$$\text{Re}\left\{\hat{h}^* r\right\} \underset{\hat{s}=s_2}{\overset{\hat{s}=s_1}{\gtrless}} 0 \tag{2.16}$$

where Re $\{\cdot\}$ indicates the real part of a complex number. The decision rule (2.16) is stated in [17, eq. (16)].

The receiver in (2.16) is a coherent receiver that treats the estimated channel as the true channel, i.e. just a matched filter that is matched to the channel estimate. The knowledge of $\sigma_e^2$ is not needed to implement the receiver in (2.16). However, as we will show in the following, $\sigma_e^2$ is a vital parameter in designing the ML receiver for orthogonal modulation.

**Orthogonal Signalling**

In this part, we derive the structure of the ML receiver for binary orthogonal signals.

In orthogonal signalling, if $\boldsymbol{s}_1 = (\sqrt{E_b}, 0)$ is transmitted the received vector $\boldsymbol{r}$ from (2.2) and (2.4) can be written as

$$\boldsymbol{r} = h\boldsymbol{s}_1 + \boldsymbol{n} = \left(\hat{h} + e\right)\boldsymbol{s}_1 + \boldsymbol{n} = \left(\sqrt{E_b}\hat{h} + \sqrt{E_b}e + n_1, n_2\right) = \left(\sqrt{E_b}\hat{h} + n_1', n_2\right) \tag{2.17}$$

where $n_1'$ is defined as

$$n_1' = \sqrt{E_b}e + n_1 \tag{2.18}$$

Since independent random variables $e$ and $n_1$ are circularly symmetric Gaussian distributed, $n_1'$ in (2.18) is also circularly symmetric Gaussian distributed, i.e. $n_1' \sim CN\left(0, 2\left(E_b\sigma_e^2 + \sigma_n^2\right)\right)$.

On the other hand, if $\boldsymbol{s}_2 = (0, \sqrt{E_b})$ is transmitted, from (2.2) and (2.4) the received vector $\boldsymbol{r}$ is

$$\boldsymbol{r} = h\boldsymbol{s}_2 + \boldsymbol{n} = \left(\hat{h} + e\right)\boldsymbol{s}_2 + \boldsymbol{n} = \left(n_1, \sqrt{E_b}\hat{h} + \sqrt{E_b}e + n_2\right) = \left(n_1, \sqrt{E_b}\hat{h} + n_2'\right) \tag{2.19}$$

where $n_2'$ is defined as

$$n_2' = \sqrt{E_b}e + n_2 \tag{2.20}$$

and $n_2' \sim CN\left(0, 2\left(E_b\sigma_e^2 + \sigma_n^2\right)\right)$ since independent random variables $e$ and $n_2$ are circularly symmetric Gaussian distributed.

Based on the ML criterion, the decision rule is

$$p_{r_1,r_2}\left(r_1, r_2|\hat{h}, \boldsymbol{s}_1\right) \underset{\hat{\boldsymbol{s}}=\boldsymbol{s}_2}{\overset{\hat{\boldsymbol{s}}=\boldsymbol{s}_1}{\gtrless}} p_{r_1,r_2}\left(r_1, r_2|\hat{h}, \boldsymbol{s}_2\right) \tag{2.21}$$

where $r_1$ and $r_2$ are the first and second elements of the vector $\boldsymbol{r}$, respectively, and $\hat{\boldsymbol{s}}$ denotes the estimate of the transmitted vector $\boldsymbol{s}$.

From (2.17), the left-hand side of (2.21) can be written as

$$p_{r_1,r_2}\left(r_1, r_2|\hat{h}, \boldsymbol{s}_1\right) = p_{n_1',n_2}\left(r_1 - \sqrt{E_b}\hat{h}, r_2|\hat{h}\right) = p_{n_1'}\left(r_1 - \sqrt{E_b}\hat{h}\right)p_{n_2}\left(r_2\right) \tag{2.22}$$

in which we have used the fact that $n_1'$ in (2.18) and $n_2$ are mutually independent, and both are independent of $\hat{h}$.

Since $n_1' \sim CN\left(0, 2\left(E_b\sigma_e^2 + \sigma_n^2\right)\right)$ and $n_2 \sim CN\left(0, 2\sigma_n^2\right)$, equation (2.22) can be expressed

as

$$p_{r_1,r_2}\left(r_1,r_2|\hat{h},\boldsymbol{s}_1\right)=\frac{1}{(2\pi)^2\,\sigma_n^2\left(E_b\sigma_e^2+\sigma_n^2\right)}\exp\left(-\frac{\left|r_1-\sqrt{E_b}\hat{h}\right|^2}{2\left(E_b\sigma_e^2+\sigma_n^2\right)}-\frac{|r_2|^2}{2\sigma_n^2}\right) \tag{2.23}$$

Similarly, from (2.19), the right-hand side of (2.21) can be expressed as

$$p_{r_1,r_2}\left(r_1,r_2|\hat{h},\boldsymbol{s}_2\right)=p_{n_1,n_2'}\left(r_1,r_2-\sqrt{E_b}\hat{h}|\hat{h}\right)=p_{n_1}\left(r_1\right)p_{n_2'}\left(r_2-\sqrt{E_b}\hat{h}\right) \tag{2.24}$$

Now, since $n_1\sim CN\left(0,2\sigma_n^2\right)$ and $n_2'\sim CN\left(0,2\left(E_b\sigma_e^2+\sigma_n^2\right)\right)$, expression (2.24) is the same as

$$p_{r_1,r_2}\left(r_1,r_2|\hat{h},\boldsymbol{s}_2\right)=\frac{1}{(2\pi)^2\,\sigma_n^2\left(E_b\sigma_e^2+\sigma_n^2\right)}\exp\left(-\frac{|r_1|^2}{2\sigma_n^2}-\frac{\left|r_2-\sqrt{E_b}\hat{h}\right|^2}{2\left(E_b\sigma_e^2+\sigma_n^2\right)}\right) \tag{2.25}$$

By substituting (2.23) and (2.25) in (2.21), the ML decision rule can be expressed as

$$\frac{\left|r_1-\sqrt{E_b}\hat{h}\right|^2}{E_b\sigma_e^2+\sigma_n^2}+\frac{|r_2|^2}{\sigma_n^2}\underset{\hat{\boldsymbol{s}}=\boldsymbol{s}_2}{\overset{\hat{\boldsymbol{s}}=\boldsymbol{s}_1}{\lessgtr}}\frac{|r_1|^2}{\sigma_n^2}+\frac{\left|r_2-\sqrt{E_b}\hat{h}\right|^2}{E_b\sigma_e^2+\sigma_n^2} \tag{2.26}$$

which can be simplified to

$$\frac{\sqrt{E_b}\sigma_e^2}{2\sigma_n^2}|r_1|^2+\text{Re}\left\{\hat{h}^*r_1\right\}\underset{\hat{\boldsymbol{s}}=\boldsymbol{s}_2}{\overset{\hat{\boldsymbol{s}}=\boldsymbol{s}_1}{\lessgtr}}\frac{\sqrt{E_b}\sigma_e^2}{2\sigma_n^2}|r_2|^2+\text{Re}\left\{\hat{h}^*r_2\right\} \tag{2.27}$$

Therefore, in contrast to the ML receiver for binary antipodal modulation in (2.16), the ML receiver for binary orthogonal signals in (2.27) is not just a coherent receiver that treats the estimated channel as the true channel. In fact, the ML receiver in (2.27) is a linear combination of the matched filter receiver and the square-law detector, the ML receivers for coherent and non-coherent detection approaches, respectively. The combining weights depend on $\sigma_e^2$.

In the extreme case of purely coherent reception ($\hat{h}=h$), we have $e=0$ and $\sigma_e^2=0$, and thus,

the receiver in (2.27) simplifies to

$$\mathrm{Re}\left\{h^* r_1\right\} \underset{\hat{\boldsymbol{s}}=\boldsymbol{s}_2}{\overset{\hat{\boldsymbol{s}}=\boldsymbol{s}_1}{\gtrless}} \mathrm{Re}\left\{h^* r_2\right\} \tag{2.28}$$

which is the matched filter receiver, as expected.

In the other limiting case of non-coherent reception ($\sigma_e^2 = \sigma_h^2$), $\sigma_{\hat{h}}^2 = 0$ and $\hat{h} = 0$, and (2.27) reduces to

$$|r_1|^2 \underset{\hat{\boldsymbol{s}}=\boldsymbol{s}_2}{\overset{\hat{\boldsymbol{s}}=\boldsymbol{s}_1}{\gtrless}} |r_2|^2 \tag{2.29}$$

which is the square-law detector, as expected.

Note that in order to implement (2.27), $\sigma_e^2$ should be available at the receiver. In Subsection 2.1.5, we investigate the decision rule (2.27) in both quasi-static and time-varying fading channels. In that subsection, we will derive analytical expressions for $\sigma_e^2$, and then the ML receiver structure can be obtained by substituting the derived $\sigma_e^2$ in (2.27).

### 2.1.3 Average Bit Error Probability Performance

In this subsection, we analyze the performance of the receivers (2.16) and (2.27) in Rayleigh fading channels for equiprobable transmitted signals. First, we review the derivation of the average BEP expression of receiver (2.16) for antipodal modulation which is presented in [17] and [51]. Then, we derive the exact closed-form expression of the average BEP of the ML receiver (2.27) for orthogonal signalling. The average BEP expressions in this subsection are general and functions of $\sigma_e^2$ and $\bar{\gamma}_b$. In Subsection 2.1.5, we will study quasi-static and time-varying channels as two special cases.

#### Antipodal Signalling

In this part, we review the derivation of the average BEP expression for the receiver in (2.16), which was presented in [17] and [51].

For equiprobable transmitted bits, the BEP of antipodal signalling is equal to the BEP when $s_1$ is transmitted. Therefore, the BEP conditioned on $\hat{h}$ can be written as

$$P_b\left(E|\hat{h}\right) = P_b\left(E|\hat{h}, s = s_1\right) = P\left(\hat{s} = s_2|\hat{h}, s = s_1\right) = P\left(\text{Re}\left\{\hat{h}^* r\right\} < 0|\hat{h}, s = s_1\right) \quad (2.30)$$

From (2.6), the output of the matched filter when $s_1$ is transmitted is equal to

$$\hat{h}^* r = \sqrt{E_b}\left|\hat{h}\right|^2 + \hat{h}^* n' = \sqrt{E_b}\left|\hat{h}\right|^2 + z \quad (2.31)$$

where $z$ is defined as

$$z = \hat{h}^* n' \quad (2.32)$$

and from (2.8) is distributed as

$$z \sim CN\left(0, 2\left|\hat{h}\right|^2\left(E_b\sigma_e^2 + \sigma_n^2\right)\right) \quad (2.33)$$

Now, from (2.31) and (2.33), we get

$$\text{Re}\left\{\hat{h}^* r\right\} \sim N\left(\sqrt{E_b}\left|\hat{h}\right|^2, \left|\hat{h}\right|^2\left(E_b\sigma_e^2 + \sigma_n^2\right)\right) \quad (2.34)$$

where $N(m, \sigma^2)$ denotes a normal distribution for a real random variable with mean $m$ and variance $\sigma^2$.

Now, from (2.34), the error probability in (2.30) can be expressed as

$$P_b(E|\hat{h}) = Q\left(\sqrt{\frac{E_b\left|\hat{h}\right|^2}{E_b\sigma_e^2 + \sigma_n^2}}\right) = Q\left(\sqrt{2\gamma_\varepsilon}\right) \quad (2.35)$$

where $Q(x)$ is the Gaussian Q-function defined as

$$Q(x) = \frac{1}{\sqrt{2\pi}} \int_x^\infty \exp\left(-\frac{t^2}{2}\right) dt \tag{2.36}$$

and the effective SNR $\gamma_\varepsilon$ is defined as

$$\gamma_\varepsilon = \frac{E_b \left|\hat{h}\right|^2}{2\left(E_b\sigma_e^2 + \sigma_n^2\right)} \tag{2.37}$$

To compute the average BEP, we average the conditional BEP in (2.35) over the PDF of $\gamma_\varepsilon$. Since $\hat{h}$ is circularly symmetric Gaussian distributed, $\gamma_\varepsilon$ in (2.37) is Rayleigh distributed and its PDF is given by

$$f_{\gamma_\varepsilon}(\gamma_\varepsilon) = \frac{1}{\bar{\gamma}_\varepsilon} \exp\left(-\frac{\gamma_\varepsilon}{\bar{\gamma}_\varepsilon}\right) \tag{2.38}$$

where

$$\bar{\gamma}_\varepsilon = E(\gamma_\varepsilon) = \frac{E_b\left(\sigma_h^2 - \sigma_e^2\right)}{E_b\sigma_e^2 + \sigma_n^2} = \frac{\bar{\gamma}_b\left(\sigma_h^2 - \sigma_e^2\right)}{\bar{\gamma}_b\sigma_e^2 + \sigma_h^2} \tag{2.39}$$

where the average SNR $\bar{\gamma}_b$ is defined in (2.3).

Now, from (2.35) and (2.38), the average BEP can be written as

$$P_b(E) = \int_0^\infty P_b(E|\gamma_\varepsilon) p_{\gamma_\varepsilon}(\gamma_\varepsilon) d\gamma_\varepsilon = \int_0^\infty \frac{1}{\bar{\gamma}_\varepsilon} \exp\left(-\frac{\gamma_\varepsilon}{\bar{\gamma}_\varepsilon}\right) Q\left(\sqrt{2\gamma_\varepsilon}\right) d\gamma_\varepsilon$$

By using [6, eq. (5.6)], the average BEP of the ML receiver for antipodal binary signals can be computed as

$$P_b(E) = \frac{1}{2}\left(1 - \sqrt{\frac{\bar{\gamma}_\varepsilon}{1+\bar{\gamma}_\varepsilon}}\right) = \frac{1}{2}\left(1 - \sqrt{\frac{\left(\sigma_h^2 - \sigma_e^2\right)\bar{\gamma}_b}{\sigma_h^2 + \sigma_h^2\bar{\gamma}_b}}\right) \tag{2.40}$$

The expression (2.40) is stated in [17, eq. (38)] and [51, eq. (23)].

In purely coherent reception $(\sigma_e^2 = 0)$ , expression (2.40) simplifies to

$$P_b(E) = \frac{1}{2}\left(1 - \sqrt{\frac{\bar{\gamma}_b}{1+\bar{\gamma}_b}}\right) \tag{2.41}$$

which is a well-known result [1, eq. (14.3-7)].

As a sanity check, for non-coherent reception $(\sigma_e^2 = \sigma_h^2)$, the average BEP expression in (2.40) reduces to

$$P_b(E) = \frac{1}{2} \tag{2.42}$$

The result in (2.42) is expected since when there is no channel information available at the receiver, there is no basis for the decision for antipodal signals. In other words, when $\sigma_e^2 = \sigma_h^2$, we get $\sigma_{\hat{h}}^2 = 0$ and $\hat{h} = 0$, and thus from (2.16) there is no basis for a decision.

**Orthogonal Signalling**

In this part, we derive the average BEP expression of the proposed receiver in (2.27).

First, we rewrite the decision rule in (2.27) as

$$|r_1'|^2 \underset{\hat{\boldsymbol{s}}=\boldsymbol{s}_2}{\overset{\hat{\boldsymbol{s}}=\boldsymbol{s}_1}{\gtrless}} |r_2'|^2 \tag{2.43}$$

where

$$r_1' = \frac{\sqrt{E_b}\sigma_e^2}{\sigma_n^2} r_1 + \hat{h} \tag{2.44}$$

and

$$r_2' = \frac{\sqrt{E_b}\sigma_e^2}{\sigma_n^2} r_2 + \hat{h} \tag{2.45}$$

For binary orthogonal signals modeled in (2.2), the BEP when transmitted signals $\boldsymbol{s}_1$ and $\boldsymbol{s}_2$ are equiprobable is equal to the BEP when $\boldsymbol{s}_1$ is transmitted. So, from (2.43) we have

$$P_b\left(E|\hat{h}\right) = P_b\left(E|\hat{h}, \boldsymbol{s}_1\right) = P\left(|r_2'| > |r_1'|\,|\hat{h}, \boldsymbol{s}_1\right) \tag{2.46}$$

If $\boldsymbol{s}_1$ is transmitted, from (2.17) we get

$$r_1|\hat{h}, \boldsymbol{s}_1 = \sqrt{E_b}\hat{h} + n_1' \sim CN\left(\sqrt{E_b}\hat{h}, 2\left(E_b\sigma_e^2 + \sigma_n^2\right)\right) \tag{2.47}$$

and

$$r_2|\hat{h}, \boldsymbol{s}_1 = n_2 \sim CN\left(0, 2\sigma_n^2\right) \tag{2.48}$$

Since $n_1'$ and $n_2$ are independent, random variables $r_1|\hat{h}, \boldsymbol{s}_1$ and $r_2|\hat{h}, \boldsymbol{s}_1$ in (2.47) and (2.48) are also independent.

Now, from (2.47) and (2.48), if $\boldsymbol{s}_1$ is transmitted random variables $r_1'$ and $r_2'$ in (2.44) and (2.45) conditioned on $\hat{h}$ are distributed as

$$r_1'|\hat{h}, \boldsymbol{s}_1 \sim CN\left(\frac{\hat{h}\left(E_b\sigma_e^2 + \sigma_n^2\right)}{\sigma_n^2}, \frac{2E_b\sigma_e^4\left(E_b\sigma_e^2 + \sigma_n^2\right)}{\sigma_n^4}\right) \tag{2.49}$$

and

$$r_2'|\hat{h}, \boldsymbol{s}_1 \sim CN\left(\hat{h}, \frac{2E_b\sigma_e^4}{\sigma_n^2}\right) \tag{2.50}$$

Since $r_1|\hat{h}, \boldsymbol{s}_1$ and $r_2|\hat{h}, \boldsymbol{s}_1$ in (2.47) and (2.48) are independent, from (2.44) and (2.45) random variables $r_1'|\hat{h}, \boldsymbol{s}_1$ and $r_2'|\hat{h}, \boldsymbol{s}_1$ are also independent. Therefore, $|r_1'|\,|\hat{h}, \boldsymbol{s}_1$ and $|r_2'|\,|\hat{h}, \boldsymbol{s}_1$ are mutually independent as well. Now, from (2.49) and (2.50), $|r_1'|\,|\hat{h}, \boldsymbol{s}_1$ and $|r_2'|\,|\hat{h}, \boldsymbol{s}_1$ are Rician distributed. The probability that in a pair of independent Rice random variables one is greater than another is computed in [4, App. A] in terms of $Q(x, y)$, the first-order Marcum's Q-function, defined as

$$Q(x, y) = \int_y^\infty t \exp\left(-\frac{t^2 + x^2}{2}\right) I_0(xt)dt \tag{2.51}$$

and $I_0(.)$ denotes the zeroth-order modified Bessel function of the first kind.

So, by using the results in [4, App. A], the conditional BEP in (2.46) is equal to

$$P_b(E|\hat{h}) = \frac{\zeta^2}{1+\zeta^2}\left(1 - Q\left(\mu\sqrt{\gamma_o}, \lambda\sqrt{\gamma_o}\right)\right) + \frac{1}{1+\zeta^2}Q\left(\lambda\sqrt{\gamma_o}, \mu\sqrt{\gamma_o}\right) \tag{2.52}$$

where $\gamma_o$ is defined as

$$\gamma_o = \frac{\bar{\gamma}_b \left|\hat{h}\right|^2}{\bar{\gamma}_b\sigma_e^2 + 2\sigma_h^2} \tag{2.53}$$

and $\lambda$, $\mu$ and $\zeta$ are defined as

$$\lambda = \frac{\sigma_h^2}{\bar{\gamma}_b\sigma_e^2}; \quad \mu = \frac{\bar{\gamma}_b\sigma_e^2 + \sigma_h^2}{\bar{\gamma}_b\sigma_e^2}; \quad \zeta = \frac{1}{\sigma_h}\sqrt{\bar{\gamma}_b\sigma_e^2 + \sigma_h^2} \tag{2.54}$$

where $\bar{\gamma}_b$ is defined in (2.3).

To derive the average BEP, the conditional BEP in (2.52) should be averaged over the PDF of $\gamma_o$. Since $\hat{h}$ is circularly symmetric Gaussian distributed, $\gamma_o$ in (2.53) has an exponential distribution [93, p. 190] with the following PDF

$$f_{\gamma_o}(\gamma_o) = \frac{1}{\bar{\gamma}_o}\exp\left(-\frac{\gamma_o}{\bar{\gamma}_o}\right), \quad \gamma_o \geq 0 \tag{2.55}$$

where

$$\bar{\gamma}_o = E(\gamma_o) = \frac{2\bar{\gamma}_b\sigma_{\hat{h}}^2}{\bar{\gamma}_b\sigma_e^2 + 2\sigma_h^2} = \frac{2\bar{\gamma}_b\left(\sigma_h^2 - \sigma_e^2\right)}{\bar{\gamma}_b\sigma_e^2 + 2\sigma_h^2} \tag{2.56}$$

Now, by integrating (2.52) over the PDF in (2.55), the average BEP can be written as

$$\begin{aligned} P_b(E) &= \int_0^\infty P_b(E|\gamma_o) f_{\gamma_o}(\gamma_o) d\gamma_o \\ &= \frac{\zeta^2}{1+\zeta^2}\left(1 - \int_0^\infty \frac{1}{\bar{\gamma}_o}\exp\left(-\frac{\gamma_o}{\bar{\gamma}_o}\right) Q\left(\mu\sqrt{\gamma_o}, \lambda\sqrt{\gamma_o}\right) d\gamma_o\right) \\ &\quad + \frac{1}{1+\zeta^2}\int_0^\infty \frac{1}{\bar{\gamma}_o}\exp\left(-\frac{\gamma_o}{\bar{\gamma}_o}\right) Q\left(\lambda\sqrt{\gamma_o}, \mu\sqrt{\gamma_o}\right) d\gamma_o \end{aligned} \tag{2.57}$$

The integral terms in (2.57) can be calculated by using the results in [6, eqs. (5.50)-(5.53)], and (2.57) can be simplified to

$$P_b(E) = \frac{1}{2}\left(1 - \frac{(1+\zeta^2)(\mu^2-\lambda^2)\frac{\bar{\gamma}_o}{2} + \zeta^2 - 1}{(1+\zeta^2)\sqrt{\left(1+(\lambda^2+\mu^2)\frac{\bar{\gamma}_o}{2}\right)^2 - \lambda^2\mu^2\bar{\gamma}_o^2}}\right) \tag{2.58}$$

By substituting (2.54) and (2.56) in (2.58), the average BEP of the ML receiver for binary orthogonal signals can be expressed as

$$P_b(E) = \frac{1}{2}\left(1 - \sqrt{\frac{\bar{\gamma}_b\left(\bar{\gamma}_b\sigma_e^2 + 2\left(\sigma_h^2 - \sigma_e^2\right)\right)}{\left(\bar{\gamma}_b+2\right)\left(\bar{\gamma}_b\sigma_e^2 + 2\sigma_h^2\right)}}\right) \tag{2.59}$$

In the extreme case of $\sigma_e^2 = 0$ (perfectly coherent reception), expression (2.59) simplifies to

$$P_b(E) = \frac{1}{2}\left(1 - \sqrt{\frac{\bar{\gamma}_b}{2+\bar{\gamma}_b}}\right) \tag{2.60}$$

which is identical to [1, eq. (14.3-8)], the average BEP of the coherent receiver, as expected.

For the other limiting case of $\sigma_e^2 = \sigma_h^2$ (noncoherent reception), (2.59) reduces to

$$P_b(E) = \frac{1}{2}\left(1 - \frac{\bar{\gamma}_b}{2+\bar{\gamma}_b}\right) = \frac{1}{2+\bar{\gamma}_b} \tag{2.61}$$

which is equal to [1, eq. (14.3-12)], the average BEP for noncoherent reception.

### 2.1.4 Performance Comparison

In this subsection, we compare the performance of orthogonal signalling with antipodal modulation in the presence of Gaussian channel estimation error. By comparing (2.59) with (2.40), orthogonal signalling has smaller average BEP than antipodal signalling if

$$\frac{1}{2}\left(1 - \sqrt{\frac{\bar{\gamma}_b\left(\bar{\gamma}_b\sigma_e^2 + 2\left(\sigma_h^2 - \sigma_e^2\right)\right)}{\left(\bar{\gamma}_b+2\right)\left(\bar{\gamma}_b\sigma_e^2 + 2\sigma_h^2\right)}}\right) < \frac{1}{2}\left(1 - \sqrt{\frac{\left(\sigma_h^2 - \sigma_e^2\right)\bar{\gamma}_b}{\sigma_h^2\left(1+\bar{\gamma}_b\right)}}\right) \tag{2.62}$$

which can be simplified to

$$\sigma_e^2 > \frac{\sigma_h^2}{1 + 0.5\bar{\gamma}_b}, \tag{2.63}$$

otherwise, antipodal modulation has smaller average BEP.

It is evident from (2.63) that for $\sigma_e^2 = 0$ (coherent reception) antipodal modulation has a better performance than orthogonal signalling while for $\sigma_e^2 = \sigma_h^2$ (non-coherent reception) orthogonal signals result in a smaller average BEP, as expected. In fact, (2.63) gives the threshold of $\sigma_e^2$ beyond which orthogonal signalling leads to a better performance.

### 2.1.5 Gaussian Channel Estimation Error Scenarios

In Subsections 2.1.2 and 2.1.3, we studied the structure and performance of the ML receivers for a general case when the variance of Gaussian-distributed error is given by $2\sigma_e^2$. This variance is used to express the receiver structure in (2.27) and average BEP expressions in (2.40) and (2.59). In this subsection, we study the structure and performance of ML receivers for two special cases: quasi-static and time-varying fading channels. First, we show that in both cases the estimation error is Gaussian-distributed, and then, we find the variance of error analytically. Subsequently, the structure of the ML receiver for orthogonal signalling as well as the average BEP for antipodal and orthogonal signals will be obtained by substituting the derived variance of error into the expressions (2.27), (2.40) and (2.59), respectively. The summary of the mentioned applications with Gaussian channel estimation error is shown in Fig. 2.1.

#### Quasi-Static Fading Channel

In a quasi-static fading channel, the channel remains constant during a whole frame of symbols but varies independently from frame to frame. In order to estimate this type of channel, predetermined symbols (pilot symbols) are transmitted over the channel. Note that in quasi-static fading channels the channel during transmission of pilot symbols in a frame is the same as the channel during

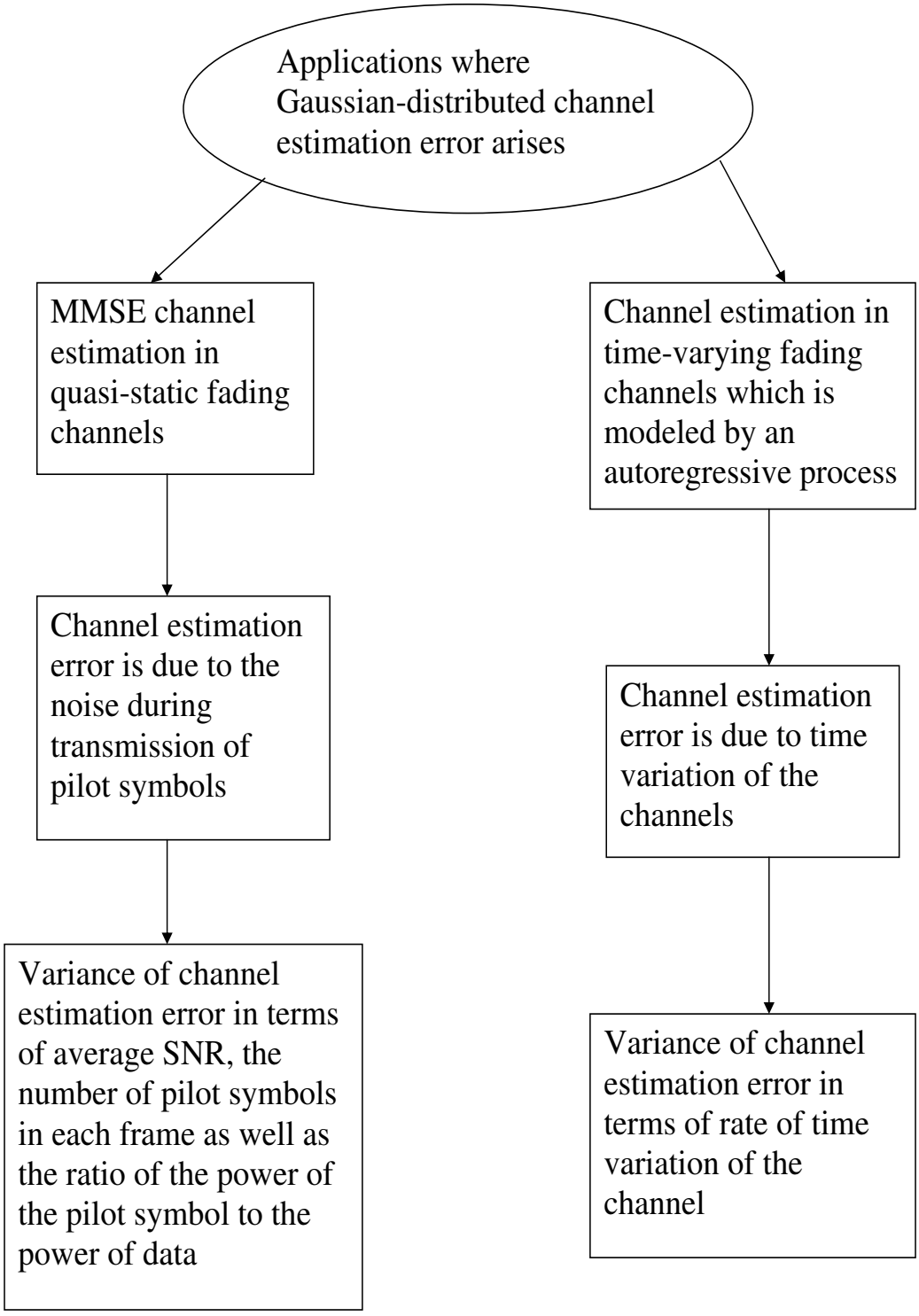


Figure 2.2: Applications with Gaussian channel estimation error

transmission of data symbols in that frame. The received signals during this training period are used to estimate the channel, and the estimate is used in the rest of the frame in which data symbols are transmitted. We use an MMSE channel estimator in this subsection. The number of pilot symbols and data symbols in each frame are denoted by $K$ and $M$, respectively.

We study the performance of the ML receivers in (2.16) and (2.27) when multiple pilot symbols are transmitted during the training period. For antipodal signalling, we assume that the pilot symbols are $\sqrt{\beta}s_1 = \sqrt{\beta E_b}$ where the scalar $\beta$ is the ratio of the power of the pilot symbol to the power of data symbol. The pilot symbols are assumed to be transmitted over $K$ symbol intervals, and hence, the $K \times 1$ observed vector during transmission of $K$ pilot symbols can be expressed as

$$\boldsymbol{x} = \sqrt{\beta E_b} h \mathbf{1}_K + \boldsymbol{\eta} \tag{2.64}$$

where the channel $h$ is fixed during the whole frame, $\mathbf{1}_K$ denotes a $K \times 1$ vector of ones, and the vector $\boldsymbol{\eta}$ is the AWGN during transmission of pilot symbols. The vector $\boldsymbol{\eta}$ is assumed to be independent from channel $h$ and also independent from $n$ in (2.1), the noise during transmission of data symbols. We assume that $\boldsymbol{\eta} \sim CN_K\left(\mathbf{0}, 2\sigma_n^2 \boldsymbol{I}_K\right)$ where $CN_p(\boldsymbol{\theta}, \boldsymbol{\Phi})$ denotes a complex Gaussian distribution for a $p$-dimensional complex random vector with mean $\boldsymbol{\theta}$ and covariance matrix $\boldsymbol{\Phi}$, and $\boldsymbol{I}_K$ is the $K \times K$ identity matrix.

Note that the model (2.64) can also be used for orthogonal signalling when pilot symbols are $\sqrt{\beta}\boldsymbol{s}_1 = \left(\sqrt{\beta E_b}, 0\right)$ and the observed vector $\boldsymbol{x}$ consists of first elements of the received signal vectors.

In the following, we will derive the MMSE channel estimate as a function of the observed vector $\boldsymbol{x}$ in (2.64) and then calculate the variance of the channel estimation error. We will show that the channel estimate $\hat{h}$ and estimation error $e$ satisfy the conditions mentioned for the model in (2.4), i.e. $\hat{h}$ and $e$ are circularly symmetric Gaussian distributed and mutually independent.

The observed vector in (2.64) is of the form of the Bayesian linear model described in chapter

10 of [8]. Therefore, by using theorems 10.3 and 11.1 of [8], the MMSE channel estimate is

$$\hat{h} = E\left(h|\boldsymbol{x}\right) = C_{h\boldsymbol{x}} C_{\boldsymbol{x}\boldsymbol{x}}^{-1} \boldsymbol{x} \tag{2.65}$$

where matrices $C_{h\boldsymbol{x}}$ and $C_{\boldsymbol{x}\boldsymbol{x}}$ are defined as

$$C_{h\boldsymbol{x}} = E\left(h\boldsymbol{x}^H\right); \;\; C_{\boldsymbol{x}\boldsymbol{x}} = E\left(\boldsymbol{x}\boldsymbol{x}^H\right) \tag{2.66}$$

By substituting (2.64) in (2.66), we get

$$C_{h\boldsymbol{x}} = 2\sqrt{\beta E_b}\sigma_h^2 \mathbf{1}_K^H \tag{2.67}$$

and

$$C_{\boldsymbol{x}\boldsymbol{x}} = 2\beta E_b \sigma_h^2 \mathbf{1}_{K\times K} + 2\sigma_n^2 \boldsymbol{I}_K = 2\beta E_b \sigma_h^2 \left(\mathbf{1}_{K\times K} + \frac{1}{\beta\bar{\gamma}_b}\boldsymbol{I}_K\right) \tag{2.68}$$

where $\mathbf{1}_{K\times K}$ denotes a $K \times K$ matrix of ones.

By applying the matrix inversion Lemma [19], the inverse of the matrix $C_{xx}$ in (2.68) can be written as

$$C_{\boldsymbol{x}\boldsymbol{x}}^{-1} = \frac{\bar{\gamma}_b}{2E_b\sigma_h^2}\left(\boldsymbol{I}_K - \frac{\beta\bar{\gamma}_b}{1+K\beta\bar{\gamma}_b}\mathbf{1}_{K\times K}\right) \tag{2.69}$$

Now, by substituting (2.67) and (2.69) in (2.65) we get

$$\hat{h} = \frac{\sqrt{\beta}\bar{\gamma}_b}{\sqrt{E_b}}\mathbf{1}_K^H\left(\boldsymbol{I}_K - \frac{\beta\bar{\gamma}_b}{1+K\beta\bar{\gamma}_b}\mathbf{1}_{K\times K}\right)\boldsymbol{x} = \frac{\sqrt{\beta}\bar{\gamma}_b}{\sqrt{E_b}\left(1+K\beta\bar{\gamma}_b\right)}\mathbf{1}_K^H\boldsymbol{x} \tag{2.70}$$

Expression (2.70) shows how the channel estimate $\hat{h}$ should be computed at the receiver as a function of the observed vector $\boldsymbol{x}$ in (2.64).

To facilitate calculating the variance of channel estimation error and to show that the derived channel estimate and the channel estimation error are independent and Gaussian distributed, we

rewrite the channel estimate $\hat{h}$ as a function of $h$ and $\boldsymbol{\eta}$ by substituting (2.64) in (2.70) to obtain

$$\hat{h} = \frac{\sqrt{\beta}\bar{\gamma}_b}{\sqrt{E_b}\left(1+K\beta\bar{\gamma}_b\right)}\mathbf{1}_K^H\left(\sqrt{\beta E_b}h\mathbf{1}_K+\boldsymbol{\eta}\right) = \frac{K\beta\bar{\gamma}_b}{1+K\beta\bar{\gamma}_b}h + \frac{\sqrt{\beta}\bar{\gamma}_b}{\sqrt{E_b}\left(1+K\beta\bar{\gamma}_b\right)}\mathbf{1}_K^H\boldsymbol{\eta} \quad (2.71)$$

From (2.71), the channel estimation error is equal to

$$e = h - \hat{h} = \frac{1}{1+K\beta\bar{\gamma}_b}h - \frac{\sqrt{\beta}\bar{\gamma}_b}{\sqrt{E_b}\left(1+K\beta\bar{\gamma}_b\right)}\mathbf{1}_K^H\boldsymbol{\eta} \quad (2.72)$$

Equation (2.72) shows that $e$ is caused by $\boldsymbol{\eta}$ (the noise during transmission of pilot symbols), and hence, $e$ is independent of the AWGN during transmission of data signals. Note that $\hat{h}$ and $e$ in (2.71) and (2.72) are circularly symmetric Gaussian distributed since $h$ and the elements of vector $\boldsymbol{\eta}$ are circularly symmetric Gaussian distributed and mutually independent. Also note that $\hat{h}$ and $e$ are jointly circularly symmetric Gaussian distributed since from (2.71) and (2.72) any linear combination of $\hat{h}$ and $e$ is also circularly symmetric Gaussian distributed. Now, it can be seen from (2.71) and (2.72) that $E\left(\hat{h}^*e\right) = 0$, i.e. random variables $\hat{h}$ and $e$ are uncorrelated, and hence independent. Therefore, $\hat{h}$ and $e$ satisfy the conditions mentioned for the model in (2.4).

Now, from (2.72), $\sigma_e^2$ is equal to

$$\sigma_e^2 = \frac{1}{2}E\left(|e|^2\right) = \frac{1}{2}\left(\frac{2\sigma_h^2}{\left(1+K\beta\bar{\gamma}_b\right)^2} + \frac{2K\beta\bar{\gamma}_b^2\sigma_n^2}{E_b\left(1+K\beta\bar{\gamma}_b\right)^2}\right) = \frac{\sigma_h^2}{1+K\beta\bar{\gamma}_b} \quad (2.73)$$

From (2.73), the variance of channel estimation error decreases as $K$ or $\beta$ or $\bar{\gamma}_b$ increases, as expected.

Now, from (2.16), for antipodal signals the ML receiver for $s[m]$, the $m$th data symbol, is

$$\text{Re}\left\{\hat{h}^* r[m]\right\} \underset{\hat{s}[m]=s_2}{\overset{\hat{s}[m]=s_1}{\gtrless}} 0 \quad \text{for } m = 1, \ldots, M \quad (2.74)$$

where $r[m]$ is the received signal when $s[m]$ is transmitted, $\hat{s}[m]$ is the $m$th estimated data symbol and $\hat{h}$ is given by (2.70).

By substituting (2.73) in (2.40), the average BEP of the ML receiver (2.74) during the whole frame of $M$ data symbols can be written as

$$P_b(E) = \frac{1}{2}\left(1 - \frac{\sqrt{K\beta}\bar{\gamma}_b}{\sqrt{1+(K\beta+1)\bar{\gamma}_b + K\beta\bar{\gamma}_b^2}}\right) \tag{2.75}$$

For $K = 0$, the average BEP in (2.75) is 0.5, i.e. the BEP expression in (2.42) for non-coherent reception, as expected. For one-symbol observation ($K = 1$), when $\beta = 1$ the expression (2.75) simplifies to

$$P_b(E) = \frac{1}{2}\left(1 - \frac{\bar{\gamma}_b}{1+\bar{\gamma}_b}\right) = \frac{1}{2\,(1+\bar{\gamma}_b)} \tag{2.76}$$

which is equal to the average BEP of binary DPSK [1, eq. (14.3-10)]. In other words, with only one pilot symbol the BEP of DPSK can be achieved. Therefore, for $K > 1$ a better performance than DPSK modulation is expected, which shows how efficient the MMSE estimator is. Note that as $K \to \infty$, the expression (2.75) reduces to the expression in (2.41), the average BEP of purely coherent reception for antipodal signalling.

For binary orthogonal signals, by substituting (2.73) in (2.27), the ML receiver for the $m$th data symbol, $\boldsymbol{s}[m]$, has the following structure for $m = 1, \ldots, M$

$$\frac{\bar{\gamma}_b}{2\sqrt{E_b}\,(1+K\beta\bar{\gamma}_b)}\,|r_1[m]|^2 + \text{Re}\left\{\hat{h}^* r_1[m]\right\} \underset{\hat{\boldsymbol{s}}[m]=\boldsymbol{s}_2}{\overset{\hat{\boldsymbol{s}}[m]=\boldsymbol{s}_1}{\gtrless}} \frac{\bar{\gamma}_b}{2\sqrt{E_b}\,(1+K\beta\bar{\gamma}_b)}\,|r_2|^2\,[m] + \text{Re}\left\{\hat{h}^* r_2[m]\right\} \tag{2.77}$$

where $r_1[m]$ and $r_2[m]$ are the first and second elements of the received vector, respectively, when $\boldsymbol{s}[m]$ is transmitted, $\hat{\boldsymbol{s}}[m]$ is the estimate of $\boldsymbol{s}[m]$, and $\hat{h}$ is given by (2.70).

By substituting (2.73) in (2.59), the average BEP of the ML receiver in (2.77) over the whole frame of $M$ data symbols can be written as

$$P_b(E) = \frac{1}{2}\left(1 - \frac{\sqrt{2K\beta+1}\bar{\gamma}_b}{\sqrt{4+4(K\beta+1)\bar{\gamma}_b + (2K\beta+1)\,\bar{\gamma}_b^2}}\right) \tag{2.78}$$

For $K = 0$, expression (2.78) reduces to (2.61), the average BEP for non-coherent reception. On the other hand, as $K \to \infty$, (2.78) converges to the expression (2.60), the average BEP for purely coherent reception, as expected.

To compare antipodal modulation with orthogonal modulation, by substituting (2.73) in (2.63) we find that orthogonal signalling has a better performance than antipodal if

$$\frac{\sigma_h^2}{1 + K\beta\bar{\gamma}_b} > \frac{\sigma_h^2}{1 + 0.5\bar{\gamma}_b} \tag{2.79}$$

which can be simplified to

$$K\beta < 0.5 \tag{2.80}$$

Note that the condition in (2.80) is unlikely to be met in practice since $K \geq 1$, and usually $\beta$ is at least equal to one in practical applications.

The result in (2.80) can also be obtained by comparing (2.75) and (2.78).

**Time-Varying Fading Channels**

Now, consider time-varying fading channels where the channel does not remain constant over a whole frame. It is assumed that each frame consists of a training sequence and $M$ data symbols and the channel estimate at the end of each training period is perfect. The results of this subsection can be easily generalized to the case when the channel estimate at the end of a training sequence is subject to Gaussian error. The channel estimate obtained in the training period prior to data transmission is then used to obtain estimates of channels during transmission of data symbols. As we will see, channel estimation error here is caused by time variations of the channel, in contrast to quasi-static fading channels.

A well-known model to represent a time-varying process is the autoregressive (AR) model [19]. In an AR model of order $P$, the current realization of the channel can be obtained from $P$ previous channel realizations and a sample of a white random process. AR models have been used in the literature to simulate time-varying fading channels [20]-[23]. In this subsection, we model

time variation of the fading channel with autoregressive process of order one for simplicity. The results of this subsection can be extended to higher orders of the AR model as well.

In [20]-[21], an AR model of order one has also been used to model the time-varying channel. In those papers, it is shown that for orthogonal signals the ML receiver is a linear combination of the matched filter and square-law detector, but only an upper bound for the average BEP of this receiver is derived. In this subsection, we verify the optimality of the mentioned receiver, and in addition obtain an exact closed-form expression for its average BEP by using the results for the general case of Gaussian channel estimation error.

In discrete time, the channel coefficient at the end of the training sequence is denoted by $h[0]$, and channels for data symbols in the next $M$ intervals are denoted by $h[m]$ for $m = 1, \ldots, M$ where $M$ is again the number of data symbols in a frame. In Rayleigh fading channels, $h[m] \sim CN(0, 2\sigma_h^2)$ for $m = 0, \ldots, M$. By modeling the time-varying fading channel with an AR process of order one, we get

$$h[m] = \alpha h[m-1] + w[m] \quad \text{for } m = 1, \ldots, M \tag{2.81}$$

where $w[m]$ is a white Gaussian random process with $w[m] \sim CN\left(0, 2\sigma_h^2\left(1-\alpha^2\right)\right)$, and $w[m]$ is independent of $h[0]$. The real scalar parameter $\alpha$ determines the channel variation rate and $0 \leq \alpha \leq 1$. As $\alpha$ decreases channel variation rate increases, i.e. when $\alpha = 0$, the random process $h[m]$ is white, while $\alpha = 1$ corresponds to quasi-static channels. The value of $\alpha$, in practice, is very close to one and can be determined by the Doppler spread and transmission bandwidth [24]. We assume that $\alpha$ is known at the receiver. The model in (2.81) is also known as the first-order Gauss-Markov model in the literature [24].

From (2.81), $h[m]$ can be written in terms of $h[0]$ as

$$h[m] = \alpha^m h[0] + w'[m] \quad \text{for } m = 1, \ldots, M \tag{2.82}$$

where

$$w'[m] = w[m] + \alpha w[m-1] + \alpha^2 w[m-2] + \ldots + \alpha^{m-1} w[1] \quad \text{for } m = 1, \ldots, M \tag{2.83}$$

Since $w[m]$ is a white random process with $w[m] \sim CN\left(0, 2\sigma_h^2\left(1-\alpha^2\right)\right)$, $w'[m]$ in (2.83) is distributed as $w'[m] \sim CN\left(0, 2\sigma_h^2\left(1-\alpha^{2m}\right)\right)$. Note that since random process $w[m]$ in (2.81) is assumed to be independent of $h[0]$, random process $w'[m]$ in (2.83) is also independent of $h[0]$

The channel $h[0]$, i.e the channel at the end of the training period prior to data transmission, is assumed to be estimated perfectly at the receiver. Now, from (2.82), based on the MMSE criterion $\hat{h}[m]$, the estimate of $h[m]$, can be written as

$$\hat{h}[m] = E\left(h[m]|h[0]\right) = \alpha^m h[0] \quad \text{for } m = 1, \ldots, M \tag{2.84}$$

in which we have used the assumption that $w'[m]$ in (2.82) is independent of $h[0]$. Equation (2.84) shows how the receiver should estimate the channel for the $m$th data symbol based on $h[0]$.

Now, from (2.84) and (2.82), the channel estimation error is equal to

$$e[m] = h[m] - \hat{h}[m] = w'[m] \quad \text{for } m = 1, \ldots, M \tag{2.85}$$

From (2.84) and (2.85), $\hat{h}[m]$ and $e[m]$ are circularly symmetric Gaussian distributed and mutually independent, and hence, the conditions mentioned for the model in (2.4) are satisfied. Now, from (2.85) we get

$$\sigma_e^2[m] = \frac{1}{2}E\left(|e[m]|^2\right) = \sigma_h^2\left(1-\alpha^{2m}\right) \quad \text{for } m = 1, \ldots, M \tag{2.86}$$

Equation (2.86) indicates that the estimation error is caused by time variations of the channel as reflected in $\alpha$, and hence, $e$ is independent from the noise during transmission of data symbols. As channel variation vanishes ($\alpha \rightarrow 1$), the estimation error converges to zero. Note that as time

index $m$ increases, the variance of channel estimation error increases. This is expected since the correlation between $h[m]$ and $h[0]$ decreases as $m$ increases.

For antipodal signalling, from (2.16), the ML receiver for the $m$th data symbol, $s[m]$, is

$$\text{Re}\left\{\hat{h}^*[m]r[m]\right\} \underset{\hat{s}[m]=s_2}{\overset{\hat{s}[m]=s_1}{\gtrless}} 0 \quad \text{for } m = 1, \ldots, M \tag{2.87}$$

where $r[m]$ is the received signal when $s[m]$ is transmitted, $\hat{s}[m]$ is the estimate of $s[m]$, and $\hat{h}[m]$ is given by (2.84). By substituting (2.86) in (2.40), the average BEP of the ML receiver in (2.87) for the $m$th data symbol is equal to

$$P_b[m] = \frac{1}{2}\left(1 - \alpha^m \sqrt{\frac{\bar{\gamma}_b}{1+\bar{\gamma}_b}}\right) \quad \text{for } m = 1, \ldots, M \tag{2.88}$$

Now, from (2.88), the average BEP during the whole frame of data for antipodal signals is

$$P_b(E) = \frac{1}{M}\sum_{m=1}^{M} P_b[m] = \frac{1}{2}\left(1 - \frac{\alpha - \alpha^{M+1}}{M\,(1-\alpha)}\sqrt{\frac{\bar{\gamma}_b}{1+\bar{\gamma}_b}}\right) \tag{2.89}$$

which is equal to the result in [20, eq. 10]. Note that as $\bar{\gamma}_b \to \infty$, the expression (2.89) converges to the following error floor

$$\lim_{\bar{\gamma}_b \to \infty} P_b(E) = \frac{1}{2}\left(1 - \frac{\alpha - \alpha^{M+1}}{M\,(1-\alpha)}\right) \tag{2.90}$$

For orthogonal signals, by substituting (2.86) in (2.27), the structure of the ML receiver for the $m$th data symbol, $\boldsymbol{s}[m]$, for $m = 1, \ldots, M$ can be written as

$$\frac{\bar{\gamma}_b\,(1-\alpha^{2m})}{2\sqrt{E_b}}\,|r_1[m]|^2 + \text{Re}\left\{\hat{h}^*[m]r_1[m]\right\} \underset{\hat{\boldsymbol{s}}[m]=\boldsymbol{s}_2}{\overset{\hat{\boldsymbol{s}}[m]=\boldsymbol{s}_1}{\gtrless}} \frac{\bar{\gamma}_b\,(1-\alpha^{2n})}{2\sqrt{E_b}}\,|r_2[m]|^2 + \text{Re}\left\{\hat{h}^*[m]r_2[m]\right\} \tag{2.91}$$

where $r_1[m]$ and $r_2[m]$ are the first and second elements of the received vector, respectively, when $\boldsymbol{s}[m]$ is transmitted, $\hat{\boldsymbol{s}}[m]$ is the estimate of $\boldsymbol{s}[m]$, and $\hat{h}[m]$ is given by (2.84). Equation (2.91) is

identical to the receiver in [20, eq. 15].

In [20]-[21], only an upper bound for the average BEP of the receiver (2.91) was obtained. The derivation of the bound is based on that the receiver (2.91) performs better than the best of coherent and non-coherent receives for any $\alpha$ and $m$. As the quality of the channel estimate degrades with $m$, non-coherent receiver will outperform coherent receiver after $m$ reaches a threshold, $M_t$. For $m$ less than $M_t$, the BEP of coherent receiver is used while for $m$ greater than $M_t$ BEP of non-coherent receiver is used. Then those BEPs are averaged over $m$.

However, in this subsection, we derive the exact average BEP of (2.91). By substituting (2.86) in (2.59), the exact average BEP of the receiver (2.91) for the $m$th data symbol can be written as

$$P_b[m] = \frac{1}{2}\left(1-\sqrt{\frac{\bar{\gamma}_b\left(\bar{\gamma}_b\left(1-\alpha^{2m}\right)+2\alpha^{2m}\right)}{\left(\bar{\gamma}_b+2\right)\left(\bar{\gamma}_b\left(1-\alpha^{2m}\right)+2\right)}}\right) \quad \text{for } m=1,\ldots,M \tag{2.92}$$

Now, from (2.92), the average BEP of orthogonal signals over a whole frame of data is equal to

$$P_b(E)=\frac{1}{M}\sum_{m=1}^{M}P_b[m]=\frac{1}{2}\left(1-\frac{1}{M}\sqrt{\frac{\bar{\gamma}_b}{\bar{\gamma}_b+2}}\sum_{m=1}^{M}\sqrt{\frac{\bar{\gamma}_b\left(1-\alpha^{2m}\right)+2\alpha^{2m}}{\bar{\gamma}_b\left(1-\alpha^{2m}\right)+2}}\right) \tag{2.93}$$

Note that in contrast to the average BEP of antipodal signals in (2.89), there is no error floor for the average BEP of orthogonal signals in (2.93). Therefore, it is expected that for a large enough $\bar{\gamma}_b$, orthogonal modulation outperforms antipodal signalling in terms of the average BEP. This statement can also be verified by the following explanation.

By substituting (2.86) in (2.63), for the $m$th data symbol orthogonal modulation outperforms antipodal signalling if

$$1-\alpha^{2m}>\frac{1}{1+0.5\bar{\gamma}_b}, \tag{2.94}$$

which can be written as

$$\bar{\gamma}_b>\frac{2\alpha^{2m}}{1-\alpha^{2m}} \tag{2.95}$$

From (2.95), for the $m$th data symbol orthogonal signalling performs better than antipodal modulation if the average SNR is greater than a threshold. Therefore, we expect that for orthogonal modulation the average BEP over time would be smaller than antipodal signalling if $\bar{\gamma}_b$ is larger than a threshold. The numerical results in the next subsection also confirm this remark.

### 2.1.6 Numerical Results

In this subsection, we study the performance of the ML receivers presented in the previous subsections for flat Rayleigh fading channels.

First, the ML receivers are examined in quasi-static fading channels when an MMSE channel estimator is applied at the receiver with pilot symbols, as explained in Subsection 2.1.5. Figs. 2.3 and 2.4 show the average BEP of the receivers in (2.16) and (2.77) versus the average SNR $\bar{\gamma}_b$ for binary antipodal and orthogonal signals, respectively, by both theory (expressions (2.75) and (2.78)) and simulation. The curves are plotted for different numbers of pilot symbols $K$ when $\beta$, the ratio of the power of the pilot symbol to the power of data symbol, is equal to one. The Monte Carlo simulations are performed until $10^4$ samples of errors are observed for each data point. It is evident that the analytical results match precisely the Monte Carlo simulations. The average BEP of coherent receiver for antipodal signals in (2.41) as well as the average BEP of non-coherent and coherent receivers for orthogonal signals in (2.60) and (2.61) have also been added for comparison in Figs. 2.3 and 2.4, respectively. It is clear that the performance of the receivers improve as the number of pilot symbols $K$ increases, as expected.

The average BEP of antipodal and orthogonal modulations in quasi-static fading channels are compared in Fig. 2.5 for different values of $K\beta$. As can be seen, for $K\beta < 0.5$ orthogonal signalling has a better performance while for $K\beta > 0.5$ antipodal modulation outperforms orthogonal signalling. For $K\beta = 0.5$, both modulations have a same average BEP. These results are expected from (2.80).

Now, we present numerical results for the performance of the receivers (2.16) and (2.91) in time-varying fading channels modeled by (2.81). The average BEP of ML receivers for antipodal

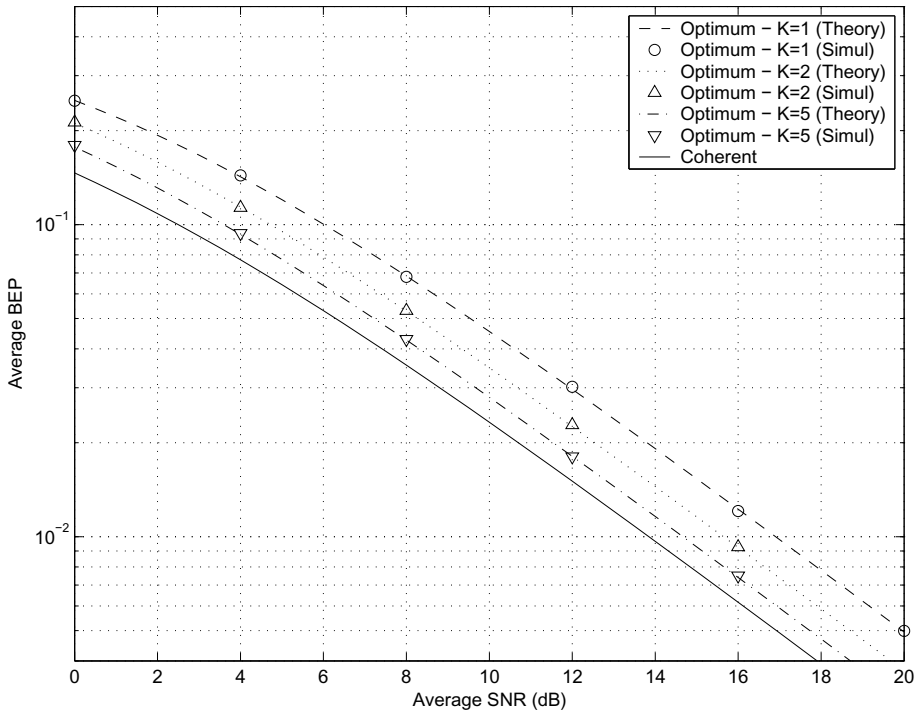


Figure 2.3: Average BEP versus the average SNR for binary antipodal signals in quasi-static fading channels for different numbers of $K$ when $\beta = 1$.

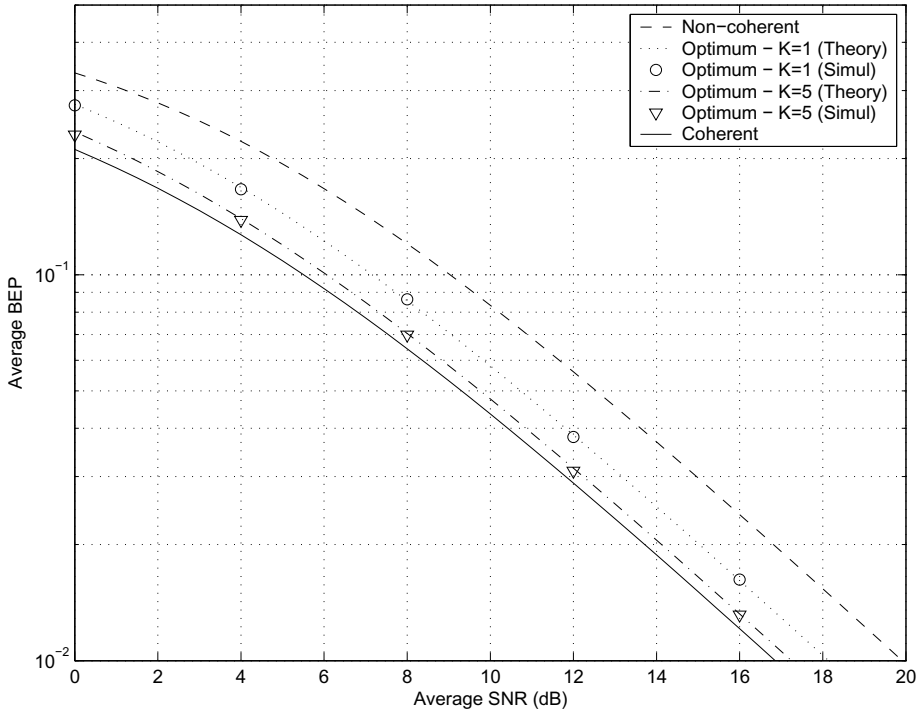


Figure 2.4: Average BEP versus the average SNR for binary orthogonal signals in quasi-static fading channels for different numbers of $K$ when $\beta = 1$.

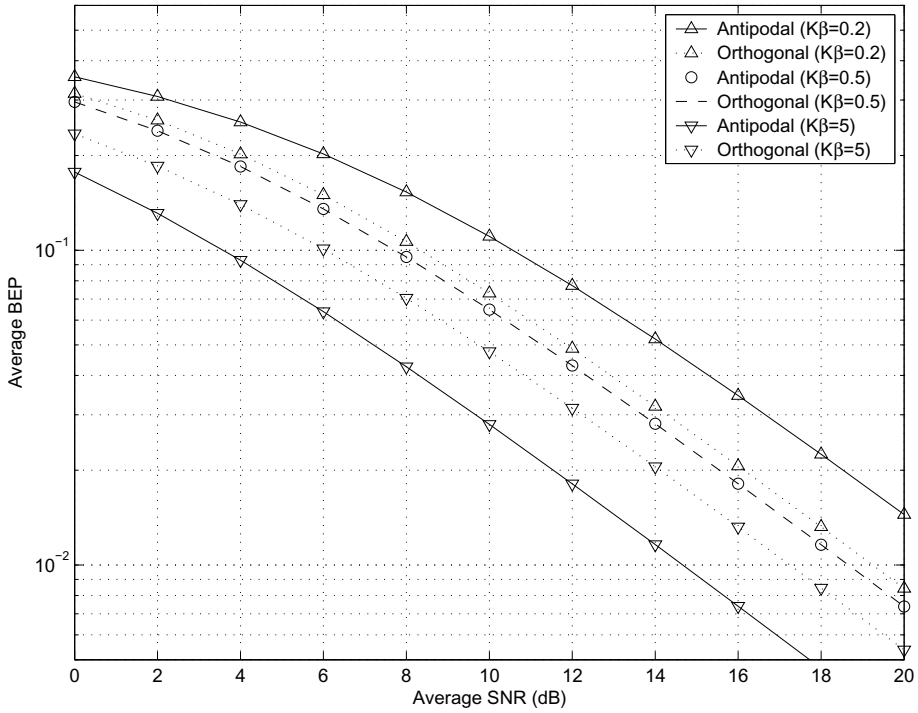


Figure 2.5: Comparison of the average BEP of antipodal signals with orthogonal signals in quasi-static fading channels for different values of $K\beta$.

and orthogonal signals are plotted versus $\bar{\gamma}_b$ in Figs. 2.6 and 2.7, respectively, by both analytical expressions in (2.89) and (2.93) and simulation results. The results are shown for different values of $\alpha$ when the number of data symbols in a frame is $M = 50$. The Monte Carlo simulations are performed until $10^5$ samples of errors are observed for each data point. As can be seen, analytical results coincide exactly with Monte Carlo simulations. We observe that the performance of the receivers improve as the channel variation rate decreases, i.e. $\alpha$ increases. It is evident from Fig. 2.6 the ML receiver for antipodal modulation results in an error floor as $\bar{\gamma}_b \to \infty$. The error floor from Fig 2.6 for $\alpha = 0.997$ is $3.64 \times 10^{-2}$, for $\alpha = 0.999$ is $1.25 \times 10^{-2}$, and for $\alpha = 0.9999$ is $1.27 \times 10^{-3}$. These results can also be obtained by equation (2.90). We see that the error floor is very sensitive to $\alpha$. Our analysis highlights the importance of applying the appropriate value of $\alpha$ when predicting the performance of a communication system in a fading channel, as even small model mismatches can lead to substantial differences in results.

The performance of the ML receivers in time-varying fading channels is compared in Fig.

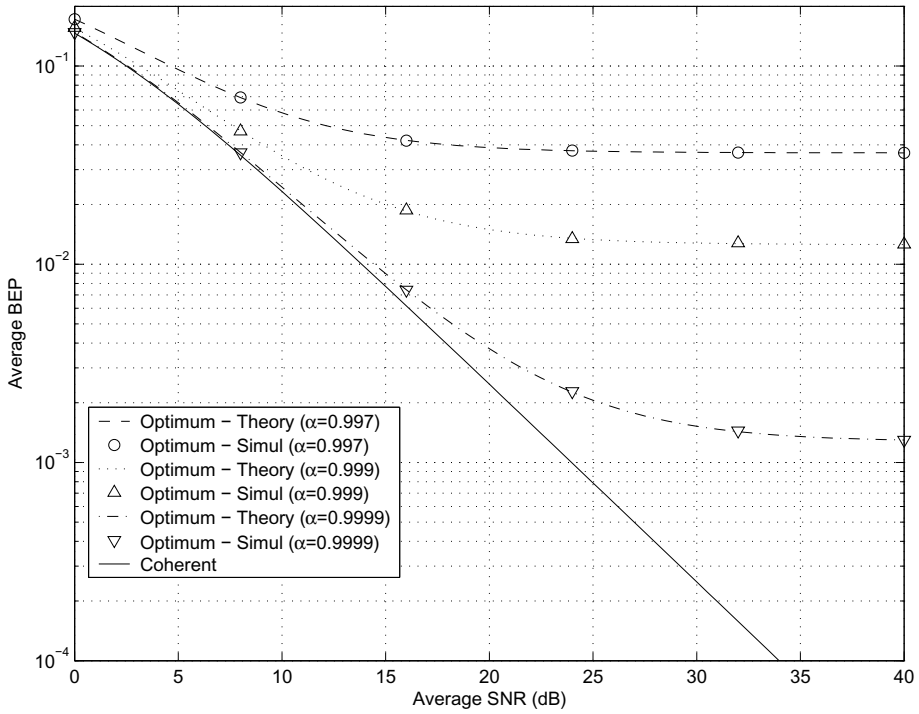


Figure 2.6: Average BEP versus the average SNR for binary antipodal signals in time-varying fading channels for different values of $\alpha$ when $M = 50$.

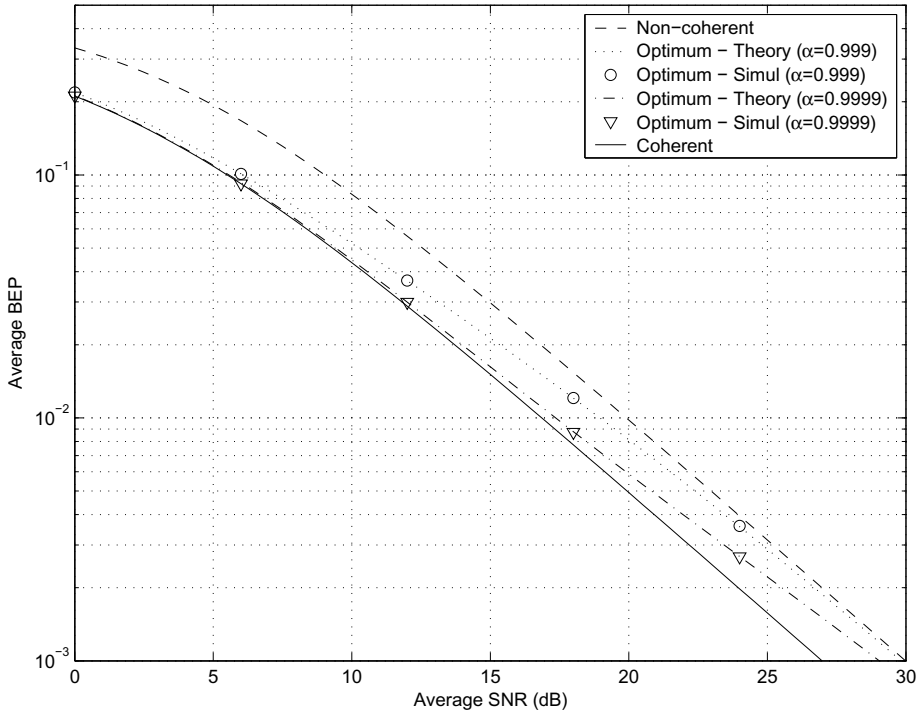


Figure 2.7: Average BEP versus the average SNR for binary orthogonal signals in time-varying fading channels for different values of $\alpha$ when $M = 50$.

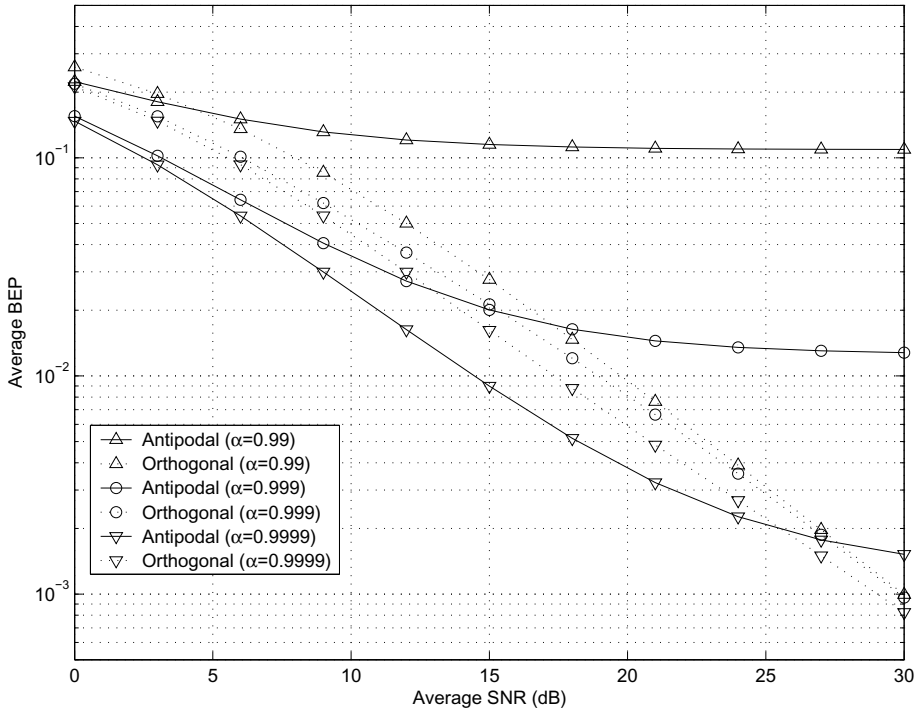


Figure 2.8: Comparison of the average BEP of antipodal signals with orthogonal signals in time-varying fading channels for different values of $\alpha$ when $M = 50$.

2.8 for different values for $\alpha$ when $M = 50$. It is evident that the ML receiver for orthogonal signalling outperforms the antipodal one for $\alpha = 0.9999$ when $\bar{\gamma}_b > 25.65$ dB, for $\alpha = 0.999$ when $\bar{\gamma}_b > 15.55$ dB, and for $\alpha = 0.99$ when $\bar{\gamma}_b > 4.62$ dB. Therefore, as channel variation rate increases, i.e. $\alpha$ decreases, there is a larger range of $\bar{\gamma}_b$ where orthogonal signaling results in a lower average BEP compared with antipodal modulation. This observation can also be justified by equation (2.95) derived in the last subsection.

## 2.2 Maximum-likelihood Detection of QPSK Signals

Up to this point in this chapter, we have only considered binary modulation formats. In this section, we extend the analysis to include QPSK signals. We derive the structure of ML receiver for QPSK signals in the presence of Gaussian channel estimation error and AWGN for single-antenna reception. We derive an exact closed-form theoretical expression for the average BEP of this receiver in Rayleigh fading channels. Then, the performance of the receiver is analyzed for a special case

where Gaussian-distributed channel estimation error arises, which is an MMSE channel estimator with pilot symbols, as in Subsection 2.1.5.

The system model of this section is similar to Section 2.1. For QPSK signalling, the transmitted baseband symbol $s$ is chosen from the set of $\{s_1, s_2, s_3, s_4\}$ where $s_1 = \sqrt{E_b} + j\sqrt{E_b}$, $s_2 = -\sqrt{E_b} + j\sqrt{E_b}$, $s_3 = -\sqrt{E_b} - j\sqrt{E_b}$, $s_4 = \sqrt{E_b} - j\sqrt{E_b}$, and $E_b$ is the energy per bit again.

### 2.2.1 Maximum-likelihood Receiver Structure

From (2.4), the received signal $r$ in (2.1) can be expressed as

$$r = \begin{cases} \sqrt{E_b}\hat{h}(1+j) + n^{(1)} & \text{if } s = s_1 \\ \sqrt{E_b}\hat{h}(-1+j) + n^{(2)} & \text{if } s = s_2 \\ \sqrt{E_b}\hat{h}(-1-j) + n^{(3)} & \text{if } s = s_3 \\ \sqrt{E_b}\hat{h}(1-j) + n^{(4)} & \text{if } s = s_4 \end{cases} \tag{2.96}$$

where

$$n^{(i)} = \begin{cases} \sqrt{E_b}e(1+j) + n & \text{if } i = 1 \\ \sqrt{E_b}e(-1+j) + n & \text{if } i = 2 \\ \sqrt{E_b}e(-1-j) + n & \text{if } i = 3 \\ \sqrt{E_b}e(1-j) + n & \text{if } i = 4 \end{cases} \tag{2.97}$$

Since $e$ and $n$ are circularly symmetric Gaussian distributed and mutually independent, $n^{(i)}$'s in (2.97) are also circularly symmetric Gaussian distributed, and we get

$$n^{(i)} \sim CN\left(0, 2\left(2E_b\sigma_e^2 + \sigma_n^2\right)\right) \quad \text{for } i = 1, 2, 3, 4 \tag{2.98}$$

Based on the ML criterion, $\hat{s}$, the estimate of the transmitted symbol $s$, is

$$\hat{s} = s_i \text{ if } i = \arg\left\{\max_i \; p_r\left(r|\hat{h}, s_i\right)\right\} \tag{2.99}$$

where $p_r\left(r|\hat{h}, s_i\right)$ is the conditional probability of the received signal $r$ given $\hat{h}$ when $s_i$ is transmitted. These conditional probabilities from (2.96) and (2.98) are

$$p_r\left(r|\hat{h}, s_i\right) = \begin{cases} A\exp\left(-\frac{\left|r-\sqrt{E_b}\hat{h}(1+j)\right|^2}{2(2E_b\sigma_e^2+\sigma_n^2)}\right) & \text{if } i=1 \\ A\exp\left(-\frac{\left|r-\sqrt{E_b}\hat{h}(-1+j)\right|^2}{2(2E_b\sigma_e^2+\sigma_n^2)}\right) & \text{if } i=2 \\ A\exp\left(-\frac{\left|r-\sqrt{E_b}\hat{h}(-1-j)\right|^2}{2(2E_b\sigma_e^2+\sigma_n^2)}\right) & \text{if } i=3 \\ A\exp\left(-\frac{\left|r-\sqrt{E_b}\hat{h}(1-j)\right|^2}{2(2E_b\sigma_e^2+\sigma_n^2)}\right) & \text{if } i=4 \end{cases} \tag{2.100}$$

where $A$ is a constant equal to $A = \left(2\pi\left(2E_b\sigma_e^2 + \sigma_n^2\right)\right)^{-1}$.

Now, from (2.99) and (2.100), the receiver estimates the transmitted symbol as

$$\hat{s} = \begin{cases} s_1 & \text{if Re}\left\{\hat{h}^* r\right\} > 0 \text{ and Im}\left\{\hat{h}^* r\right\} > 0 \\ s_2 & \text{if Re}\left\{\hat{h}^* r\right\} < 0 \text{ and Im}\left\{\hat{h}^* r\right\} > 0 \\ s_3 & \text{if Re}\left\{\hat{h}^* r\right\} < 0 \text{ and Im}\left\{\hat{h}^* r\right\} < 0 \\ s_4 & \text{if Re}\left\{\hat{h}^* r\right\} > 0 \text{ and Im}\left\{\hat{h}^* r\right\} < 0 \end{cases} \tag{2.101}$$

where Re$\{.\}$ and Im$\{.\}$ denote the real part and the imaginary part of a complex number, respectively.

Therefore, the ML receiver for QPSK modulation in (2.101) like the receiver for BPSK signals in (2.16) is a matched filter that is matched to the channel estimate. However, the receiver (2.16) needs only to calculate Re$\left\{\hat{h}^* r\right\}$ while the receiver (2.101) should compute both Re$\left\{\hat{h}^* r\right\}$ and Im$\left\{\hat{h}^* r\right\}$.

### 2.2.2 Average Bit Error Probability Performance

In this subsection, we analyze the performance of the receiver (2.101) in Rayleigh fading channels for equiprobable transmitted signals. We derive the exact closed-form expression of the average

BEP of the receiver (2.101). The derived average BEP expression in this subsection is general and is a function of $\sigma_e^2$ and $\bar{\gamma}_b$. In Subsection 2.2.3, we will study an MMSE estimator with pilot signals as a special case.

We consider QPSK signals when Gray code bit mapping [1], [6] is applied. In this mapping, nearest neighboring symbols correspond to bit groups that differ by only one bit. Therefore, for QPSK signals if we denote two consecutive bits by $a_1$ and $a_2$, the transmitter maps these two bits to the following symbols which be will be transmitted over the channel

$$s = \begin{cases} s_1 & \text{if } a_1 = 0 \text{ and } a_2 = 0 \\ s_2 & \text{if } a_1 = 0 \text{ and } a_2 = 1 \\ s_3 & \text{if } a_1 = 1 \text{ and } a_2 = 1 \\ s_4 & \text{if } a_1 = 1 \text{ and } a_2 = 0 \end{cases} \tag{2.102}$$

For QPSK signals the BEP when transmitted symbols are equiprobable is equal to the BEP when $s_1$ is transmitted. Note that when $s = s_1$, from (2.102) if $\hat{s} = s_2$ or $\hat{s} = s_4$ the bit estimates are incorrect with a probability of $\frac{1}{2}$, while if $\hat{s} = s_3$, the bit error probability is 1. Therefore, the BEP conditioned on $\hat{h}$ can be written as

$$\begin{aligned} P_b\left(E|\hat{h}\right) &= P_b\left(E|\hat{h}, s = s_1\right) \\ &= \frac{1}{2}P\left(\hat{s} = s_2|\hat{h}, s = s_1\right) + P\left(\hat{s} = s_3|\hat{h}, s = s_1\right) + \frac{1}{2}P\left(\hat{s} = s_4|\hat{h}, s = s_1\right) \end{aligned} \tag{2.103}$$

From (2.96), the output of the matched filter when $s_1$ is transmitted is equal to

$$\hat{h}^* r = \sqrt{E_b}\left|\hat{h}\right|^2 (1+j) + \hat{h}^* n^{(1)} = \sqrt{E_b}\left|\hat{h}\right|^2 (1+j) + z \tag{2.104}$$

where $z$ is defined as

$$z = \hat{h}^* n^{(1)} \tag{2.105}$$

and from (2.98) is distributed as

$$z \sim CN\left(0, 2\left|\hat{h}\right|^2\left(2E_b\sigma_e^2+\sigma_n^2\right)\right) \tag{2.106}$$

Now, from (2.104) and (2.106), we get

$$\text{Re}\left\{\hat{h}^* r\right\} \sim N\left(\sqrt{E_b}\left|\hat{h}\right|^2, \left|\hat{h}\right|^2\left(2E_b\sigma_e^2+\sigma_n^2\right)\right) \tag{2.107}$$

and

$$\text{Im}\left\{\hat{h}^* r\right\} \sim N\left(\sqrt{E_b}\left|\hat{h}\right|^2, \left|\hat{h}\right|^2\left(2E_b\sigma_e^2+\sigma_n^2\right)\right) \tag{2.108}$$

where $N(m, \sigma^2)$ denotes a normal distribution for a real random variable with mean $m$ and variance $\sigma^2$. Note that the random variables Re $\left\{\hat{h}^* r\right\}$ and Im $\left\{\hat{h}^* r\right\}$ in (2.107) and (2.108) are independent since $z$ in (2.104) is circularly symmetric Gaussian distributed.

Now, from (2.101), (2.107) and (2.108) we get

$$P\left(\hat{s}=s_2|\hat{h}, s=s_1\right) = P\left(\hat{s}=s_4|\hat{h}, s=s_1\right) = Q\left(\sqrt{2\gamma_\epsilon}\right)\left(1-Q\left(\sqrt{2\gamma_\epsilon}\right)\right) \tag{2.109}$$

and

$$P\left(\hat{s}=s_3|\hat{h}, s=s_1\right) = Q^2\left(\sqrt{2\gamma_\epsilon}\right) \tag{2.110}$$

where $Q(x)$ is defined in (2.36) and $\gamma_\varepsilon$ is defined as

$$\gamma_\epsilon = \frac{E_b\left|\hat{h}\right|^2}{2\left(2E_b\sigma_e^2+\sigma_n^2\right)} \tag{2.111}$$

By substituting (2.109) and (2.110) in (2.103), the conditional BEP can be expressed as

$$P_b(E|\hat{h}) = Q\left(\sqrt{2\gamma_\epsilon}\right) \tag{2.112}$$

To derive the average BEP, the conditional BEP in (2.112) should be averaged over the PDF of $\gamma_\epsilon$. Since $\hat{h}$ is circularly symmetric Gaussian distributed, $\gamma_\epsilon$ in (2.111) has an exponential distribution [93, p. 190] with the following PDF

$$f_{\gamma_\epsilon}(\gamma_\epsilon) = \frac{1}{\bar{\gamma}_\epsilon}\exp\left(-\frac{\gamma_\epsilon}{\bar{\gamma}_\epsilon}\right), \quad \gamma_\epsilon \geq 0 \tag{2.113}$$

where

$$\bar{\gamma}_\epsilon = E(\gamma_\epsilon) = \frac{2E_b\sigma_{\hat{h}}^2}{2\left(2E_b\sigma_e^2 + \sigma_n^2\right)} = \frac{\bar{\gamma}_b\sigma_{\hat{h}}^2}{2\bar{\gamma}_b\sigma_e^2 + \sigma_h^2} = \frac{\bar{\gamma}_b\left(\sigma_h^2 - \sigma_e^2\right)}{2\bar{\gamma}_b\sigma_e^2 + \sigma_h^2} \tag{2.114}$$

Now, by integrating (2.112) over the PDF in (2.113), the average BEP can be written as

$$P_b(E) = \int_0^\infty P_b(E|\gamma_\varepsilon) f_{\gamma_\varepsilon}(\gamma_\varepsilon) d\gamma_\varepsilon = \int_0^\infty \frac{1}{\bar{\gamma}_\varepsilon}\exp\left(-\frac{\gamma_\varepsilon}{\bar{\gamma}_\varepsilon}\right) Q\left(\sqrt{2\gamma_\varepsilon}\right) d\gamma_\varepsilon \tag{2.115}$$

By using [6, eq. (5.6)], the integral term in (2.115) can be computed as

$$P_b(E) = \frac{1}{2}\left(1 - \sqrt{\frac{\bar{\gamma}_\varepsilon}{1+\bar{\gamma}_\varepsilon}}\right) = \frac{1}{2}\left(1 - \sqrt{\frac{\left(\sigma_h^2 - \sigma_e^2\right)\bar{\gamma}_b}{\sigma_h^2 + \left(\sigma_h^2 + \sigma_e^2\right)\bar{\gamma}_b}}\right) \tag{2.116}$$

Note that from (2.40) and (2.116) for a given $\sigma_e^2$, BPSK results in a lower average BEP compared with QPSK when $\sigma_e^2 \neq 0$ and $\sigma_e^2 \neq 1$. However, we will see in the next subsection that for QPSK signals an MMSE channel estimator results in a smaller $\sigma_e^2$ compared with BPSK provided that both modulations use the same number of pilot symbols as well as the same ratio of power of pilot symbol to the power of data symbol. This result leads to almost the same average BEP by both modulations when $\bar{\gamma}_b \gg 1$.

For ideal coherent reception ($\sigma_e^2 = 0$), expression (2.116) reduces to

$$P_b(E) = \frac{1}{2}\left(1 - \sqrt{\frac{\bar{\gamma}_b}{1+\bar{\gamma}_b}}\right) \tag{2.117}$$

which is a well-known result [1, eq. (14.4-41)] and is identical to the average BEP of ideal coherent BPSK in (2.41).

In noncoherent reception ($\sigma_e^2 = \sigma_h^2$), the average BEP expression in (2.40) simplifies to

$$P_b(E) = \frac{1}{2} \tag{2.118}$$

as expected.

### 2.2.3 MMSE Channel Estimator

In this subsection, we study the performance of the receiver in (2.101) for the special case of quasi-static flat Rayleigh fading channels when an MMSE channel estimator is employed at the receiver with pilot symbols. As mentioned before, in a quasi-static fading channel, the channel remains constant during a whole frame of symbols but varies independently from frame to frame. By using an MMSE estimator, the received signals during the training period are used to estimate the channel, and then, this estimate is used in the rest of the frame.

For QPSK signalling, we assume that the pilot symbols are $\sqrt{\beta}s_1 = \sqrt{\beta E_b} + j\sqrt{\beta E_b}$ where the scalar $\beta$ is again the ratio of the power of the pilot symbol to the power of data symbol. Pilot symbols are transmitted over $K$ symbol intervals, and hence, the observed vector during transmission of pilot symbols can be expressed as

$$\boldsymbol{x} = \sqrt{\beta E_b}(1+j)h\mathbf{1}_K + \boldsymbol{\eta} \tag{2.119}$$

where the vector $\boldsymbol{\eta}$ is distributed as $\boldsymbol{\eta} \sim CN_K(\mathbf{0}, 2\sigma_n^2 \boldsymbol{I}_K)$ and is independent of noise $n$ and channel $h$.

Similar to (2.65) in Section 2.1, the MMSE channel estimate is

$$\hat{h} = E\left(h|\boldsymbol{x}\right) = C_{h\boldsymbol{x}} C_{\boldsymbol{xx}}^{-1} \boldsymbol{x} \tag{2.120}$$

where matrices $C_{h\boldsymbol{x}}$ and $C_{\boldsymbol{xx}}$ are defined as

$$C_{h\boldsymbol{x}} = E\left(h\boldsymbol{x}^H\right);\ \ C_{\boldsymbol{xx}} = E\left(\boldsymbol{x}\boldsymbol{x}^H\right) \tag{2.121}$$

By substituting (2.119) in (2.121), we get

$$C_{h\boldsymbol{x}} = 2\sqrt{\beta E_b}\sigma_h^2(1-j)\mathbf{1}_K^H \tag{2.122}$$

and

$$C_{\boldsymbol{xx}} = 4\beta E_b\sigma_h^2\mathbf{1}_{K\times K} + 2\sigma_n^2\boldsymbol{I}_K = 4\beta E_b\sigma_h^2\left(\mathbf{1}_{K\times K} + \frac{1}{2\beta\bar{\gamma}_b}\boldsymbol{I}_K\right) \tag{2.123}$$

where $\mathbf{1}_{K\times K}$ denotes a $K \times K$ matrix of ones.

By using the matrix inversion Lemma , the inverse of the matrix in (2.123) can be written as

$$C_{\boldsymbol{xx}}^{-1} = \frac{\bar{\gamma}_b}{2E_b\sigma_h^2}\left(\boldsymbol{I}_K - \frac{2\beta\bar{\gamma}_b}{1+2K\beta\bar{\gamma}_b}\mathbf{1}_{K\times K}\right) \tag{2.124}$$

Now, by substituting (2.122) and (2.124) in (2.120), the MMSE channel estimate is equal to

$$\hat{h} = \frac{\sqrt{\beta}\bar{\gamma}_b(1-j)}{\sqrt{E_b}}\mathbf{1}_K^H\left(\boldsymbol{I}_K - \frac{2\beta\bar{\gamma}_b}{1+2K\beta\bar{\gamma}_b}\mathbf{1}_{K\times K}\right)\boldsymbol{x} = \frac{\sqrt{\beta}\bar{\gamma}_b(1-j)}{\sqrt{E_b}\left(1+2K\beta\bar{\gamma}_b\right)}\mathbf{1}_K^H\boldsymbol{x} \tag{2.125}$$

Expression (2.125) shows how the MMSE estimator should compute the channel estimate $\hat{h}$ as a function of $\boldsymbol{x}$ in (2.119).

By substituting (2.119) in (2.125), $\hat{h}$ can be rewritten as

$$\hat{h} = \frac{\sqrt{\beta}\bar{\gamma}_b(1-j)}{\sqrt{E_b}\left(1+2K\beta\bar{\gamma}_b\right)}\mathbf{1}_K^H\left(\sqrt{\beta E_b}(1+j)h\mathbf{1}_K + \boldsymbol{\eta}\right) = \frac{2K\beta\bar{\gamma}_b}{1+2K\beta\bar{\gamma}_b}h + \frac{\sqrt{\beta}\bar{\gamma}_b(1-j)}{\sqrt{E_b}\left(1+2K\beta\bar{\gamma}_b\right)}\mathbf{1}_K^H\boldsymbol{\eta} \tag{2.126}$$

and hence, the channel estimation error is equal to

$$e = h - \hat{h} = \frac{1}{1 + 2K\beta\bar{\gamma}_b} h - \frac{\sqrt{\beta}\bar{\gamma}_b(1-j)}{\sqrt{E_b}\,(1 + 2K\beta\bar{\gamma}_b)} \mathbf{1}_K^H \boldsymbol{\eta} \tag{2.127}$$

From (2.127), channel estimation error $e$ is caused by $\boldsymbol{\eta}$ (the noise during transmission of pilot symbols), and hence, $e$ is independent of the AWGN during transmission of data signals. Note that since $h$ and the elements of vector $\boldsymbol{\eta}$ are circularly symmetric Gaussian distributed and mutually independent random variables $\hat{h}$ and $e$ in (2.126) and (2.127) are circularly symmetric Gaussian distributed. It can also be seen from (2.126) and (2.127) that $E\left(\hat{h}^* e\right) = 0$, i.e. $\hat{h}$ and $e$ are orthogonal, and hence, are independent. Therefore, $\hat{h}$ and $e$ satisfy the conditions mentioned for the model in (2.4).

Now, from (2.127), $\sigma_e^2$ is equal to

$$\sigma_e^2 = \frac{1}{2} E\left(|e|^2\right) = \frac{1}{2}\left(\frac{2\sigma_h^2}{(1 + 2K\beta\bar{\gamma}_b)^2} + \frac{4K\beta\bar{\gamma}_b^2\sigma_n^2}{E_b\,(1 + 2K\beta\bar{\gamma}_b)^2}\right) = \frac{\sigma_h^2}{1 + 2K\beta\bar{\gamma}_b} \tag{2.128}$$

We can see that $\sigma_e^2$ for QPSK modulation in (2.128) is smaller than that of BPSK in (2.73) of Section 2.1. In fact, for $\bar{\gamma}_b \gg 1$, $\sigma_e^2$ in (2.128) is half of (2.73). However, we will show later that BPSK and QPSK modulations result in approximately the same average BEP when $\bar{\gamma}_b \gg 1$.

By substituting (2.128) in (2.116), the average BEP of the receiver in (2.101) can be expressed as

$$P_b(E) = \frac{1}{2}\left(1 - \frac{\sqrt{2K\beta}\bar{\gamma}_b}{\sqrt{1 + 2(K\beta + 1)\bar{\gamma}_b + 2K\beta\bar{\gamma}_b^2}}\right) \tag{2.129}$$

For one-symbol observation ($K = 1$), when $\beta = 1$ the expression (2.129) reduces to

$$P_b(E) = \frac{1}{2}\left(1 - \frac{\sqrt{2}\bar{\gamma}_b}{\sqrt{1 + 4\bar{\gamma}_b + 2\bar{\gamma}_b^2}}\right) \tag{2.130}$$

which is equal to the average BEP of differential quadrature phase-shift keying (DQPSK) [6, eq.

(8.210)]. Therefore, with only one pilot symbol the BEP of DQPSK can be obtained, which shows again how effective an MMSE channel estimator is. As $K \to \infty$, expression (2.129) converges to (2.117), the average BEP of the ideal coherent reception.

**Performance Comparison of BPSK and QPSK**

In this part, we compare the performance of ML receivers of BPSK and QPSK for large average SNR ($\bar{\gamma}_b \gg 1$) when an MMSE channel estimator is used with pilot symbols, as described in Subsection 2.1.5 and this Subsection. The performance comparison is performed by using average BEP expressions in (2.75) and (2.129).

For $\bar{\gamma}_b \gg 1$, by using the Taylor series, the average BEP expression of BPSK in (2.75) can be approximated as

$$P_b(E) \approx \frac{K\beta + 1}{4K\beta\bar{\gamma}_b} \quad \text{for } \bar{\gamma}_b \gg 1 \tag{2.131}$$

For QPSK signals, the average BEP expression in (2.129) when $\bar{\gamma}_b \gg 1$ by using the Taylor series is approximately equal to

$$P_b(E) \approx \frac{K\beta + 1}{4K\beta\bar{\gamma}_b} \quad \text{for } \bar{\gamma}_b \gg 1 \tag{2.132}$$

Therefore, from (2.131) and (2.132), BPSK and QPSK modulations result in approximately the same average BEP for $\bar{\gamma}_b \gg 1$ when in both modulations an MMSE channel estimator is used with the same value of $K\beta$. The numerical results in the next section verify this result.

### 2.2.4 Numerical Results

In this subsection, we study the performance of the receiver in (2.101). We consider quasi-static flat Rayleigh fading channels when an MMSE channel estimator is applied at the receiver with pilot symbols, as explained in Subsection 2.2.3.

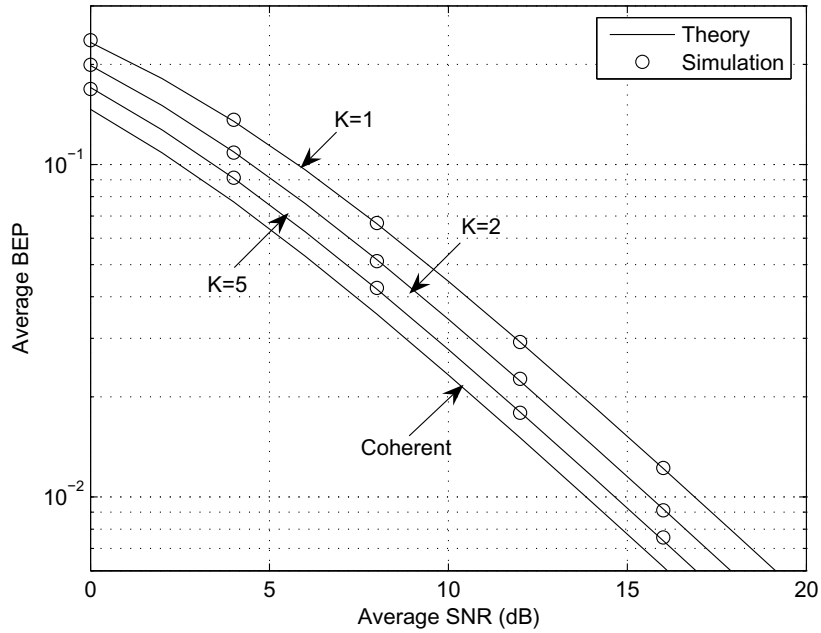


Figure 2.9: Average BEP versus the average SNR for QPSK signals for different numbers of $K$ when $\beta = 1$.

Fig. 2.9 shows the average BEP of the receivers in (2.101) versus the average SNR $\bar{\gamma}_b$ for QPSK signals by both theory (expressions (2.129)) and Monte-Carlo simulation. The curves are plotted for different numbers of pilot symbols $K$ when $\beta$, the ratio of the power of the pilot symbol to the power of data symbol, is equal to one. The Monte Carlo simulations are performed until $10^4$ samples of errors are observed for each data point. It is evident that the analytical result matches precisely the Monte Carlo simulations. The average BEP of ideal coherent QPSK in (2.117) has also been added for comparison in Fig 2.9. The performance of the ML receiver improves as the number of pilot symbols $K$ increases, as expected.

The average BEP's of BPSK and QPSK modulations are compared in Fig. 2.10 by using theoretical expressions (2.75) and (2.129) for different numbers of $K$ when $\beta = 1$. For small values of $\bar{\gamma}_b$, QPSK has a slight advantage over BPSK in terms of the average BEP. However, it is clear from the figure that for $\bar{\gamma}_b \gg 1$ QPSK and BPSK have almost the same average BEP, which is expected from (2.131) and (2.132).

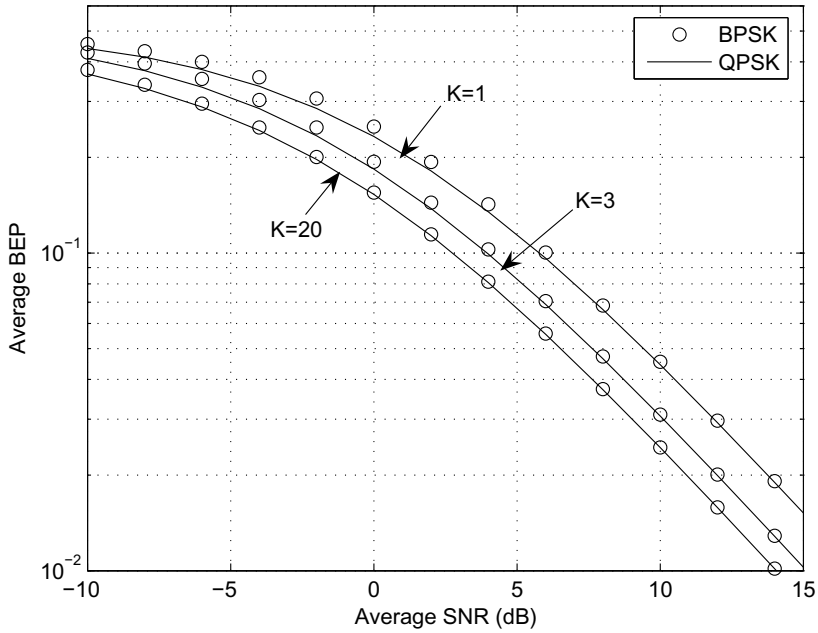


Figure 2.10: Comparison of the average BEP of BPSK signals with QPSK signals for different numbers of $K$ when $\beta = 1$.

## 2.3 Summary

In the first section of this chapter, we derived the ML receiver for binary orthogonal signals in the presence of Gaussian channel estimation error. The ML receiver is a linear combination of the matched filter and the square-law detector. An exact closed-form expression was derived for the average BEP of the proposed ML receiver in Rayleigh fading channels. It was shown that in the presence of channel estimation error if a certain condition is satisfied then orthogonal modulation outperforms antipodal signalling, and we stated that condition analytically. We also analyzed the performance of the proposed ML receiver for two special cases of fading channels: first quasi-static Rayleigh fading channels with an MMSE channel estimator, and second, time-varying Rayleigh fading channels modeled with an AR process. In both cases, we proved that the channel estimation error is Gaussian, and hence, the receiver proposed for the general case of Gaussian estimation error can be used for these cases.

In the second section, we derived the ML receiver for QPSK signals in the presence of Gaussian

channel estimation error. We found that the ML receiver is a matched filter which is matched to the channel estimate. An exact closed-form expression is derived for the average BEP of the ML receiver of QPSK signals in Rayleigh fading channels. We also analyzed the performance of the ML receiver of QPSK signals for the special case of quasi-static Rayleigh fading channels with an MMSE channel estimator. It was found that in quasi-static Rayleigh fading channels with an MMSE channel estimator, both BPSK and QPSK modulations result in almost the same average BEP for high enough average SNR.

## 2.4 List of Publications

The material of this chapter can be found in the following papers:

- A. A. Basri and T. J. Lim, "Optimum detection of binary signals in Rayleigh fading channels with imperfect channel estimates," in *Proc. IEEE Global Telecommun. Conf. (GLOBECOM 2006)*, pp. 1-5, Nov.- Dec. 2006.

- A. A. Basri and T. J. Lim, "Binary demodulation in Rayleigh fading with noisy channel estimates – Detector structures and performance," to appear in *Proc. IEEE Veh. Technol. Conf. (VTC-2008 Spring)*.

# Chapter 3

# Maximal Ratio Combining in the Presence of Multiple Interferers

In the last chapter, we studied single-antenna transceivers with imperfect channel estimates. In this chapter, multi-antenna receivers are assumed, with the spatial dimension used for multi-user interference suppression. The design of the base station receiver on the uplink of a wireless network that experiences multi-user interference, either from other cells or non-orthogonal users within a cell, is our exclusive focus.

This chapter comprises two main sections. In the first section, we examine the performance of the maximal ratio combining technique in the uplink of wireless communication systems in the presence of multiple interferers when channel estimates at the receiver are perfect. We derive an exact closed-form expression for the average BEP of binary phase-shift keying signals over Rayleigh fading channels. In the second section, the performance of MRC is studied when the channel estimates are subject to Gaussian-distributed channel estimation error. For this case, closed-form expressions for several performance measures, such as the outage probability and average bit-error probability, are derived.

## 3.1 Maximal Ratio Combining with Perfect Channel Estimates

In this section, we study the performance of MRC in the presence of multiple interferers and additive white Gaussian noise with perfect channel estimates and binary phase-shift keying signals.

### 3.1.1 System Model

We consider the uplink (mobile to base station) of a wireless communication systems where there is one desired user transmitting with one antenna over a flat fading channel, and $L$ other interfering users are also each transmitting over flat fading channels with one antenna, as shown in Fig. 3.1. The receiver is equipped with $N$ antenna elements. The $N \times 1$ baseband received signal vector $\boldsymbol{r}$ is given by

$$\boldsymbol{r} = \sqrt{P_0}\boldsymbol{h}_0 d_0 + \sum_{j=1}^{L} \sqrt{P_j}\boldsymbol{h}_j d_j + \boldsymbol{n} \tag{3.1}$$

where $d_0$ and $d_j$ are independent transmitted symbols of the desired and the $j$th interfering users, respectively. We assume that the transmitted symbols are equiprobable with BPSK modulation, i.e $d_0, \ldots, d_L \in \{-1, +1\}$. The $N \times 1$ circularly symmetric Gaussian vectors $\boldsymbol{h}_0$ and $\boldsymbol{h}_j$ correspond to the flat Rayleigh fading channels for the desired user and the $j$th interferer and are mutually independent. It is assumed that the antennas at the receiver are far enough apart so that the fading coefficients at different antennas are independent, i.e. $E[\boldsymbol{h}\boldsymbol{h}^H] = E[\boldsymbol{h}_j\boldsymbol{h}_j^H] = 2\boldsymbol{I}_N$, where $\boldsymbol{I}_N$ is an $N \times N$ identity matrix, and the factor 2 comes from the real and imaginary parts of the channels. Therefore, $\boldsymbol{h}_0 \sim CN_N(\boldsymbol{0}, 2\boldsymbol{I}_N)$ and $\boldsymbol{h}_j \sim CN_N(\boldsymbol{0}, 2\boldsymbol{I}_N)$ where $CN_p(\boldsymbol{\eta}, \boldsymbol{\Phi})$ denotes a complex multivariate normal distribution for a $p$-dimensional random vector with mean $\boldsymbol{\eta}$ and covariance matrix $\boldsymbol{\Phi}$ [91]. $P_0$ and $P_j$ correspond to the received signal powers of the desired user and the $j$th interfering user, respectively. The vector $\boldsymbol{n}$ represents the AWGN and $\boldsymbol{n} \sim CN_N(\boldsymbol{0}, 2\sigma_n^2\boldsymbol{I}_N)$, where $\sigma_n^2$ is the noise variance per real dimension.

In MRC, the array combining weight vector is equal to the desired user's channel, $\boldsymbol{h}_0$. Therefore, if $\boldsymbol{h}_0$ can be estimated perfectly at the receiver, from (3.1), the decision variable at the output

of the maximal ratio combiner can be written as

$$z = \boldsymbol{h}_0^H \boldsymbol{r} = \sqrt{P_0}\boldsymbol{h}_0^H \boldsymbol{h}_0 d_0 + z_{in} \tag{3.2}$$

where $z_{in}$ is the interference-plus-noise term at the output of the combiner and is equal to

$$z_{in} = \sum_{j=1}^{L} \sqrt{P_j}\boldsymbol{h}_0^H \boldsymbol{h}_j d_j + \boldsymbol{h}_0^H \boldsymbol{n} \tag{3.3}$$

From (3.2) and (3.3), the SINR $\gamma$ at the output of the maximal ratio combiner can be expressed as

$$\gamma = \frac{P_0 \left(\boldsymbol{h}_0^H \boldsymbol{h}_0\right)^2}{\boldsymbol{h}_0^H \left(\sum_{j=1}^{L} P_j \boldsymbol{h}_j \boldsymbol{h}_j^H + 2\sigma_n^2 \boldsymbol{I}_N\right) \boldsymbol{h}_0} \tag{3.4}$$

### 3.1.2 Performance Analysis

In this section, we investigate the average BEP of BPSK signals at the output of the maximal ratio combiner. First, we review the conventional PDF-based method and then derive an exact expression for the average BEP by using the proposed method.

#### PDF-Based Method

The PDF-based method is based on the following two-step procedure: First, find the BEP conditioned on $\boldsymbol{h}_0, \boldsymbol{h}_1, \ldots, \boldsymbol{h}_L$ and then average the result over the joint distribution of $\boldsymbol{h}_0, \boldsymbol{h}_1, \ldots, \boldsymbol{h}_L$. In other words, the average BEP $P_b(E)$ can be derived by

$$P_b(E) = \int \cdots \int P_b(E|\boldsymbol{h}_0, \boldsymbol{h}_1, \ldots, \boldsymbol{h}_L) f_{\boldsymbol{h}_0, \boldsymbol{h}_1, \ldots, \boldsymbol{h}_L}(\boldsymbol{h}_0, \boldsymbol{h}_1, \ldots, \boldsymbol{h}_L) d\boldsymbol{h}_0 d\boldsymbol{h}_1 \cdots d\boldsymbol{h}_L \tag{3.5}$$

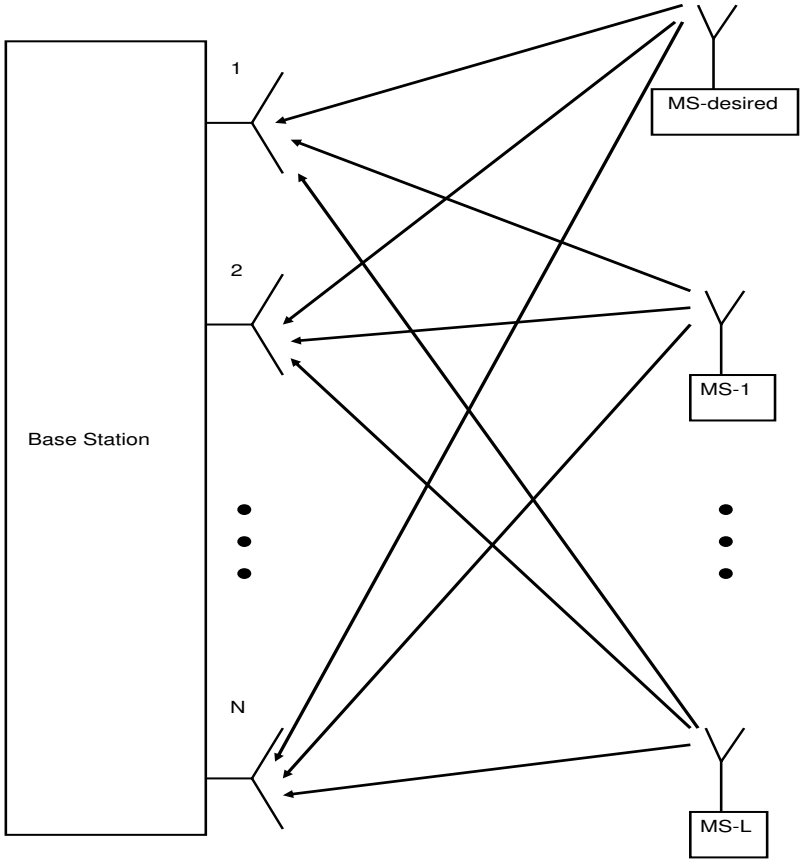


Figure 3.1: Uplink of single-input-multiple-output wireless systems

where $P_b(E|\boldsymbol{h}_0, \boldsymbol{h}_1, \ldots, \boldsymbol{h}_L)$ is the conditional BEP for a given set of fading channels $\boldsymbol{h}_0, \boldsymbol{h}_1, \ldots, \boldsymbol{h}_L$, and $f_{\boldsymbol{h}_0,\boldsymbol{h}_1,\ldots,\boldsymbol{h}_L}(\boldsymbol{h}_0, \boldsymbol{h}_1, \ldots, \boldsymbol{h}_L)$ is the joint PDF of $\boldsymbol{h}_0, \boldsymbol{h}_1, \ldots, \boldsymbol{h}_L$.

To calculate the conditional BEP $P_b(E|\boldsymbol{h}_0, \boldsymbol{h}_1, \ldots, \boldsymbol{h}_L)$ note that when transmitted signals $d_0 = -1$ and $d_0 = +1$ are equiprobable the BEP is equal to the BEP when $d_0 = -1$ is transmitted, and hence, from (3.2) we have

$$\begin{aligned} P_b\left(E|\boldsymbol{h}_0, \boldsymbol{h}_1, \ldots, \boldsymbol{h}_L\right) &= P_b\left(E|\boldsymbol{h}_0, \boldsymbol{h}_1, \ldots, \boldsymbol{h}_L, d_0 = -1\right) = P\left(\Re\left(z\right) > 0|\boldsymbol{h}_0, \boldsymbol{h}_1, \ldots, \boldsymbol{h}_L, d_0 = -1\right) \\ &= P\big(-\sqrt{P_0}\boldsymbol{h}_0^H\boldsymbol{h}_0 + z_{in}^R > 0|\boldsymbol{h}_0, \boldsymbol{h}_1, \ldots, \boldsymbol{h}_L\big) \end{aligned} \tag{3.6}$$

where $z_{in}^R$ is the real part of $z_{in}$ in (3.3).

Calculating the conditional BEP in (3.6) is difficult since it requires conditioning on all the interfering bits, and thus, its computational complexity increases exponentially in the number of users [18, pp. 113-114]. Moreover, the conditional BEP in (3.6) would be a complicated function of fading channels of all users, i.e. $\boldsymbol{h}_0, \boldsymbol{h}_1, \ldots, \boldsymbol{h}_L$, and therefore, integrating that complex conditional BEP over the joint PDF of $\boldsymbol{h}_0, \boldsymbol{h}_1, \ldots, \boldsymbol{h}_L$ would be a very difficult process in order to obtain the average BEP. Therefore, in the literature to find a simple expression for the conditional BEP in (3.6) it is assumed that $z_{in}|\boldsymbol{h}_0, \boldsymbol{h}_1, \ldots, \boldsymbol{h}_L$ is circularly symmetric Gaussian distributed [41]–[43]. We will see that based on this assumption, the conditional BEP in (3.6) can be expressed as a function of just $\gamma$ in (3.4), and then, the average BEP can be obtained by averaging the conditional BEP over the PDF of $\gamma$.

So, if we assume that $z_{in}$ in (3.3) conditioned on $\boldsymbol{h}_0, \boldsymbol{h}_1, \ldots, \boldsymbol{h}_L$ is distributed as

$$z_{in}|\boldsymbol{h}_0, \boldsymbol{h}_1, \ldots, \boldsymbol{h}_L \sim CN\left(0, \boldsymbol{h}_0^H\left(\sum_{j=1}^{L} P_j\boldsymbol{h}_j\boldsymbol{h}_j^H + 2\sigma_n^2\boldsymbol{I}_N\right)\boldsymbol{h}_0\right) \tag{3.7}$$

then the distribution of $z_{in}^R|\boldsymbol{h}_0, \boldsymbol{h}_1, \ldots, \boldsymbol{h}_L$ is

$$z_{in}^R|\boldsymbol{h}_0, \boldsymbol{h}_1, \ldots, \boldsymbol{h}_L \sim N\left(0, \frac{1}{2}\boldsymbol{h}_0^H\left(\sum_{j=1}^{L} P_j\boldsymbol{h}_j\boldsymbol{h}_j^H + 2\sigma_n^2\boldsymbol{I}_N\right)\boldsymbol{h}_0\right) \tag{3.8}$$

where $N(\eta, \sigma^2)$ denotes a normal distribution for a real random variable with mean $\eta$ and variance $\sigma^2$ [93].

Now, from (3.8), the conditional BEP in (3.6) can be expressed in terms of $\gamma$ in (3.4) as

$$P_b\left(E|\boldsymbol{h}_0, \boldsymbol{h}_1, \ldots, \boldsymbol{h}_L\right) = Q\left(\sqrt{2\gamma}\right) \tag{3.9}$$

where the Gaussian $Q$ function is defined in (2.36).

Therefore, assumption (3.7) has made it possible to derive a simple expression for the conditional BEP in (3.9) as a function of just $\gamma$. So, to find the average BEP, we should integrate (3.9) over the PDF of $\gamma$. Finding the PDF of $\gamma$ is not an easy procedure itself since $\gamma$ in (3.4) is a function of fading channels of all users, i.e. $\boldsymbol{h}_0, \boldsymbol{h}_1, \ldots, \boldsymbol{h}_L$. Now, from (3.9), the average BEP can be written as

$$P_b(E) = \int_0^\infty P_b(E|\gamma) f_\gamma(\gamma) d\gamma = \int_0^\infty Q\left(\sqrt{2\gamma}\right) f_\gamma(\gamma) d\gamma \tag{3.10}$$

where $P_b(E|\gamma)$ is the conditional error probability for a given $\gamma$, and $f_\gamma(\gamma)$ is the PDF of $\gamma$.

Note that from (3.3), assumption (3.7) is only valid for two cases: either when the transmitted symbols of the interfering users, $d_j$'s for $j = 1, \ldots, L$, are circularly symmetric Gaussian distributed, i.e. $d_j \sim CN(0, 1)$ for $j = 1, \ldots, L$, or when the number of interfering users goes to infinity and then the central limit theorem can be applied (as explained in [41]). However, in practice we deal with the case where the number of users is finite and the transmitted symbols are not Gaussian distributed. Therefore, in practice the average BEP expression in (3.10), which is derived with assumption (3.7), can be viewed only as an approximate result.

The PDF-based method has been used in [41]–[43]. For independent Rayleigh fading channels and BPSK signals the authors in [41] have found the PDF of SIR at the output of the maximal ratio combiner when the system is interference-limited and interfering sources have equal powers. Then, they have used (3.10) to find the approximate expression for the average BEP of MRC in [41, eq. (47)]. Their results have been generalized to other types of fading in [42], [43].

**Exact Method**

In this section, we propose a new method for deriving the exact average BEP of BPSK signals for MRC based on the decision variable at the output of the combiner conditioned only on the fading channel of the desired user. This method is again a two-step procedure, but the conditional BEP in the first step is conditioned on $\boldsymbol{h}_0$ and not on $\boldsymbol{h}_0, \boldsymbol{h}_1, \ldots, \boldsymbol{h}_L$. We will find that the distribution of interference-plus-noise term in (3.3) conditioned on the fading channel of the desired user is exactly Gaussian, which helps us find an exact expression for the conditional BEP. Then, we average this conditional BEP to get an exact expression for the average BEP. We will see that in contrast to the PDF-based method explained in the last part, in the proposed method there is no need to find the PDF of the output SINR in (3.4).

The conditional BEP $P_b(E|\boldsymbol{h}_0)$ when transmitted signals $d_0 = -1$ and $d_0 = +1$ are equiprobable is equal to the BEP when $d_0 = -1$ is transmitted, and hence from the decision variable in (3.2) we have

$$P_b\left(E|\boldsymbol{h}_0\right) = P_b\left(E|\boldsymbol{h}_0, d_0 = -1\right) = P\left(\Re\left(z\right) > 0|\boldsymbol{h}_0, d_0 = -1\right) = P\left(-\sqrt{P_0}\boldsymbol{h}_0^H\boldsymbol{h}_0 + z_{in}^R > 0|\boldsymbol{h}_0\right) \tag{3.11}$$

where $z_{in}^R$ is the real part of $z_{in}$ in (3.3).

To determine the conditional BEP in (3.11), we first need to find the distribution of $z_{in}^R$ conditioned on $\boldsymbol{h}_0$. Note that since random vectors $\boldsymbol{h}_j$'s for $j = 1, \ldots, L$ are distributed as $\boldsymbol{h}_j \sim CN_N\left(\boldsymbol{0}, 2\boldsymbol{I}_N\right)$ and $\boldsymbol{h}_0$ is independent from $\boldsymbol{h}_j$'s for $j = 1, \ldots, L$, we get $\sqrt{P_j}\boldsymbol{h}_0^H\boldsymbol{h}_j|\boldsymbol{h}_0 \sim CN\left(0, 2P_j\boldsymbol{h}_0^H\boldsymbol{h}_0\right)$ for $j = 1, \ldots, L$. Now, since for BPSK signals $d_j \in \{-1, +1\}$, the distribution of $\sqrt{P_j}\boldsymbol{h}_0^H\boldsymbol{h}_j d_j|\boldsymbol{h}_0$ conditioned on $d_j$ can be written as

$$\sqrt{P_j}\boldsymbol{h}_0^H\boldsymbol{h}_j d_j|\boldsymbol{h}_0, d_j \sim CN\left(0, 2P_j\boldsymbol{h}_0^H\boldsymbol{h}_0\left|d_j\right|^2\right) = CN\left(0, 2P_j\boldsymbol{h}_0^H\boldsymbol{h}_0\right) \text{ for } j = 1, \ldots, L \tag{3.12}$$

We can see from (3.12) that the PDF of $\sqrt{P_j}\boldsymbol{h}_0^H\boldsymbol{h}_j d_j|\boldsymbol{h}_0$ conditioned on $d_j$ is not a function of $d_j$. Therefore, $\sqrt{P_j}\boldsymbol{h}_0^H\boldsymbol{h}_j d_j|\boldsymbol{h}_0$ is independent from $d_j$, and thus, the distribution of $\sqrt{P_j}\boldsymbol{h}_0^H\boldsymbol{h}_j d_j|\boldsymbol{h}_0$ conditioned on $d_j$ is equal to the distribution of $\sqrt{P_j}\boldsymbol{h}_0^H\boldsymbol{h}_j d_j|\boldsymbol{h}_0$ itself. So, from (3.12) we have

$$\sqrt{P_j}\boldsymbol{h}_0^H\boldsymbol{h}_j d_j|\boldsymbol{h}_0 \sim CN\left(0, 2P_j\boldsymbol{h}_0^H\boldsymbol{h}_0\right) \quad \text{for } j = 1, \ldots, L \tag{3.13}$$

Now, since $\boldsymbol{h}_j$'s for $j = 1, \ldots, L$ are independent, from (3.13) we get

$$\sum_{j=1}^{L}\sqrt{P_j}\boldsymbol{h}_0^H\boldsymbol{h}_j d_j|\boldsymbol{h}_0 \sim CN\left(0, 2\boldsymbol{h}_0^H\boldsymbol{h}_0\sum_{j=1}^{L}P_j\right) \tag{3.14}$$

and therefore, $z_{in}$ in (3.3) conditioned on $\boldsymbol{h}_0$ is distributed as

$$z_{in}|\boldsymbol{h}_0 \sim CN\left(0, 2\boldsymbol{h}_0^H\boldsymbol{h}_0\left(\sigma_n^2 + \sum_{j=1}^{L}P_j\right)\right) \tag{3.15}$$

From (3.15), the distribution of $z_{in}^R|\boldsymbol{h}_0$ is

$$z_{in}^R|\boldsymbol{h}_0 \sim N\left(0, \boldsymbol{h}_0^H\boldsymbol{h}_0\left(\sigma_n^2 + \sum_{j=1}^{L}P_j\right)\right) \tag{3.16}$$

The result in (3.16) is a crucial outcome which shows that the distribution of $z_{in}^R|\boldsymbol{h}_0$ is exactly Gaussian. Therefore, from (3.16), the conditional BEP in (3.11) is precisely

$$P_b\left(E|\boldsymbol{h}_0\right) = Q\left(\sqrt{2\gamma_\varepsilon}\right) \tag{3.17}$$

where $\gamma_\varepsilon$ in (3.17) is given as

$$\gamma_\varepsilon = \frac{P_0\boldsymbol{h}_0^H\boldsymbol{h}_0}{2\left(\sigma_n^2 + \sum_{j=1}^{L}P_j\right)} \tag{3.18}$$

and the $Q$ function is defined in (2.36).

Note that in contrast to the conditional BEP expression of the PDF-based method in (3.9) which was derived under the assumption of (3.8), the expression in (3.17) is exact since (3.16) is exact.

Now, to derive the exact expression of the average BEP, we should average the conditional BEP in (3.17) over the PDF of $\gamma_\varepsilon$. To proceed with obtaining the PDF of $\gamma_\varepsilon$, from (3.18) we have

$$\gamma_\varepsilon = \frac{P_0}{2\left(\sigma_n^2 + \sum_{j=1}^{L} P_j\right)} \sum_{k=1}^{N} |h_{0,k}|^2 \tag{3.19}$$

where $h_{0,k}$ is the $k$th element of vector $\boldsymbol{h}_0$. Since it is assumed that $h_{0,k} \sim CN(0,2)$ we get $|h_{0,k}|^2 \sim \chi_2^2$ where $\chi_n^2$ denotes a chi-square distribution with $n$ degrees of freedom [93]. Note that the degrees of freedom for $|h_{0,k}|^2$ is equal to two because the complex Gaussian random variable $h_{0,k}$ consists of two independent Gaussian random variables (the real part and the imaginary part) each with unit variance. Now $\sum_{k=1}^{N} |h_{0,k}|^2$ in (3.19) is a summation of $N$ independent chi-square random variables. It is known that if independent random variables $x_1$ and $x_2$ are distributed as $x_1 \sim \chi_{\nu_1}^2$ and $x_2 \sim \chi_{\nu_2}^2$, then the sum $x_1 + x_2$ has a distribution of $\chi_{\nu_1+\nu_2}^2$ [93, p. 260]. Therefore, $\sum_{k=1}^{N} |h_{0,k}|^2 \sim \chi_{2N}^2$, and hence, $\gamma_\varepsilon$ in (3.19) has the following PDF

$$f_{\gamma_\varepsilon}(\gamma_\varepsilon) = \frac{N^N \gamma_\varepsilon^{N-1}}{(N-1)!\,(\bar{\gamma}_\varepsilon)^N} \exp\left(-\frac{N\gamma_\varepsilon}{\bar{\gamma}_\varepsilon}\right), \quad \gamma_\varepsilon \geq 0 \tag{3.20}$$

where

$$\bar{\gamma}_\varepsilon = E(\gamma_\varepsilon) = \frac{NP_0}{\sigma_n^2 + \sum_{j=1}^{L} P_j} \tag{3.21}$$

Now, the average BEP can be obtained by averaging the conditional BEP in (3.17) over the PDF of $\gamma_\varepsilon$ in (3.20) as

$$P_b(E) = \int_0^\infty P_b(E|\gamma_\varepsilon)\, f_{\gamma_\varepsilon}(\gamma_\varepsilon)\, d\gamma_\varepsilon = \int_0^\infty Q\left(\sqrt{2\gamma_\varepsilon}\right) \frac{N^N \gamma_\varepsilon^{N-1}}{(N-1)!\,(\bar{\gamma}_\varepsilon)^N} \exp\left(-\frac{N\gamma_\varepsilon}{\bar{\gamma}_\varepsilon}\right) d\gamma_\varepsilon \tag{3.22}$$

The integral in (3.22) can be calculated by using the result in [1, eq. (14.4-15)] as

$$P_b(E) = \frac{1}{2^N}\left(1-\sqrt{\frac{\bar{\gamma}_c}{1+\bar{\gamma}_c}}\right)^N \sum_{k=0}^{N-1}\frac{1}{2^k}\begin{pmatrix} N-1+k \\ k \end{pmatrix}\left(1+\sqrt{\frac{\bar{\gamma}_c}{1+\bar{\gamma}_c}}\right)^k \quad (3.23)$$

where $\bar{\gamma}_c$ is defined as

$$\bar{\gamma}_c = \frac{\bar{\gamma}_\varepsilon}{N} = \frac{P_0}{\sigma_n^2 + \sum_{j=1}^{L} P_j} \quad (3.24)$$

which is the ratio of the desired signal's power to the summation of the interfering users' powers plus the power of the noise.

Note that the expression in (3.23) is equal to the result derived in [1, eq. (14.4-15)] for the single-user systems (with AWGN and no CCI) where the average SNR per channel is replaced by $\bar{\gamma}_c$ in (3.24). The expression in (3.23) is also mentioned in [62] and [79] for the average BEP of MRC in the presence of CCI. In those papers, the authors have replaced the average SNR per channel by the ratio of the desired signal's power to the total power of interference plus noise to obtain what appeared to be an approximation of the average BEP of MRC (in [62] for the single-interferer case and in [79] for the case of multiple equal-power interferers). However, we have shown in this section that actually the expression in (3.23) is the exact expression of the average BEP of BPSK signals for MRC when fading channels of users are independent with Rayleigh statistics. In other words, replacing the average SNR per channel of the expression in [1, eq. (14.4-15)] (which is derived for the single-user case) by the ratio of the desired user's power to the total power of the interfering users plus noise in (3.24) gives an exact expression of the average BEP.

The proposed exact method has several advantages over the PDF-based method explained earlier. First, finding the PDF of SINR is a complicated task, but for the exact method there is no need to find the PDF of $\gamma$ in (3.4). Second, the result of the exact method is valid in the presence of thermal noise with either equal-power or unequal-power interferers. However, the results of the PDF-based method in [41] is limited to the case of interference-limited systems, i.e. $\sigma_n^2 = 0$, with

equal-power interferers, i.e. $P_j$'s for $j = 1, \ldots, L$ are equal. Finally, the result of the PDF-based method is only exact when the assumption (3.7) is valid which is not the case in practical systems, for example for a system with finite $L$ and BPSK modulated signals. However, the result in (3.23) is precise and no approximation is involved.

The results of the proposed exact method can be easily generalized to M-PSK modulation. In M-PSK, the transmitted symbols are chosen from the set of $\left\{\exp\left(\frac{j2\pi m}{M}\right) | m = 0, 1, \ldots, M-1\right\}$ where $M$ is the number of points in the signal constellation. So, for these types of signals the magnitude of the transmitted symbols is also unity, i.e. $|d_j|^2 = 1$ for $j = 1, \ldots, L$, and hence, formulas (3.12) and (3.13) can be applied again. Therefore, the distribution of interference-plus-noise term conditioned on the fading channel of the desired user would be Gaussian as well, and the exact expressions for the conditional BEP and average BEP can be similarly obtained.

### 3.1.3 Numerical Results

In this section, we present a set of numerical results for the average BEP of BPSK signals for MRC in the presence of CCI. The fading channels of different users are assumed to be independent with Rayleigh statistics.

The average BEP is studied in Fig. 3.2 by both theory (expression (3.23)) and simulation for a system with equal-power interferers, i.e. $P_j = P_I$ for $j = 1, \ldots, L$ where $P_I$ is a constant. The average BEP in Fig. 3.2 is plotted versus $P_0/P_I$ (the power of the desired user to the power of one interferer) for different numbers of interfering users $L$ when the number of antennas is $N = 3$. The power of the noise is assumed to be equal to the power of one of the interfering users, i.e. $\sigma_n^2 = P_I$. We can see that as $L$ increases the average BEP also increases, as expected. The Monte Carlo simulations are performed until $10^5$ samples of errors are observed for each data point. Theoretical results in Fig. 3.2 match precisely the Monte Carlo simulations, which verifies the derived analytical expression in (3.23).

In Fig. 3.3, we compare the average BEP expression derived by the conventional PDF-based

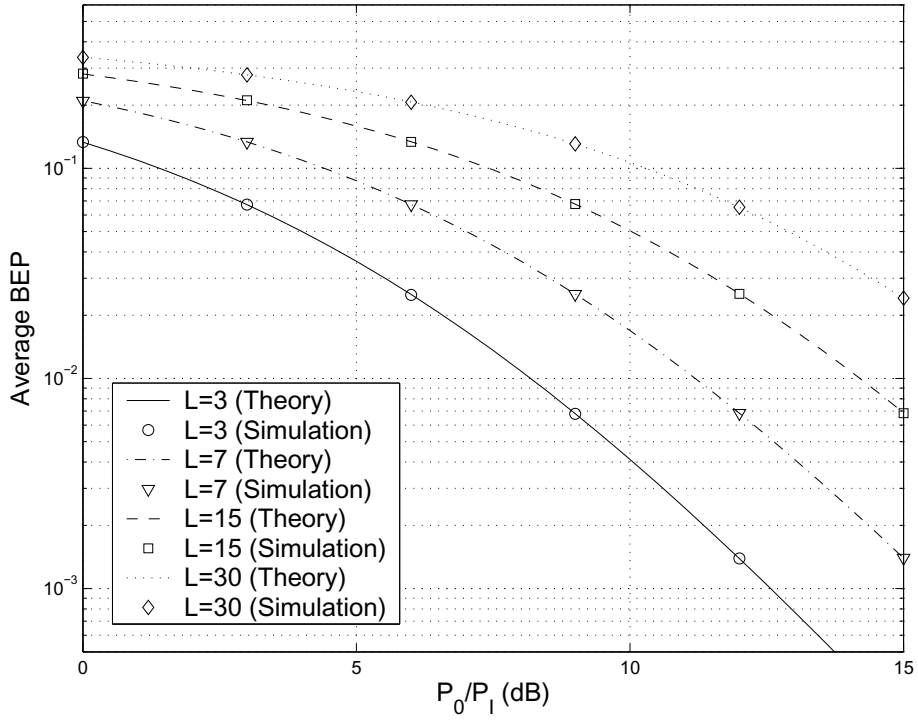


Figure 3.2: Average BEP versus $P_0/P_I$ for different numbers of interfering users in a system with equal-power interferers when $N = 3$ and $\sigma_n^2 = P_I$.

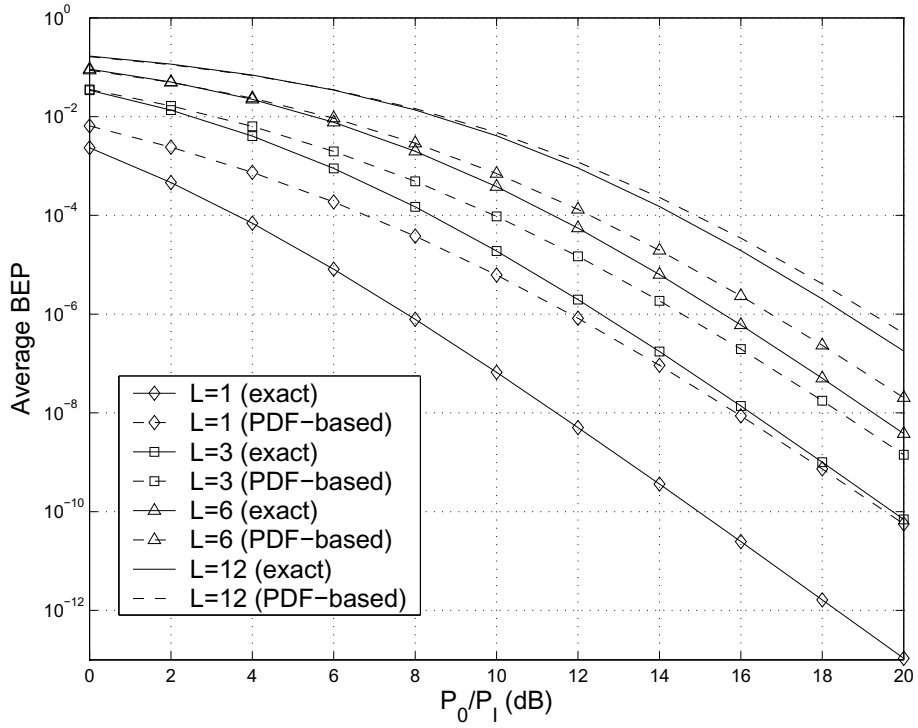


Figure 3.3: Average BEP versus $P_0/P_I$ for different numbers of interfering users in an interference-limited system with equal-power interferers when $N = 6$.

method in [41, eq. (47)] with expression (3.23). Since the results in [41] are obtained for interference-limited systems with equal-power interferers, we consider the case where $\sigma_n^2 = 0$ and $P_j = P_I$ for $j = 1, \ldots, L$, where $P_I$ is a constant. In Fig. 3.3, we have shown the average BEP versus $P_0/P_I$ for different numbers of interfering users $L$ when the number of antennas is $N = 6$. As we can see, for $L = 1$ there is a large gap between the the approximate result of the PDF-based approach and the exact expression. However, it is evident that as the number of interfering users increases the difference between the exact and approximate results decreases. This is because with increasing numbers of interfering users the distribution of $z_{in}$ in (3.3) conditioned on $\boldsymbol{h}_0, \boldsymbol{h}_1, \ldots, \boldsymbol{h}_L$ converges to a Gaussian distribution by the Central Limit Theorem, and hence, the assumption (3.7) in the PDF-based method becomes increasingly accurate.

## 3.2 Maximal Ratio Combining with Imperfect Channel Estimates

In this section, we analyze the performance of MRC in the presence of channel estimation errors and multiple interferers in a flat Rayleigh fading environment. We assume that the system is interference-limited, i.e. the power of noise can be neglected, and the interfering users have equal power. The PDF of the signal-to-interference-plus-noise ratio at the output of the maximal ratio combiner has been derived in prior work [59], assuming Gaussian channel estimation errors. We use that PDF to derive analytical expressions for a number of important performance measures such as the outage probability and the average bit error probability for different modulation formats in interference-limited systems. These expressions are useful tools to examine the performance degradation of MRC in the presence of channel estimation error.

### 3.2.1 System Model

We consider the uplink of a wireless communication system in the presence of $L$ interferers. The receiver is equipped with $N$ antenna elements, and $N \leq L$. The system is assumed to be

interference-limited and all the interferers are received with the same average power. Note that these assumptions are different from the ones in Section 3.1. The $N \times 1$ baseband received signal vector $\boldsymbol{r}$ is given by

$$\boldsymbol{r} = \sqrt{P_D}\boldsymbol{h}d + \sum_{j=1}^{L} \sqrt{P_I}\boldsymbol{h}_j d_j \tag{3.25}$$

where $d$ and $d_j$ are independent transmitted symbols of the desired and the $j$th interfering users, respectively, each with zero mean and unit variance. The $N \times 1$ circularly symmetric Gaussian vectors $\boldsymbol{h}$ and $\boldsymbol{h}_j$ correspond to the flat Rayleigh fading channels for the desired user and the $j$th interferer, and are mutually independent. It is assumed that receiver antennas are far enough apart so that the fading coefficients at different antennas are independent, i.e. $E[\boldsymbol{h}\boldsymbol{h}^H] = E[\boldsymbol{h}_j\boldsymbol{h}_j^H] = 2\boldsymbol{I}_N$. Received signal powers $P_D$ and $P_I$ correspond to the desired and the interfering users, respectively.

When the desired user's channel vector $\boldsymbol{h}$ can be estimated perfectly, the combining weight vector of MRC is equal to $\boldsymbol{h}$. However, since in practice the receiver cannot estimate the channels without error, diversity combining is based on the estimated channels. Therefore, the weight vector of MRC is the desired user's channel estimate vector, and we have

$$\boldsymbol{u}^{mrc} = \hat{\boldsymbol{h}} \tag{3.26}$$

where $\hat{\boldsymbol{h}}$ denotes the channel estimate vector for the desired user.

From (3.25) and (3.26), the output of the combiner can be written as

$$z = \left(\boldsymbol{u}^{mrc}\right)^H \boldsymbol{r} = \sqrt{P_D}\hat{\boldsymbol{h}}^H\boldsymbol{h}d + \sum_{j=1}^{L} \sqrt{P_I}\hat{\boldsymbol{h}}^H\boldsymbol{h}_j d_j \tag{3.27}$$

Now, from (3.27) the SIR $\gamma^{mrc}$ at the output of the maximal ratio combiner can be written as

$$\gamma^{mrc} = \frac{P_D \hat{\boldsymbol{h}}^H \boldsymbol{h}\boldsymbol{h}^H \hat{\boldsymbol{h}}}{P_I \hat{\boldsymbol{h}}^H \left( \sum_{j=1}^{L} \boldsymbol{h}_j \boldsymbol{h}_j^H \right) \hat{\boldsymbol{h}}} \tag{3.28}$$

The channel estimation error vector for the desired user is defined as

$$\boldsymbol{e} = \boldsymbol{h} - \hat{\boldsymbol{h}} \tag{3.29}$$

The vector $\boldsymbol{e}$ in (3.29) is assumed to be circularly symmetric Gaussian distributed and independent from the channel estimate vector $\hat{\boldsymbol{h}}$. Channel estimate vector $\hat{\boldsymbol{h}}$ is also assumed to be circularly symmetric Gaussian distributed. These assumptions are valid for an MMSE estimator in the Bayesian linear model, where the channel estimation error is circularly symmetric Gaussian distributed and the estimate and the error are orthogonal [8]. The elements of the error vector $\boldsymbol{e}$ are assumed to be independent. Hence, we have $E[\boldsymbol{e}\boldsymbol{e}^H] = diag(2\sigma_1^2, \ldots, 2\sigma_N^2)$ where $2\sigma_k^2$ is the variance of $e_k$, the $k$th element of the channel estimation error vector $\boldsymbol{e}$. Similarly, the elements of the channel estimate vector $\hat{\boldsymbol{h}}$ are independent, and from (3.29), the variance of $\hat{h}_k$, the $k$th element of the vector $\hat{\boldsymbol{h}}$, is $2(1-\sigma_k^2)$. Since $\boldsymbol{h}$ and $\boldsymbol{e}$ are circularly symmetric Gaussian distributed and mutually independent, we can find from (3.29) that $\hat{\boldsymbol{h}}$ and $\boldsymbol{h}$ are jointly circularly symmetric Gaussian vectors, and the correlation coefficient between the $k$th elements of $\boldsymbol{h}$ and $\hat{\boldsymbol{h}}$, $h_k$ and $\hat{h}_k$ respectively, can be written as

$$\rho_k = \frac{E\left(\hat{h}_k^* h_k\right)}{\sqrt{E\left(|h_k|^2\right) E\left(\left|\hat{h}_k\right|^2\right)}} = \sqrt{1-\sigma_k^2} \tag{3.30}$$

Throughout this section, we assume that for all elements the correlation coefficients are equal, i.e. $\rho_k = \rho \ \forall\, k$. This assumption is reasonable because all the channels are estimated under the same conditions using the same method.

### 3.2.2 Performance Analysis

In this section, we analyze the performance of MRC in the presence of Gaussian-distributed channel estimation error.

In the presence of Gaussian-distributed channel estimation error, the PDF of $\gamma^{mrc}$ is derived in [59] and for interference-limited systems can be expressed as

$$f_{\gamma^{mrc}}\left(\gamma^{mrc}\right) = \left(\frac{P_D}{P_I}\right)^L \sum_{j=0}^{N-1} \frac{\binom{N-1}{j}(1-\rho^2)^{N-1-j}\left(\rho^2\right)^j \left(\gamma^{mrc}\right)^j}{B(j+1,L)\left(\frac{P_D}{P_I}+\gamma^{mrc}\right)^{j+L+1}} \tag{3.31}$$

where the beta function $B(p,q)$ is defined in (A.3) and (A.4) in Appendix A.

Now, we use the PDF expression in (3.31) to derive analytical expressions for the outage probability and average BEP of MRC.

#### Outage Probability

From (3.31), the outage probability of $\gamma^{mrc}$ for a certain threshold, say $\gamma_0$, is

$$\begin{aligned} P_{out} &= \int_0^{\gamma_0} f_{\gamma^{mrc}}\left(\gamma^{mrc}\right) d\gamma^{mrc} \\ &= \left(\frac{P_D}{P_I}\right)^L \sum_{j=0}^{N-1} \frac{\binom{N-1}{j}(1-\rho^2)^{N-1-j}\left(\rho^2\right)^j}{B(j+1,L)} \int_0^{\gamma_0} \frac{\left(\gamma^{mrc}\right)^j}{\left(\frac{P_D}{P_I}+\gamma^{mrc}\right)^{j+L+1}} d\gamma^{mrc} \end{aligned} \tag{3.32}$$

From (A.5), the integral term in (3.32) can be written in terms of the incomplete beta function as

$$\int_0^{\gamma_0} \frac{\left(\gamma^{mrc}\right)^j}{\left(\frac{P_D}{P_I}+\gamma^{mrc}\right)^{j+L+1}} d\gamma^{mrc} = \frac{B_{\frac{\gamma_0}{\frac{P_D}{P_I}+\gamma_0}}(j+1,L)}{\left(\frac{P_D}{P_I}\right)^L} \tag{3.33}$$

Now, from (3.33), the outage probability expression in (3.32) can be simplified to

$$\begin{aligned} P_{out} &= \sum_{j=0}^{N-1} \frac{\binom{N-1}{j}(1-\rho^2)^{N-1-j}\,(\rho^2)^j}{B(j+1,L)} B_{\frac{\gamma_0}{\frac{P_D}{P_I}+\gamma_0}}(j+1,L) \\ &= \sum_{j=0}^{N-1} \binom{N-1}{j}(1-\rho^2)^{N-1-j}\left(\rho^2\right)^j I_{\frac{\gamma_0}{\frac{P_D}{P_I}+\gamma_0}}(j+1,L) \end{aligned} \tag{3.34}$$

where the regularized incomplete beta function $I_w(a,b)$ is defined in (A.6) and can be evaluated directly in MATLAB.

### Average Bit Error Probability

To evaluate this important measure of performance for our multi-user system in the presence of channel estimation errors, first we should find the BEP conditioned on the true and estimated fading channels of all users. Then, the conditional BEP should be averaged over the joint distribution of the true and estimated channels of all users which is an enormously complicated process. But if the conditional BEP can be expressed as a function of SIR, then we can easily average the conditional BEP over the PDF of SIR to get the average BEP instead of sophisticated averaging over the joint PDF of the true and estimated channels.

Now, we show that in the presence of channel estimation errors, the conditional BEP for coherent modulation formats is not a function only of SIR, but for non-coherent modulation formats, e.g. binary DPSK and binary NCFSK, it is just a function of SIR.

In this section, we assume that the interference component of $z$ in (3.27) conditioned on $\hat{\boldsymbol{h}}$ and $\boldsymbol{h}_j$'s is circularly symmetric Gaussian distributed. The Gaussian interference assumption can be justified by Cramér's central limit theorem [100] as the number of interfering users goes to infinity[1]. Therefore, the channel in (3.27) conditioned on $\hat{\boldsymbol{h}}$, $\boldsymbol{h}$ and $\boldsymbol{h}_j$'s resembles an AWGN channel, with unknown phase. The unknown phase is due to imperfect channel estimation of $\boldsymbol{h}$ at the receiver resulting in $\hat{\boldsymbol{h}}^H\boldsymbol{h}$ having non-zero phase. If coherent antipodal binary phase-shift

[1]Cramér's central limit theorem is one variation of the cental limit theorem in which the assumption of identically distributed random variables is abandoned in favor additional restrictions.

keying modulation is used, the slicer input would be $\Re\{z\}$, the real part of $z$, and the resulting conditional BEP will not be determined only by $\gamma^{mrc}$ defined in (3.28). However, for binary DPSK and NCFSK signals, the BEP in an AWGN channel with unknown phase is a function only of SNR [1]. Therefore, the BEP conditioned on $\hat{\boldsymbol{h}}$, $\boldsymbol{h}$ and $\boldsymbol{h}_j$'s for binary DPSK and binary NCFSK is a function only of $\gamma^{mrc}$ in (3.28) and can be expressed as

$$P_b\left(E|\hat{\boldsymbol{h}}, \boldsymbol{h}, \boldsymbol{h}_1, \ldots, \boldsymbol{h}_L\right) = P_b\left(E|\gamma^{mrc}\right) = \frac{1}{2}\exp\left(-\alpha\gamma^{mrc}\right) \tag{3.35}$$

where

$$\alpha = \begin{cases} 1, & \text{for binary DPSK} \\ \frac{1}{2}, & \text{for binary NCFSK} \end{cases} \tag{3.36}$$

Now, by averaging the conditional BEP in (3.35) over the PDF of SIR in (3.31), the average BEP of MRC can be written as

$$\begin{aligned} P_b(E) &= \int_0^\infty P_b(E|\gamma^{mrc}) f_{\gamma^{mrc}}(\gamma^{mrc}) d\gamma^{mrc} \\ &= \left(\frac{P_D}{P_I}\right)^L \sum_{j=0}^{N-1} \frac{\binom{N-1}{j}(1-\rho^2)^{N-1-j}\left(\rho^2\right)^j}{B(j+1, L)} \int_0^\infty \frac{\left(\gamma^{mrc}\right)^j \exp\left(-\alpha\gamma^{mrc}\right)}{2\left(\frac{P_D}{P_I} + \gamma^{mrc}\right)^{j+L+1}} d\gamma^{mrc} \end{aligned} \tag{3.37}$$

From (A.4), the average BEP expression of MRC in (3.37) can be simplified to

$$P_b(E) = \frac{1}{2\Gamma(L)} \sum_{j=0}^{N-1} \binom{N-1}{j} (1-\rho^2)^{N-1-j} \left(\rho^2\right)^j \Gamma(j+L+1) U\left(j+1, 1-L, \frac{\alpha P_D}{P_I}\right) \tag{3.38}$$

where the confluent hypergeometric function $U(a, b, x)$ is defined in (A.7) and can be evaluated either directly using Mathematica, or by using the exponential integral functions [98, eq. (5.1.4)] in MATLAB.

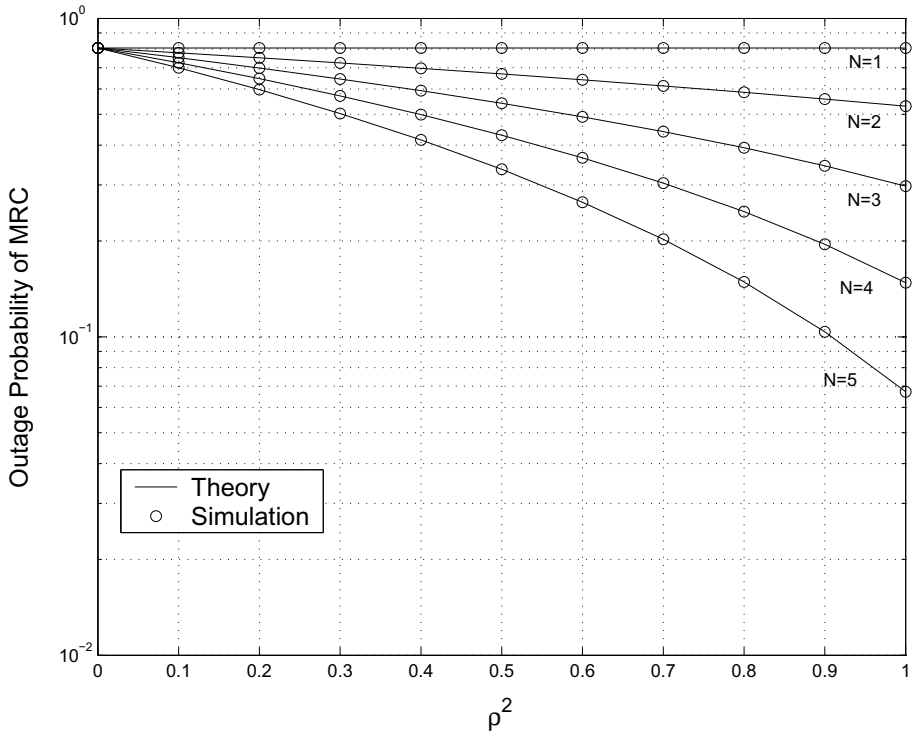


Figure 3.4: Outage probability of MRC versus the square of correlation coefficient for different numbers of antennas when $\gamma_0 = 5$ dB and $L = 6$.

### 3.2.3 Numerical Results

In this section, we present a set of numerical results for the outage probability and the average BEP of MRC and OC with imperfect channel estimates when the number of interferers is $L = 6$, and $P_D/P_I = 10$.

The outage probability of MRC for threshold $\gamma_0 = 5$ dB is plotted in Fig. 3.4 versus the square of the correlation coefficient for different numbers of antennas, $N$, by both theory (expression (3.34)) and simulation. We can see that except for $N = 1$, the outage probability decreases as $\rho$ increases, and this improvement is more significant when there is a larger number of antennas at the receiver. For instance, as $\rho^2$ increases from 0.9 to 1, the outage probability decreases from $0.1037$ to $6.72 \times 10^{-2}$ for $N = 5$, while it only improves from $0.5582$ to $0.5305$ for $N = 2$. Theoretical results in Fig. 3.4 match precisely the Monte Carlo simulations, which verifies the derived analytical expression in (3.34).

Fig. 3.5 shows the theoretical and simulation results of the average BEP of MRC against $\rho^2$

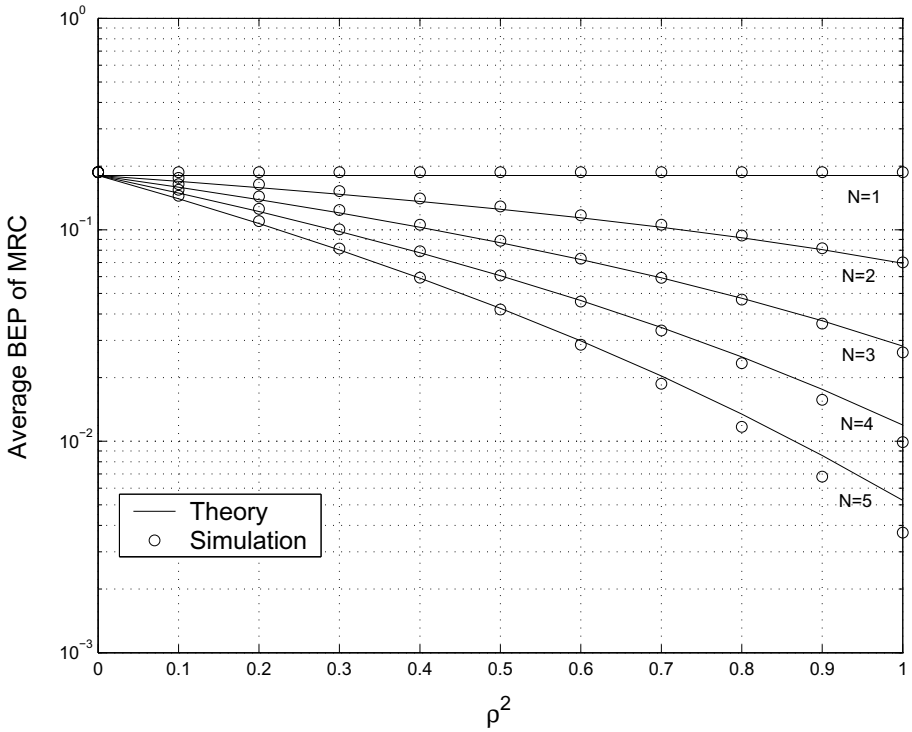


Figure 3.5: Average BEP of MRC versus the square of correlation coefficient for DPSK signals and $N = 1, \ldots, 5$ when $L = 6$.

for DPSK signals with several values of $N$. For the theoretical results we have used expression (3.38) with $\alpha = 1$. We observe again that the performance improvement due to increasing $\rho$ is more substantial with a larger number of antennas. For example, as $\rho^2$ increases from 0.9 to 1, the analytical average BEP decreases only from $8.06 \times 10^{-2}$ to $6.95 \times 10^{-2}$ when $N = 2$, whereas it decreases significantly from $8.57 \times 10^{-3}$ to $5.25 \times 10^{-3}$ for $N = 5$. Although the average BEP in (3.38) is derived under the Gaussian distributed interference assumption, we can see a very good match between the theory and simulation in Fig. 3.5.

## 3.3 Summary

In the first section of this chapter, we examined the performance of MRC technique in the uplink of wireless communication systems in the presence of multiple interferers and AWGN when the fading channels are perfectly estimated. An exact closed-form expression of the average BEP for

BPSK signals is derived when the the fading channels of different users are assumed to be independent from each other with Rayleigh statistics. The derivation is based on the decision variable at the output of the combiner conditioned on the fading channel of the desired user. We found that by conditioning only on the fading channel of the desired user, the distribution of interference-plus-noise term is exactly Gaussian, which results in exact expressions for the conditional BEP and average BEP. Moreover, the proposed method is much less complex than the conventional PDF-based technique since there is no need to find the PDF of the SINR. We found that the exact expression of the average BEP in the presence of CCI can be obtained from the expression for the average BEP of MRC in single-user systems (with AWGN and no CCI) by replacing the average SNR per channel with the ratio of the desired signal's power to the total power of the interfering users plus noise. We studied the difference between the results of the PDF-based method and exact results and found that this difference is considerable in the presence of a smaller number of interfering users. The results of the proposed exact method can be easily generalized to M-PSK modulation as well since for this type of modulation the distribution of interference-plus-noise term conditioned on the fading channel of the desired user is also exactly Gaussian.

In the second section of this chapter, we investigated the performance of MRC in the presence of circularly symmetric Gaussian-distributed channel estimation errors and multiple interferers over Rayleigh fading channels for interference-limited systems with equal-power interferers. We derived analytical expressions for the outage probability and the average BEP of MRC for binary DPSK and NCFSK signals. These expressions are useful tools for performance analysis and easier to compute than time-consuming Monte Carlo simulations. We studied the performance improvement of MRC as the correlation between the true and estimated channels increases and found that this improvement is more substantial when there is a larger number of antennas at the receiver. The derived expressions in this section will be used in Chapter 4 to compare the performance of MRC with OC in the presence of multiple interferers and Gaussian-distributed channel estimation errors.

## 3.4 List of Publications

The material of this chapter can be found in the following papers:

- A. A. Basri and T. J. Lim, "Exact average bit-error probability for maximal ratio combining with multiple cochannel interferers and Rayleigh fading," in *Proc. IEEE Int. Conf. on Commun. (ICC 2007)*, pp. 1102-1107, Jun. 2007.

- A. A. Basri and T. J. Lim, "Performance of maximal ratio and optimum combining with channel estimation errors and multiple interferers in Rayleigh fading channels," in *Proc. IEEE Veh. Technol. Conf. (VTC-2006 Fall)*, pp. 1345-1349, Sep. 2006.

# Chapter 4

# Optimum Combining in the Presence of Multiple Interferers

In this chapter, we investigate the effect of imperfect channel estimation on the performance of OC in the uplink of wireless communication systems. We consider the same setup as in the previous chapter, i.e. space diversity reception in a flat Rayleigh fading channel in the presence of multiple interferers and channel estimation errors. The word ”optimum” in OC accurately describes this receiver only when the channel estimates and true channel coefficients are equal – however, we continue to use the term OC in the presence of estimation errors in order not to introduce another term into the lexicon, with the understanding that the noisy estimates are used directly in place of the true coefficients. It is assumed that the channel estimation errors are circularly symmetric Gaussian distributed. We assume that the interferers have equal powers and the number of interferers is no less than the number of antenna elements. The main contribution of this chapter is applying multivariate statistical analysis to derive an exact closed-form expression for the PDF of the output SIR in terms of hypergeometric functions. This PDF expression is then utilized to obtain expressions for the moments of SIR, outage probability and the average bit error probability. The analytical expressions are verified by Monte Carlo simulations and are useful for studying the impact of imperfect channel estimation on the receiver performance. Clearly, the performance of

OC is expected to improve as the correlation between the true and estimated channels increases– our analysis shows quantitatively that this improvement becomes more significant as the number of antennas at the receiver increases.

## 4.1 System Model

Similar to Section 3.2, we consider the uplink of a single-input-multiple-output wireless communication system in the presence of $L$ interferers. We assume that each interfering user has one antenna and the receiver is equipped with $N$ antenna elements. The system is assumed to be interference-limited and all the interferers are received with the same average power. The baseband received signal vector $\boldsymbol{r}$ is given by

$$\boldsymbol{r} = \sqrt{P_D}\boldsymbol{h}d + \sum_{j=1}^{L} \sqrt{P_I}\boldsymbol{h}_j d_j \tag{4.1}$$

where $d$ and $d_j$ are independent symbols with zero mean and unit variance for the desired and the $j$th interfering users, respectively. The $N \times 1$ circularly symmetric Gaussian vectors $\boldsymbol{h}$ and $\boldsymbol{h}_j$ correspond to the flat Rayleigh fading channels for the desired user and the $j$th interferer and are mutually independent. It is assumed that receiver antennas are far enough apart so that the fading coefficients at different antennas are independent. Therefore, $\boldsymbol{h} \sim CN_N(\boldsymbol{0}, 2\boldsymbol{I}_N)$ and $\boldsymbol{h}_j \sim CN_N(\boldsymbol{0}, 2\boldsymbol{I}_N)$. Received signal powers $P_D$ and $P_I$ correspond to the desired and the interfering users, respectively. Denoting the $N \times 1$ array combining weight vector as $\boldsymbol{u}$, the output of the combiner can be written as

$$z_{out} = \boldsymbol{u}^H\boldsymbol{r} = \sqrt{P_D}\boldsymbol{u}^H\boldsymbol{h}d + \sum_{j=1}^{L} \sqrt{P_I}\boldsymbol{u}^H\boldsymbol{h}_j d_j \tag{4.2}$$

and hence, the SIR $\gamma$ at the output of the combiner is

$$\gamma = \frac{P_D \boldsymbol{u}^H \boldsymbol{h}\boldsymbol{h}^H \boldsymbol{u}}{P_I \boldsymbol{u}^H \left( \sum_{j=1}^{L} \boldsymbol{h}_j \boldsymbol{h}_j^H \right) \boldsymbol{u}} \tag{4.3}$$

where the superscript $H$ denotes the Hermitian transposition, i.e. transposition combined with complex conjugation. It can be seen that if the number of antennas at the receiver is greater than the number of interferers, i.e. $N > L$, then the denominator of (4.3) can be driven to zero in the case of perfect channel estimation, and hence, the interference vanishes completely. Throughout this chapter we assume that $L \geq N$, and hence a linear zero-forcing receiver cannot be found.

The receiver performs channel estimation in order to determine $\boldsymbol{u}$. It is assumed that the channel estimation error is Gaussian distributed and independent from the channel estimate. Therefore, we have

$$\boldsymbol{h}_j = \hat{\boldsymbol{h}}_j + \boldsymbol{e}_j \tag{4.4}$$

where mutually independent error vectors $\boldsymbol{e}_j$'s are assumed to be circularly symmetric Gaussian distributed and independent from the estimated channels $\hat{\boldsymbol{h}}_j$'s [48]. This assumption is valid for MMSE estimation in which the estimate and the error are orthogonal [8]. Moreover, channel estimate vectors $\hat{\boldsymbol{h}}_j$'s are mutually independent and circularly symmetric Gaussian distributed [48] which is also true when MMSE channel estimation is used [8]. The elements of the error vector $\boldsymbol{e}_j$ are assumed to be independent, and hence, we have $E[\boldsymbol{e}_j \boldsymbol{e}_j^H] = diag(2\sigma_{1j}^2, \ldots, 2\sigma_{Nj}^2)$ where $2\sigma_{kj}^2$ is the variance of $e_{kj}$, the $k$th complex element of the channel estimation error vector $\boldsymbol{e}_j$. Similarly, the elements of the estimated channel vector $\hat{\boldsymbol{h}}_j$ are independent, and the variance of $\hat{h}_{kj}$, the $k$th element of the vector $\hat{\boldsymbol{h}}_j$, is $2(1 - \sigma_{kj}^2)$. Since $\boldsymbol{h}_j$ and $\boldsymbol{e}_j$ are circularly symmetric Gaussian distributed and mutually independent, we can find from (4.4) that $\hat{\boldsymbol{h}}_j$ and $\boldsymbol{h}_j$ are jointly circularly symmetric Gaussian vectors, and the correlation coefficient between the $k$th elements of

$\boldsymbol{h}_j$ and $\hat{\boldsymbol{h}}_j$, $h_{kj}$ and $\hat{h}_{kj}$ respectively, can be written as

$$\rho_{kj} = \frac{E\left(\hat{h}^*_{kj} h_{kj}\right)}{\sqrt{E\left(|h_{kj}|^2\right) E\left(\left|\hat{h}_{kj}\right|^2\right)}} = \sqrt{1-\sigma^2_{kj}} \tag{4.5}$$

Note that since $E\,|h_{kj}|^2 = E\left|\hat{h}_{kj}\right|^2 + E\,|e_{kj}|^2$, then $E\,|e_{kj}|^2 \leq E\,|h_{kj}|^2 = 2$, and so $\sigma^2_{kj} = \frac{1}{2}E\,|e_{kj}|^2 \leq 1$. We see that the channel estimation model in (4.4) results in jointly circularly symmetric Gaussian distributed true and estimated channels, which is a crucial consequence that enables us to perform statistical analysis of the output SIR.

The same arguments hold for the true and estimated channels of the desired user. In other words,

$$\boldsymbol{h} = \hat{\boldsymbol{h}} + \boldsymbol{e} \tag{4.6}$$

where $\hat{\boldsymbol{h}}$ and $\boldsymbol{e}$ are the desired users' channel estimate and channel estimation error vectors, respectively. The $k$th elements of $\boldsymbol{h}$ and $\hat{\boldsymbol{h}}$, $h_k$ and $\hat{h}_k$ respectively, are jointly circularly symmetric Gaussian distributed with correlation coefficient $\rho_k$.

Throughout this chapter we assume that all the correlation coefficients are the same, i.e. $\rho_k = \rho_{kj} = \rho \;\forall\, k, j$. This assumption is reasonable if all the channels are estimated using the same type of estimator. Therefore, from (4.5), the channel estimate vectors are distributed as

$$\hat{\boldsymbol{h}} \sim CN_N(\boldsymbol{0}, 2\rho^2 \boldsymbol{I_N}) \text{ and } \hat{\boldsymbol{h}}_j \sim CN_N(\boldsymbol{0}, 2\rho^2 \boldsymbol{I_N}), \tag{4.7}$$

and for channel estimation error vectors we have

$$\boldsymbol{e} \sim CN_N\left(\boldsymbol{0}, 2\left(1-\rho^2\right)\boldsymbol{I_N}\right) \text{ and } \boldsymbol{e}_j \sim CN_N\left(\boldsymbol{0}, 2\left(1-\rho^2\right)\boldsymbol{I_N}\right). \tag{4.8}$$

To simplify the following analysis without loss of generality, we define vectors $\boldsymbol{s}$ and $\boldsymbol{s}_j$'s as

$$\boldsymbol{s} = \frac{\hat{\boldsymbol{h}}}{\rho} \text{ and } \boldsymbol{s}_j = \frac{\hat{\boldsymbol{h}}_j}{\rho} \tag{4.9}$$

Note that from (4.7) and (4.9), vectors $\boldsymbol{s}$ and $\boldsymbol{s}_j$'s are distributed as

$$\boldsymbol{s} \sim CN_N(\boldsymbol{0}, 2\boldsymbol{I}_N) \text{ and } \boldsymbol{s}_j \sim CN_N(\boldsymbol{0}, 2\boldsymbol{I}_N) \tag{4.10}$$

If the channels can be estimated without error at the receiver, the OC vector is a function of $\boldsymbol{h}$ and $\boldsymbol{h}_j$'s, the true channels of all users. However, in the presence of channel estimation errors the receiver performs diversity combining based on its channel estimates. In other words, the optimum combiner uses channel estimates $\hat{\boldsymbol{h}}$ and $\hat{\boldsymbol{h}}_j$'s instead of true channels $\boldsymbol{h}$ and $\boldsymbol{h}_j$'s. So, in this case, the OC vector would be only a function of channel estimates $\hat{\boldsymbol{h}}$ and $\hat{\boldsymbol{h}}_j$'s (or equivalently vectors $\boldsymbol{s}$ and $\boldsymbol{s}_j$'s) and can be written as [62]

$$\boldsymbol{u}^{oc} = \frac{\left(\sum_{j=1}^{L} \hat{\boldsymbol{h}}_j \hat{\boldsymbol{h}}_j^H\right)^{-1} \hat{\boldsymbol{h}}}{\left\|\left(\sum_{j=1}^{L} \hat{\boldsymbol{h}}_j \hat{\boldsymbol{h}}_j^H\right)^{-1} \hat{\boldsymbol{h}}\right\|} = \frac{\left(\sum_{j=1}^{L} \boldsymbol{s}_j \boldsymbol{s}_j^H\right)^{-1} \boldsymbol{s}}{\left\|\left(\sum_{j=1}^{L} \boldsymbol{s}_j \boldsymbol{s}_j^H\right)^{-1} \boldsymbol{s}\right\|} = \frac{\boldsymbol{R}^{-1}\boldsymbol{s}}{\left\|\boldsymbol{R}^{-1}\boldsymbol{s}\right\|} \tag{4.11}$$

where $\|.\|$ denotes the norm of a vector, and the matrix $\boldsymbol{R}$ is defined as

$$\boldsymbol{R} = \sum_{j=1}^{L} \boldsymbol{s}_j \boldsymbol{s}_j^H \tag{4.12}$$

By substituting (4.11) in (4.3), the SIR $\gamma^{oc}$ at the output of the optimum combiner is given by

$$\gamma^{oc} = \frac{P_D \boldsymbol{s}^H \boldsymbol{R}^{-1} \boldsymbol{h}\boldsymbol{h}^H \boldsymbol{R}^{-1} \boldsymbol{s}}{P_I \boldsymbol{s}^H \boldsymbol{R}^{-1} \left(\sum_{j=1}^{L} \boldsymbol{h}_j \boldsymbol{h}_j^H\right) \boldsymbol{R}^{-1} \boldsymbol{s}} \tag{4.13}$$

## 4.2 Statistical Analysis

In this section, we derive the exact expressions for the PDF of $\gamma^{oc}$ in (4.13) as well as the moments of $\gamma^{oc}$ and the outage probability. A list of mathematical functions used in this chapter is given in Appendix A.

To obtain the PDF of $\gamma^{oc}$, first we derive its PDF conditioned on channel estimates. Then the conditional PDF will be utilized to obtain the PDF of $\gamma^{oc}$.

### 4.2.1 Conditional SIR Distribution

To derive the conditional distribution of $\gamma^{oc}$, first we present a Theorem for the conditional PDF of $\gamma$ in (4.3), i.e. the SIR at the output of the combiner with an arbitrary combining vector $\boldsymbol{u}$. Then, we use that Theorem for the conditional PDF of $\gamma^{oc}$ as a special case.

**Theorem 4.1** *$\frac{LP_I}{P_D}\gamma$ conditioned on channel estimates $\boldsymbol{s}, \boldsymbol{s}_1, ..., \boldsymbol{s}_L$, for all $\boldsymbol{u}$ such that $\|\boldsymbol{u}\|^2 = 1$ and when $|\rho| < 1$, has a distribution of*

$$\frac{LP_I}{P_D}\gamma|\boldsymbol{s}, \boldsymbol{s}_1, ..., \boldsymbol{s}_L \sim F''_{2,2L}(\lambda_1, \lambda_2) \tag{4.14}$$

*where the symbol $F''_{\nu_1,\nu_2}(\delta_1, \delta_2)$ denotes a doubly noncentral F-distribution with $\nu_1, \nu_2$ degrees of freedom and non-centrality parameters $\delta_1, \delta_2$ [97]. Non-centrality parameters $\lambda_1$ and $\lambda_2$ in (4.14) can be expressed as*

$$\lambda_1 = \frac{\rho^2}{1-\rho^2}\boldsymbol{u}^H\boldsymbol{s}\boldsymbol{s}^H\boldsymbol{u}, \tag{4.15}$$

*and*

$$\lambda_2 = \frac{\rho^2}{1-\rho^2}\boldsymbol{u}^H\boldsymbol{R}\boldsymbol{u} \tag{4.16}$$

*where the matrix $\boldsymbol{R}$ is defined in (4.12).*

*From (4.14), the conditional PDF of $\gamma$ can be written as*

$$f_\gamma(\gamma|\boldsymbol{s},\boldsymbol{s}_1,...,\boldsymbol{s}_L)=f_\gamma\left(\gamma|\lambda_1,\lambda_2\right)=e^{-\left(\frac{\lambda_1+\lambda_2}{2}\right)}\sum_{j=0}^{\infty}\sum_{k=0}^{\infty}c(\gamma,j,k)\lambda_1^j\lambda_2^k \tag{4.17}$$

*where*

$$c(\gamma,j,k)=\left(\frac{P_D}{P_I}\right)^{k+L}\frac{\gamma^j}{\left(\frac{P_D}{P_I}+\gamma\right)^{j+k+L+1}2^{j+k}B(1+j,L+k)j!k!}, \tag{4.18}$$

*and the beta function $B(p,q)$ is defined in (A.3) in Appendix A.*

*Proof:* From (4.4), we have $\boldsymbol{h}_j=\hat{\boldsymbol{h}}_j+\boldsymbol{e}_j=\rho\boldsymbol{s}_j+\boldsymbol{e}_j$. Since channel estimation error vector $\boldsymbol{e}_j$ is independent from the channel estimates $\boldsymbol{s},\boldsymbol{s}_1,\ldots,\boldsymbol{s}_L$, we get

$$f_{\boldsymbol{h}_j}\left(\boldsymbol{h}_j|\boldsymbol{s},\boldsymbol{s}_1,\ldots,\boldsymbol{s}_L\right)=f_{\boldsymbol{e}_j}\left(\boldsymbol{h}_j-\rho\boldsymbol{s}_j|\boldsymbol{s},\boldsymbol{s}_1,\ldots,\boldsymbol{s}_L\right)=f_{\boldsymbol{e}_j}\left(\boldsymbol{h}_j-\rho\boldsymbol{s}_j\right) \tag{4.19}$$

Now, since from (4.8) $\boldsymbol{e}_j\sim CN_N\left(\boldsymbol{0},2\left(1-\rho^2\right)\boldsymbol{I}_N\right)$, from (4.19) we have

$$\boldsymbol{h}_j|\boldsymbol{s},\boldsymbol{s}_1,\ldots,\boldsymbol{s}_L\sim CN_N\left(\rho\boldsymbol{s}_j,2\left(1-\rho^2\right)\boldsymbol{I}_N\right) \tag{4.20}$$

As mentioned before, the diversity combining vector $\boldsymbol{u}$ is a function of estimated channel vectors. Therefore, $\boldsymbol{u}|\boldsymbol{s},\boldsymbol{s}_1,\ldots,\boldsymbol{s}_L$ is a deterministic vector, and from (4.20), we obtain

$$\boldsymbol{u}^H\boldsymbol{h}_j|\boldsymbol{s},\boldsymbol{s}_1,\ldots,\boldsymbol{s}_L\sim CN\left(\rho\boldsymbol{u}^H\boldsymbol{s}_j,2\left(1-\rho^2\right)\boldsymbol{u}^H\boldsymbol{u}\right)=CN\left(\rho\boldsymbol{u}^H\boldsymbol{s}_j,2\left(1-\rho^2\right)\right) \tag{4.21}$$

in which we have used the assumption that $\boldsymbol{u}^H\boldsymbol{u}=1$.

The equation (4.21) can also be written as

$$\frac{\boldsymbol{u}^H\boldsymbol{h}_j}{\sqrt{1-\rho^2}}\Big|\boldsymbol{s},\boldsymbol{s}_1,\ldots,\boldsymbol{s}_L\sim CN\left(\frac{\rho}{\sqrt{1-\rho^2}}\boldsymbol{u}^H\boldsymbol{s}_j,2\right) \tag{4.22}$$

If a $p$-dimensional random vector $\boldsymbol{g}$ has a multivariate normal distribution $N_p(\boldsymbol{m}, \boldsymbol{I}_p)$, then $\boldsymbol{g}^H\boldsymbol{g}$ is distributed as a noncentral chi-square with $p$ degrees of freedom and non-centrality parameter $\delta = \boldsymbol{m}^H\boldsymbol{m}$ [91, p. 60]. This distribution is denoted by $\chi_p^2(\delta)$ [90], [91] or ${\chi'_p}^2(\delta)$ [97] in the literature. In this Thesis, we use $\chi_p^2(\delta)$ to denote this distribution. So, from (4.22), we obtain

$$\varphi_j = \frac{\boldsymbol{u}^H\boldsymbol{h}_j\boldsymbol{h}_j^H\boldsymbol{u}}{1-\rho^2}\bigg|\boldsymbol{s}, \boldsymbol{s}_1, \ldots, \boldsymbol{s}_L \sim \chi_2^2\left(\frac{\rho^2}{1-\rho^2}\boldsymbol{u}^H\boldsymbol{s}_j\boldsymbol{s}_j^H\boldsymbol{u}\right) \tag{4.23}$$

The degrees of freedom for the noncentral chi-square variable in (4.23) is equal to two because the complex Gaussian random variable in (4.22) consists of two independent Gaussian random variables (the real part and the imaginary part) each with unit variance. Note that $\varphi_j$'s for $j = 1, \ldots, L$ are independent since channel estimation error vector $\boldsymbol{e}_j$'s for $j = 1, \ldots, L$ are independent. Now, to proceed with deriving the PDF of $\gamma$ in (4.3), we define $\psi$ as

$$\psi = \sum_{j=1}^{L}\varphi_j = \frac{1}{1-\rho^2}\boldsymbol{u}^H\left(\sum_{j=1}^{L}\boldsymbol{h}_j\boldsymbol{h}_j^H\right)\boldsymbol{u}\bigg|\boldsymbol{s}, \boldsymbol{s}_1, \ldots, \boldsymbol{s}_L \tag{4.24}$$

From (4.24) and (4.23), we see that $\psi$ is a summation of $L$ independent noncentral chi-square random variables. Therefore, $\psi$ in (4.24) is distributed as

$$\psi \sim \chi_{2L}^2\left(\frac{\rho^2}{1-\rho^2}\boldsymbol{u}^H\left(\sum_{j=1}^{L}\boldsymbol{s}_j\boldsymbol{s}_j^H\right)\boldsymbol{u}\right) = \chi_{2L}^2\left(\frac{\rho^2}{1-\rho^2}\boldsymbol{u}^H\boldsymbol{R}\boldsymbol{u}\right) = \chi_{2L}^2(\lambda_2) \tag{4.25}$$

where $\lambda_2$ is given by (4.16).

The equation (4.23) is written for the $j$th interfering user. A similar relation is also valid for the desired user, and we have

$$\varphi = \frac{\boldsymbol{u}^H\boldsymbol{h}\boldsymbol{h}^H\boldsymbol{u}}{1-\rho^2}\bigg|\boldsymbol{s}, \boldsymbol{s}_1, \ldots, \boldsymbol{s}_L \sim \chi_2^2\left(\frac{\rho^2}{1-\rho^2}\boldsymbol{u}^H\boldsymbol{s}\boldsymbol{s}^H\boldsymbol{u}\right) = \chi_2^2(\lambda_1) \tag{4.26}$$

where $\lambda_1$ is given by (4.15). Note that random variables $\varphi$ and $\psi$ in (4.26) and (4.24) are independent since the channel estimation error vector of the desired user, $\boldsymbol{e}$, is independent of the channel

estimation error vectors of the interfering users, $\boldsymbol{e}_j$'s.

If random variables $x_1$ and $x_2$ are independent and $x_1 \sim \chi^2_{\nu_1}(\delta_1)$ and $x_2 \sim \chi^2_{\nu_2}(\delta_2)$, then $x' = \frac{x_1/\nu_1}{x_2/\nu_2}$ has the doubly noncentral F-distribution of $F''_{\nu_1,\nu_2}(\delta_1, \delta_2)$ [97, p. 480]. Since independent random variables $\varphi$ and $\psi$ in (4.26) and (4.25) are distributed as $\varphi \sim \chi^2_2(\lambda_1)$ and $\psi \sim \chi^2_{2L}(\lambda_2)$, the distribution of $\frac{LP_I}{P_D}\gamma$ conditioned on $\boldsymbol{s}, \boldsymbol{s}_1, \ldots, \boldsymbol{s}_L$ is

$$\frac{LP_I}{P_D}\gamma|\boldsymbol{s}, \boldsymbol{s}_1, \ldots, \boldsymbol{s}_L = \frac{L\,\boldsymbol{u}^H\boldsymbol{h}\boldsymbol{h}^H\boldsymbol{u}}{\boldsymbol{u}^H\left(\sum_{j=1}^{L}\boldsymbol{h}_j\boldsymbol{h}_j^H\right)\boldsymbol{u}}\Bigg|\boldsymbol{s}, \boldsymbol{s}_1, \ldots, \boldsymbol{s}_L = \frac{\varphi/2}{\psi/(2L)} \sim F''_{2,2L}(\lambda_1, \lambda_2) \quad (4.27)$$

as stated in (4.14), and therefore, the conditional PDF of $\gamma$ is given by (4.17) [97, p. 499]. □

The following Corollary is an immediate result of Theorem 4.1.

**Corollary 4.1** *The conditional $\frac{LP_I}{P_D}\gamma^{oc}$ given channel estimates $\boldsymbol{s}, \boldsymbol{s}_1, ..., \boldsymbol{s}_L$ when $|\rho| < 1$, has a distribution of*

$$\frac{LP_I}{P_D}\gamma^{oc}\big|\boldsymbol{s}, \boldsymbol{s}_1, ..., \boldsymbol{s}_L \sim F''_{2,2L}(\lambda_1^{oc}, \lambda_2^{oc}) \quad (4.28)$$

*where*

$$\lambda_1^{oc} = \frac{\rho^2}{1-\rho^2}\frac{\left(\boldsymbol{s}^H\boldsymbol{R}^{-1}\boldsymbol{s}\right)^2}{\boldsymbol{s}^H\boldsymbol{R}^{-2}\boldsymbol{s}}, \quad (4.29)$$

*and*

$$\lambda_2^{oc} = \frac{\rho^2}{1-\rho^2}\frac{\boldsymbol{s}^H\boldsymbol{R}^{-1}\boldsymbol{s}}{\boldsymbol{s}^H\boldsymbol{R}^{-2}\boldsymbol{s}} \quad (4.30)$$

*Moreover, the conditional PDF of $\gamma^{oc}$ can be written as*

$$f_{\gamma^{oc}}\left(\gamma^{oc}|\boldsymbol{s}, \boldsymbol{s}_1, ..., \boldsymbol{s}_L\right) = f_{\gamma^{oc}}\left(\gamma^{oc}|\lambda_1^{oc}, \lambda_2^{oc}\right) = e^{-\left(\frac{\lambda_1^{oc}+\lambda_2^{oc}}{2}\right)}\sum_{j=0}^{\infty}\sum_{k=0}^{\infty} c\left(\gamma^{oc}, j, k\right)\left(\lambda_1^{oc}\right)^j\left(\lambda_2^{oc}\right)^k \quad (4.31)$$

*where $c(\gamma^{oc}, j, k)$ is given by (4.18).*

*Proof:* By substituting (4.11) in (4.15) and (4.16), the expressions of $\lambda_1^{oc}$ and $\lambda_2^{oc}$ can be derived as shown in (4.29) and (4.30). Then, by substituting (4.29) and (4.30) in (4.17) and (4.18), the PDF expression in (4.31) will be reached. □

### 4.2.2 SIR Distribution

In the last subsection, we obtained the analytical expression of conditional PDF $f_{\gamma^{oc}}\left(\gamma^{oc}|\lambda_1^{oc}, \lambda_2^{oc}\right)$ in (4.31). In this subsection, we use that conditional PDF to derive the PDF of $\gamma^{oc}$. In order to do this, first we express $\lambda_1^{oc}$ and $\lambda_2^{oc}$ in terms of auxiliary random variables with well-known distributions, and then, we average the conditional PDF in (4.31) over the joint distribution of these auxiliary random variables.

First, note that matrix $\boldsymbol{R}$ in (4.12) can be written as

$$\boldsymbol{R} = \boldsymbol{X}\boldsymbol{X}^H = (\boldsymbol{s}_1, \ldots, \boldsymbol{s}_L)\,(\boldsymbol{s}_1, \ldots, \boldsymbol{s}_L)^H \tag{4.32}$$

where $\boldsymbol{X} = (\boldsymbol{s}_1, \ldots, \boldsymbol{s}_L)$ is an $N \times L$ random matrix, and $L \geq N$. The columns of $\boldsymbol{X}$ are independent, and each column is a complex multivariate normal vector with zero mean and covariance matrix $2\boldsymbol{I}_N$, i.e. $\boldsymbol{s}_j \sim CN_N(\boldsymbol{0}, 2\boldsymbol{I}_N)$. Therefore, the matrix $\boldsymbol{R}$ has a complex Wishart distribution with $L$ degrees of freedom and covariance matrix $2\boldsymbol{I}_N$ [90], [91] denoted by

$$\boldsymbol{R} \sim CW_N(L, 2\boldsymbol{I}_N) \tag{4.33}$$

where the subscript on $CW$ shows the size of the matrix $\boldsymbol{R}$.

To proceed with expressing $\lambda_1^{oc}$ and $\lambda_2^{oc}$ in terms of random variables with well-known distributions, first we present the following Lemmas which are similar to the Theorems in [92, Ch. 3]. Those Theorems in [92, Ch. 3] are stated for the real Wishart distribution and can be generalized for the complex Wishart distribution by using the results in [99] as follows:

**Lemma 4.1** *Let $\boldsymbol{S} \sim CW_p(n, 2\boldsymbol{I}_p)$ and $\boldsymbol{\Gamma}(p \times p)$ be a constant unitary matrix, i.e. $\boldsymbol{\Gamma}^H\boldsymbol{\Gamma} = \boldsymbol{\Gamma}\boldsymbol{\Gamma}^H = \boldsymbol{I}_p$. Then $\boldsymbol{\Gamma}^H\boldsymbol{S}\boldsymbol{\Gamma} \sim CW_p(n, 2\boldsymbol{I}_p)$.*

**Lemma 4.2** *Let $\boldsymbol{S} \sim CW_p(n, 2\boldsymbol{I}_p)$ and $\boldsymbol{S} = \boldsymbol{T}\boldsymbol{T}^H$ where $\boldsymbol{T} = (t_{ij})$ is an upper triangular matrix with positive diagonal elements. Then $t_{ij}$'s for $1 \leq i \leq j \leq p$ are independently distributed, $t_{ii}^2 \sim \chi^2_{2(n-p+i)}$ for $1 \leq i \leq p$, and $t_{ij} \sim CN(0, 2)$ for $1 \leq i < j \leq p$.*

**Lemma 4.3** *Let $\boldsymbol{S} \sim CW_p(n, 2\boldsymbol{I}_p)$ and partition $\boldsymbol{S}$ as $\boldsymbol{S} = \begin{pmatrix} \boldsymbol{S}_{11} & \boldsymbol{S}_{12} \\ \boldsymbol{S}_{21} & \boldsymbol{S}_{22} \end{pmatrix}$ where $\boldsymbol{S}_{11}$ and $\boldsymbol{S}_{22}$ are $q \times q$ and $(p-q) \times (p-q)$ matrices, respectively. Then $\boldsymbol{S}_{22} \sim CW_{p-q}(n, 2\boldsymbol{I}_{p-q})$.*

**Lemma 4.4** *Let $\boldsymbol{S} \sim CW_p(n, 2\boldsymbol{I}_p)$ and $\boldsymbol{x} \sim CN_p(\boldsymbol{0}, 2\boldsymbol{I}_p)$ be independent. Then,*

$$\frac{n-p+1}{p}\boldsymbol{x}^H(\boldsymbol{C}^H\boldsymbol{C})^{-1}\boldsymbol{x} \sim F_{2p,2(n-p+1)} \tag{4.34}$$

*where $\boldsymbol{S} = \boldsymbol{C}\boldsymbol{C}^H$, the matrix $\boldsymbol{C}$ being nonsingular, and $F_{p,q}$ is the F-distribution with $p$ and $q$ degrees of freedom.*

Now, we present the following Theorem for the complex Wishart distribution, which is similar to Theorem 3.3.29 in [92] proved for the real Wishart distribution.

**Theorem 4.2** *If $\boldsymbol{A} \sim CW_p(n, 2\boldsymbol{I}_p)$, and $\boldsymbol{b}$ is a constant $p \times 1$ complex vector, and $\boldsymbol{b} \neq 0$, then we have*

$$\frac{\boldsymbol{b}^H\boldsymbol{A}^{-1}\boldsymbol{b}}{\boldsymbol{b}^H\boldsymbol{A}^{-2}\boldsymbol{b}} = \theta\xi \tag{4.35}$$

*and*

$$\frac{\left(\boldsymbol{b}^H\boldsymbol{A}^{-1}\boldsymbol{b}\right)^2}{\boldsymbol{b}^H\boldsymbol{A}^{-2}\boldsymbol{b}} = \boldsymbol{b}^H\boldsymbol{b}\theta \tag{4.36}$$

*where $\theta$ and $\xi$ are independent random variables. The PDFs of $\theta$ and $\xi$ are not functions of $\boldsymbol{b}$, and*

$$\theta \sim \textit{beta}(n-p+2, p-1) \qquad \textit{and} \qquad \xi \sim \chi^2_{2(n-p+1)} \tag{4.37}$$

*where beta$(p, q)$ denotes the beta distribution with parameters $p$ and $q$ [97], and $\chi^2_n$ indicates the chi-square distribution with $n$ degrees of freedom [93].*

*Proof:* The proof of this theorem is similar to that of Theorem $3.3.29$ in [92]. From Lemma 4.1, for $\boldsymbol{A} \sim CW_p(n, 2\boldsymbol{I}_p)$ and any unitary matrix $\boldsymbol{\Gamma}(p \times p)$ we have $\boldsymbol{\Gamma}^H \boldsymbol{A} \boldsymbol{\Gamma} \sim CW_p(n, 2\boldsymbol{I}_p)$. Let $\boldsymbol{V} = (v_{ij}) = \boldsymbol{\Gamma}^H \boldsymbol{A} \boldsymbol{\Gamma}$, and choose matrix $\boldsymbol{\Gamma} = \begin{pmatrix} (\boldsymbol{b}^H \boldsymbol{b})^{-\frac{1}{2}} \boldsymbol{b} & \boldsymbol{\Gamma}_1 \end{pmatrix}$ where $\boldsymbol{\Gamma}_1$ is a $p \times (p-1)$ matrix. Then $\boldsymbol{A}^{-1} = \boldsymbol{\Gamma} \boldsymbol{V}^{-1} \boldsymbol{\Gamma}^H$, $\boldsymbol{A}^{-2} = \boldsymbol{\Gamma} \boldsymbol{V}^{-2} \boldsymbol{\Gamma}^H$, and we get

$$\boldsymbol{b}^H \boldsymbol{A}^{-1} \boldsymbol{b} = \boldsymbol{b}^H \boldsymbol{b} v^{11} \tag{4.38}$$

and

$$\boldsymbol{b}^H \boldsymbol{A}^{-2} \boldsymbol{b} = \boldsymbol{b}^H \boldsymbol{b} \sum_{j=1}^{p} \left| v^{1j} \right|^2 \tag{4.39}$$

where $\boldsymbol{V}^{-1} = (v^{ij})$. So, from (4.38) and (4.39) we get

$$\frac{\boldsymbol{b}^H \boldsymbol{A}^{-1} \boldsymbol{b}}{\boldsymbol{b}^H \boldsymbol{A}^{-2} \boldsymbol{b}} = \frac{v^{11}}{\sum_{j=1}^{p} \left| v^{1j} \right|^2} \tag{4.40}$$

Now, let $\boldsymbol{V} = \boldsymbol{T} \boldsymbol{T}^H$, where $\boldsymbol{T}$ is an upper triangular matrix with positive diagonal elements and partition $\boldsymbol{T}$ as

$$\boldsymbol{T} = \begin{pmatrix} t_{11} & \boldsymbol{t}^H \\ 0 & \boldsymbol{T}_{22} \end{pmatrix} \tag{4.41}$$

and hence,

$$\boldsymbol{V} = \begin{pmatrix} t_{11}^2 + \boldsymbol{t}^H \boldsymbol{t} & \boldsymbol{t}^H \boldsymbol{T_{22}}^H \\ \boldsymbol{T}_{22} \boldsymbol{t} & \boldsymbol{T_{22}} \boldsymbol{T_{22}}^H \end{pmatrix} \tag{4.42}$$

where $\boldsymbol{t}^H = (t_{12}, \ldots, t_{1p})$, and $\boldsymbol{T}_{22}$ is a $(p-1) \times (p-1)$ upper triangular matrix. Then,

$$\boldsymbol{T}^{-1} = \begin{pmatrix} t_{11}^{-1} & -t_{11}^{-1}\boldsymbol{t}^H\boldsymbol{T}_{22}^{-1} \\ 0 & \boldsymbol{T}_{22}^{-1} \end{pmatrix} \tag{4.43}$$

and $\boldsymbol{V}^{-1}$ can be written as

$$\boldsymbol{V}^{-1} = \left(\boldsymbol{T}\boldsymbol{T}^H\right)^{-1} = \begin{pmatrix} t_{11}^{-2} & t_{11}^{-2}\boldsymbol{t}^H\boldsymbol{T}_{22}^{-1} \\ -t_{11}^{-2}\left(\boldsymbol{T}_{22}^H\right)^{-1}\boldsymbol{t} & \left(\boldsymbol{T}_{22}\boldsymbol{T}_{22}^H\right)^{-1} + t_{11}^{-2}\left(\boldsymbol{T}_{22}^H\right)^{-1}\boldsymbol{t}\boldsymbol{t}^H\boldsymbol{T}_{22}^{-1} \end{pmatrix} \tag{4.44}$$

From (4.40) and (4.44), we have

$$\frac{\boldsymbol{b}^H\boldsymbol{A}^{-1}\boldsymbol{b}}{\boldsymbol{b}^H\boldsymbol{A}^{-2}\boldsymbol{b}} = \frac{t_{11}^{-2}}{t_{11}^{-4} + t_{11}^{-4}\boldsymbol{t}^H\left(\boldsymbol{T}_{22}^H\boldsymbol{T}_{22}\right)^{-1}\boldsymbol{t}} = \frac{t_{11}^2}{1 + \boldsymbol{t}^H\left(\boldsymbol{T}_{22}^H\boldsymbol{T}_{22}\right)^{-1}\boldsymbol{t}} \tag{4.45}$$

From Lemma 4.2, $t_{11}$, $\boldsymbol{t}$ and $\boldsymbol{T}_{22}$ are independent, $t_{11}^2 \sim \chi^2_{2(n-p+1)}$ and $\boldsymbol{t} \sim CN_{p-1}(\boldsymbol{0}, 2\boldsymbol{I}_{p-1})$. From (4.42) by using Lemma 4.3, $\boldsymbol{T}_{22}\boldsymbol{T}_{22}^H \sim CW_{p-1}(n, 2\boldsymbol{I}_{p-1})$. Therefore, from Lemma 4.4 we get $\frac{n-p+2}{p-1}\boldsymbol{t}^H\left(\boldsymbol{T}_{22}^H\boldsymbol{T}_{22}\right)^{-1}\boldsymbol{t} \sim F_{2(p-1),2(n-p+2)}$, and hence [93], $\frac{1}{1+\boldsymbol{t}^H\left(\boldsymbol{T}_{22}^H\boldsymbol{T}_{22}\right)^{-1}\boldsymbol{t}} \sim$ beta $(n-p+2, p-1)$. So, (4.45) can be written as

$$\frac{\boldsymbol{b}^H\boldsymbol{A}^{-1}\boldsymbol{b}}{\boldsymbol{b}^H\boldsymbol{A}^{-2}\boldsymbol{b}} = \theta\xi \tag{4.46}$$

where

$$\theta = \frac{1}{1 + \boldsymbol{t}^H\left(\boldsymbol{T}_{22}^H\boldsymbol{T}_{22}\right)^{-1}\boldsymbol{t}} \sim \text{beta}(n-p+2, p-1) \qquad \text{and} \qquad \xi = t_{11}^2 \sim \chi^2_{2(n-p+1)} \tag{4.47}$$

and random variables $\theta$ and $\xi$ are independent. Equations (4.46) and (4.47) are stated in (4.35) and (4.37).

Now to derive (4.36), from (4.38) and (4.39) we have

$$\frac{\left(\boldsymbol{b}^H\boldsymbol{A}^{-1}\boldsymbol{b}\right)^2}{\boldsymbol{b}^H\boldsymbol{A}^{-2}\boldsymbol{b}} = \frac{\boldsymbol{b}^H\boldsymbol{b}\left(v^{11}\right)^2}{\sum_{j=1}^{p}\left|v^{1j}\right|^2} \tag{4.48}$$

From (4.44), equation (4.48) can be written as

$$\frac{\left(\boldsymbol{b}^H \boldsymbol{A}^{-1} \boldsymbol{b}\right)^2}{\boldsymbol{b}^H \boldsymbol{A}^{-2} \boldsymbol{b}} = \frac{\boldsymbol{b}^H \boldsymbol{b} t_{11}^{-4}}{t_{11}^{-4} + t_{11}^{-4} \boldsymbol{t}^H \left(\boldsymbol{T}_{22}^H \boldsymbol{T}_{22}\right)^{-1} \boldsymbol{t}} = \frac{\boldsymbol{b}^H \boldsymbol{b}}{1 + \boldsymbol{t}^H \left(\boldsymbol{T}_{22}^H \boldsymbol{T}_{22}\right)^{-1} \boldsymbol{t}} \tag{4.49}$$

So, from (4.47) and (4.49) we get

$$\frac{\left(\boldsymbol{b}^H \boldsymbol{A}^{-1} \boldsymbol{b}\right)^2}{\boldsymbol{b}^H \boldsymbol{A}^{-2} \boldsymbol{b}} = \boldsymbol{b}^H \boldsymbol{b} \theta \tag{4.50}$$

as expressed in (4.36). □

The next Corollary, which results from Theorem 4.2, expresses random variables $\lambda_1^{oc}$ and $\lambda_2^{oc}$ in terms of random variables with well-known distributions.

**Corollary 4.2** *Non-centrality parameters $\lambda_2^{oc}$ and $\lambda_1^{oc}$ in (4.30) and (4.29) can be written as*

$$\lambda_2^{oc} = \frac{\rho^2}{1 - \rho^2} xy \tag{4.51}$$

*and*

$$\lambda_1^{oc} = \frac{\rho^2}{1 - \rho^2} xz \tag{4.52}$$

*where $x$, $y$ and $z$ are independent random variables, and*

$$x \sim \textit{beta}(L - N + 2, N - 1), \tag{4.53}$$

$$y \sim \chi^2_{2(L-N+1)} \tag{4.54}$$

*and*

$$z \sim \chi^2_{2N} \tag{4.55}$$

*Proof:* Since the vector $\boldsymbol{s}$ and the matrix $\boldsymbol{R}$ are independent, and $\boldsymbol{R} \sim CW_N(L, 2\boldsymbol{I}_N)$, the random variables $\lambda_2^{oc}$ and $\lambda_1^{oc}$ in (4.30) and (4.29) conditioned on $\boldsymbol{s}$, according to (4.35) and (4.36) in Theorem 4.2, can be written as

$$\lambda_2^{oc}|\boldsymbol{s} = \frac{\rho^2}{1-\rho^2}(x|\boldsymbol{s})(y|\boldsymbol{s}) \tag{4.56}$$

and

$$\lambda_1^{oc}|\boldsymbol{s} = \frac{\rho^2}{1-\rho^2}\boldsymbol{s}^H\boldsymbol{s}(x|\boldsymbol{s}) \tag{4.57}$$

where $x|\boldsymbol{s}$ and $y|\boldsymbol{s}$ are independent random variables and from (4.37) are distributed as

$$x|\boldsymbol{s} \sim \text{beta}(L-N+2, N-1) \text{ and } y|\boldsymbol{s} \sim \chi^2_{2(L-N+1)} \tag{4.58}$$

Now, from (4.56) and (4.57), we get

$$\lambda_2^{oc} = \frac{\rho^2}{1-\rho^2}xy \tag{4.59}$$

and

$$\lambda_1^{oc} = \frac{\rho^2}{1-\rho^2}\boldsymbol{s}^H\boldsymbol{s}x \tag{4.60}$$

In order to find the distribution of $x$ and $y$ , note that from (4.58), the PDF's of $x|\boldsymbol{s}$ and $y|\boldsymbol{s}$ are not functions of $\boldsymbol{s}$, and hence, random variables $x$ and $y$ are independent of $\boldsymbol{s}$. Therefore, from (4.58), $x$ and $y$ are distributed as

$$x \sim \text{beta}(L-N+2, N-1) \text{ and } y \sim \chi^2_{2(L-N+1)} \tag{4.61}$$

as defined in (4.53) and (4.54). Also note that $x$ and $y$ are independent since the joint distribution of $x$ and $y$ can be written as $f_{xy}(x,y) = \int f_{xy}(x,y|\boldsymbol{s})f_{\boldsymbol{s}}(\boldsymbol{s})d\boldsymbol{s} = \int f_x(x|\boldsymbol{s})f_y(y|\boldsymbol{s})f_{\boldsymbol{s}}(\boldsymbol{s})d\boldsymbol{s} = \int f_x(x)f_y(y)f_{\boldsymbol{s}}(\boldsymbol{s})d\boldsymbol{s} = f_x(x)f_y(y)\int f_{\boldsymbol{s}}(\boldsymbol{s})d\boldsymbol{s} = f_x(x)f_y(y)$.

By defining

$$z = \boldsymbol{s}^H \boldsymbol{s} \tag{4.62}$$

non-centrality parameter $\lambda_1^{oc}$ in (4.60) can be written as

$$\lambda_1^{oc} = \frac{\rho^2}{1-\rho^2} xz \tag{4.63}$$

Since from (4.10) $\boldsymbol{s} \sim CN_N(0, 2\boldsymbol{I}_N)$, random variable $z$ in (4.62) is distributed as

$$z \sim \chi^2_{2N} \tag{4.64}$$

as defined in (4.55). Note that since random variables $x$ and $y$ are independent from $\boldsymbol{s}$, they are also independent from $z$ in (4.62). □

Now, from Corollary 4.2, we can rewrite the conditional PDF in (4.31) according to the following Corollary.

**Corollary 4.3** *The conditional PDF in (4.31) can be expressed in terms of random variables $x$, $y$ and $z$ in (4.53)-(4.55) as*

$$f_{\gamma^{oc}}(\gamma^{oc}|x,y,z) = e^{-\frac{\rho^2(xz+xy)}{2(1-\rho^2)}} \sum_{j=0}^{\infty}\sum_{k=0}^{\infty} c(\gamma^{oc},j,k) \left(\frac{\rho^2}{1-\rho^2}\right)^{j+k} x^{j+k} z^j y^k \tag{4.65}$$

where $c(\gamma^{oc}, j, k)$ is given by (4.18).

*Proof:* The expression in (4.65) can be directly obtained by substituting (4.51) and (4.52) in (4.31). □

Now, we can derive the PDF of $\gamma^{oc}$ as stated in the following Theorem.

**Theorem 4.3** *The PDF of $\gamma^{oc}$ for $|\rho| < 1$ can be expressed as*

$$f_{\gamma^{oc}}(\gamma^{oc}) = \frac{L\left(1-\rho^2\right)^{L-N+2}}{\left(\frac{P_D}{P_I}+\gamma^{oc}\right)^{L+1}} \left(\frac{P_D}{P_I}\right)^L {}_2F_2\left[L-N+2, N, L-N+1; 1, L; \frac{\rho^2\gamma^{oc}}{\frac{P_D}{P_I}+\gamma^{oc}}, \frac{\frac{P_D}{P_I}\rho^2}{\frac{P_D}{P_I}+\gamma^{oc}}\right] \tag{4.66}$$

*where $F_2[a, b, b'; c, c'; v, w]$ is the Appell hypergeometric function defined as [94]*

$$F_2[a, b, b'; c, c'; v, w] = \sum_{j=0}^{\infty} \sum_{k=0}^{\infty} \frac{(a)_{j+k}(b)_j(b')_k}{(c)_j(c')_k} \frac{v^j}{j!} \frac{w^k}{k!} \tag{4.67}$$

*and the Pochhammer symbol $(a)_j$ is defined in (A.2) in Appendix A.*

*Proof:* The PDF expression in (4.66) can be obtained by integrating the conditional PDF in (4.65) over the joint distribution of $x$, $y$ and $z$ in (4.53)-(4.55). Since according to Corollary 4.2 random variables $x$, $y$ and $z$ are independent, from (4.65) the PDF of $\gamma^{oc}$ can be written as

$$\begin{aligned} f_{\gamma^{oc}}(\gamma^{oc}) &= \int\int\int f_{\gamma^{oc}}(\gamma^{oc}|x, y, z)\, f_x(x) f_y(y) f_z(z) dx dy dz \\ &= \sum_{j=0}^{\infty} \sum_{k=0}^{\infty} c(\gamma^{oc}, j, k) \left(\frac{\rho^2}{1-\rho^2}\right)^{j+k} \\ &\quad \times \int_0^1 x^{j+k} \left(\int_0^{\infty} e^{-\frac{\rho^2 xz}{2(1-\rho^2)}} z^j f_z(z) dz\right) \left(\int_0^{\infty} e^{-\frac{\rho^2 xy}{2(1-\rho^2)}} y^k f_y(y) dy\right) f_x(x) dx \end{aligned} \tag{4.68}$$

where the PDFs of $x$, $y$, and $z$ in (4.53)-(4.55) are [93]

$$f_x(x) = \frac{\Gamma(L+1)}{\Gamma(L-N+2)\Gamma(N-1)} x^{L-N+1}(1-x)^{N-2}, \qquad 0 \le x \le 1 \tag{4.69}$$

$$f_y(y) = \frac{y^{L-N}}{2^{L-N+1}\Gamma(L-N+1)} e^{-y/2}, \qquad y \ge 0 \tag{4.70}$$

and

$$f_z(z) = \frac{z^{N-1}}{2^N \Gamma(N)} e^{-z/2}, \qquad z \ge 0 \tag{4.71}$$

where the Gamma function $\Gamma(\cdot)$ is defined in (A.1) in Appendix A.

The integral term in (4.68) can be calculated as [96, eqs. (3.381.4), (3.197.4)]

$$\begin{aligned}
&\int_0^1 x^{j+k}\left(\int_0^\infty e^{-\frac{\rho^2 xz}{2(1-\rho^2)}} z^j f_z(z)dz\right)\left(\int_0^\infty e^{-\frac{\rho^2 xy}{2(1-\rho^2)}} y^k f_y(y)dy\right) f_x(x)dx \\
&= 2^{j+k}(N)_j(L-N+1)_k \int_0^1 \left(\frac{1-\rho^2}{1+\rho^2(x-1)}\right)^{j+k+L+1} x^{j+k} f_x(x)dx \\
&= \frac{2^{j+k}(L-N+2)_{j+k}(N)_j(L-N+1)_k}{(L+1)_{j+k}}\left(1-\rho^2\right)^{L-N+j+k+2}
\end{aligned} \tag{4.72}$$

Now, by substituting (4.18) and (4.72) in (4.68), we get

$$f_{\gamma^{oc}}(\gamma^{oc}) = \frac{(1-\rho^2)^{L-N+2}}{\left(\frac{P_D}{P_I}+\gamma\right)^{L+1}}\left(\frac{P_D}{P_I}\right)^L \sum_{j=0}^{\infty}\sum_{k=0}^{\infty} \frac{(L-N+2)_{j+k}(N)_j(L-N+1)_k \rho^{2(j+k)}(\gamma^{oc})^j \left(\frac{P_D}{P_I}\right)^k}{(L+1)_{j+k}B(j+1,k+L)j!k!\left(\frac{P_D}{P_I}+\gamma^{oc}\right)^{j+k}} \tag{4.73}$$

From (A.4) and (A.2), the expression in (4.73) can be simplified to

$$\begin{aligned}
f_{\gamma^{oc}}(\gamma^{oc}) = &\frac{L\,(1-\rho^2)^{L-N+2}}{\left(\frac{P_D}{P_I}+\gamma^{oc}\right)^{L+1}}\left(\frac{P_D}{P_I}\right)^L \\
&\times \sum_{j=0}^{\infty}\sum_{k=0}^{\infty} \frac{(L-N+2)_{j+k}(N)_j(L-N+1)_k}{(1)_j(L)_k j!k!}\left(\frac{\rho^2\gamma^{oc}}{\frac{P_D}{P_I}+\gamma^{oc}}\right)^j \left(\frac{\frac{P_D}{P_I}\rho^2}{\frac{P_D}{P_I}+\gamma^{oc}}\right)^k
\end{aligned} \tag{4.74}$$

which results in (4.66). □

The infinite series in (4.67) is convergent for $|v|+|w|<1$ [94]. Therefore, for $|\rho|<1$ the PDF expression in (4.66) is convergent since $\left|\frac{\rho^2\gamma^{oc}}{\frac{P_D}{P_I}+\gamma^{oc}}\right| + \left|\frac{\frac{P_D}{P_I}\rho^2}{\frac{P_D}{P_I}+\gamma^{oc}}\right| = |\rho^2| < 1$.

For $|\rho|=1$, the PDF of $\gamma^{oc}$ is obtained in [65, eq. (13)] and can be expressed as

$$f_{\gamma^{oc}}(\gamma^{oc}) = \frac{\left(\frac{P_D}{P_I}\right)^{L-N+1}(\gamma^{oc})^{N-1}}{B(N,L-N+1)\left(\frac{P_D}{P_I}+\gamma^{oc}\right)^{L+1}} \tag{4.75}$$

Note that for $\rho = 0$, the PDF expression in (4.74) can be simplified to

$$f_{\gamma^{oc}}(\gamma^{oc}) = \frac{L\left(\frac{P_D}{P_I}\right)^L}{\left(\frac{P_D}{P_I} + \gamma^{oc}\right)^{L+1}} \qquad \text{for } \rho = 0 \tag{4.76}$$

Expression (4.76) shows that for $\rho = 0$ the PDF of SIR is not a function of $N$, the number of antennas.

Now, we study the PDF expression in (4.74) for the special case of $N = 1$. To simplify the PDF expression for $N = 1$, we use the following equation [95, eq. (1.4.9)]

$$\sum_{j=0}^{\infty}\sum_{k=0}^{\infty} g(j+k)\frac{v^j}{j!}\frac{w^k}{k!} = \sum_{l=0}^{\infty}\frac{g(l)}{l!}(v+w)^l \tag{4.77}$$

where $g(j+k)$ is a function of the sum of the indices of summation only, not involving them separately. From (4.77), the expression (4.74) for $N = 1$ can be written as

$$\begin{aligned} f_{\gamma^{oc}}(\gamma^{oc}) &= \frac{L\left(1-\rho^2\right)^{L+1}}{\left(\frac{P_D}{P_I} + \gamma^{oc}\right)^{L+1}}\left(\frac{P_D}{P_I}\right)^L \sum_{j=0}^{\infty}\sum_{k=0}^{\infty}\frac{(L+1)_{j+k}}{j!k!}\left(\frac{\rho^2\gamma^{oc}}{\frac{P_D}{P_I} + \gamma^{oc}}\right)^j\left(\frac{\frac{P_D}{P_I}\rho^2}{\frac{P_D}{P_I} + \gamma^{oc}}\right)^k \\ &= \frac{L\left(1-\rho^2\right)^{L+1}}{\left(\frac{P_D}{P_I} + \gamma^{oc}\right)^{L+1}}\left(\frac{P_D}{P_I}\right)^L \sum_{l=0}^{\infty}\frac{(L+1)_l}{l!}\left(\frac{\rho^2\gamma^{oc}}{\frac{P_D}{P_I} + \gamma^{oc}} + \frac{\frac{P_D}{P_I}\rho^2}{\frac{P_D}{P_I} + \gamma^{oc}}\right)^l \\ &= \frac{L\left(1-\rho^2\right)^{L+1}}{\left(\frac{P_D}{P_I} + \gamma^{oc}\right)^{L+1}}\left(\frac{P_D}{P_I}\right)^L \sum_{l=0}^{\infty}\frac{(L+1)_l}{l!}\left(\rho^2\right)^l \qquad \text{for } N = 1 \end{aligned} \tag{4.78}$$

To simplify the expression (4.78) further, we use the Taylor series $(1-v)^{-a} = \sum_{j=0}^{\infty}\frac{(a)_j}{j!}v^j$ to obtain

$$f_{\gamma^{oc}}(\gamma^{oc}) = \frac{L\left(1-\rho^2\right)^{L+1}}{\left(\frac{P_D}{P_I} + \gamma^{oc}\right)^{L+1}}\left(\frac{P_D}{P_I}\right)^L\left(1-\rho^2\right)^{-(L+1)} = \frac{L\left(\frac{P_D}{P_I}\right)^L}{\left(\frac{P_D}{P_I} + \gamma^{oc}\right)^{L+1}} \qquad \text{for } N = 1 \tag{4.79}$$

Expression (4.79) shows that for $N = 1$ the PDF of SIR is not a function of $\rho$. This result can

be justified as follows: For $N = 1$ no diversity combining is possible, and hence, channel estimates at the receiver cannot be used to perform any type of combining. Therefore, the quality of channel estimates, as measured by $|\rho|$, has no impact on the SIR and its PDF.

Note that (4.79) is the same expression as (4.76). Therefore, we have

$$f_{\gamma^{oc}}(\gamma^{oc}) = \frac{L\left(\frac{P_D}{P_I}\right)^L}{\left(\frac{P_D}{P_I} + \gamma^{oc}\right)^{L+1}} \qquad \text{for } N = 1 \text{ or } \rho = 0 \tag{4.80}$$

Note that since from (4.80) the PDF expression for $N = 1$ is the same for all $\rho$'s, the expression (4.80) should be equal to the result with perfect channel estimation ($\rho = 1$) when $N = 1$, and indeed (4.80) is identical to the expression for the PDF of SIR in the case of perfect channel estimation in (4.75) when $N = 1$.

## 4.3 Performance Analysis

In this section, we use PDF expression (4.66), or equivalently (4.73) , to derive analytical expressions for other measures of performance such as the moments of SIR, outage probability and average bit error probability.

### 4.3.1 Moments of SIR

The $n$th moment of $\gamma^{oc}$ when $|\rho| < 1$, from (4.73), can be written as

$$\begin{aligned} E\left((\gamma^{oc})^n\right) &= \left(1-\rho^2\right)^{L-N+2}\left(\frac{P_D}{P_I}\right)^L \sum_{j=0}^{\infty}\sum_{k=0}^{\infty} \frac{(L-N+2)_{j+k}(N)_j(L-N+1)_k\rho^{2(j+k)}\left(\frac{P_D}{P_I}\right)^k}{(L+1)_{j+k}j!k!B(j+1,k+L)} \\ &\quad \times \int_0^{\infty} \frac{(\gamma^{oc})^{j+n}}{\left(\frac{P_D}{P_I}+\gamma^{oc}\right)^{j+k+L+1}} d\gamma^{oc} \end{aligned} \tag{4.81}$$

From (A.3), the integral term in (4.81), for $n < k + L$ can be written in terms of the beta

function:

$$\int_0^\infty \frac{(\gamma^{oc})^{j+n}}{\left(\frac{P_D}{P_I}+\gamma^{oc}\right)^{j+k+L+1}} d\gamma^{oc} = \frac{B(j+n+1, k+L-n)}{\left(\frac{P_D}{P_I}\right)^{k+L-n}} \tag{4.82}$$

When $n \geq k+L$, the integral term in (4.81) is infinite since the order of the denominator is not greater than the order of the numerator plus one.

By substituting (4.82) in (4.81), and from (A.4) and (A.2), the expression of the $n$th moment of $\gamma^{oc}$ for $|\rho| < 1$ when $n < L$ can be simplified to

$$\begin{aligned} E\left((\gamma^{oc})^n\right) = & \frac{\Gamma(n+1)\Gamma(L-n)\left(1-\rho^2\right)^{L-N+2}}{\Gamma(L)} \left(\frac{P_D}{P_I}\right)^n \\ & \times \sum_{j=0}^{\infty}\sum_{k=0}^{\infty} \frac{(L-N+2)_{j+k}(N)_j(n+1)_j(L-N+1)_k(L-n)_k\rho^{2(j+k)}}{(L+1)_{j+k}(1)_j(L)_k j!k!} \end{aligned} \tag{4.83}$$

and is infinite for $n \geq L$.

Now, from (4.83), when $|\rho| < 1$ the $n$th moment of $\gamma^{oc}$ for $n \geq L$ is infinite, and for $n < L$ can be expressed as

$$\begin{aligned} E\left((\gamma^{oc})^n\right) = & \frac{\Gamma(n+1)\Gamma(L-n)\left(1-\rho^2\right)^{L-N+2}}{\Gamma(L)} \left(\frac{P_D}{P_I}\right)^n \\ & \times F_{1:1;1}^{1:2;2}\left[\begin{matrix} L-N+2 : N, n+1 \ ; \ L-N+1, L-n \ ; \\ \\ L+1 \quad : \quad 1 \quad ; \quad L \quad ; \end{matrix} \begin{matrix} \\ \\ \rho^2, \rho^2 \end{matrix}\right] \end{aligned} \tag{4.84}$$

where the Gamma function $\Gamma(\cdot)$ is defined in (A.1) in Appendix A, and the Kampé de Fériet

function $F_{1:1;1}^{1:2;2}\left[\begin{array}{ccccccc} a & : & b_1, b_2 & ; & c_1, c_2 & ; & \\ & & & & & & v, w \\ \alpha & : & \beta & ; & \gamma & ; & \end{array}\right]$ is defined as [94]

$$F_{1:1;1}^{1:2;2}\left[\begin{array}{ccccccc} a & : & b_1, b_2 & ; & c_1, c_2 & ; & \\ & & & & & & v, w \\ \alpha & : & \beta & ; & \gamma & ; & \end{array}\right] = \sum_{j=0}^{\infty}\sum_{k=0}^{\infty} \frac{(a)_{j+k}(b_1)_j(b_2)_j(c_1)_k(c_2)_k}{(\alpha)_{j+k}(\beta)_j(\gamma)_k}\frac{v^j}{j!}\frac{w^k}{k!} \quad (4.85)$$

and is convergent if $\max(|v|,|w|) < 1$. Therefore, for $|\rho| < 1$ the expression (4.84) is convergent since $\max(|\rho^2|,|\rho^2|) = |\rho^2| < 1$.

When $|\rho| = 1$, from (4.75), (A.3) and (A.4), the $n$th moment of SIR for $n < L - N + 1$ can be written as

$$\begin{aligned} E\Big((\gamma^{oc})^n\Big) &= \frac{\left(\frac{P_D}{P_I}\right)^{L-N+1}}{B(N, L-N+1)}\int_0^{\infty}\frac{(\gamma^{oc})^{N+n-1}}{\left(\frac{P_D}{P_I}+\gamma^{oc}\right)^{L+1}}d\gamma^{oc} \\ &= \frac{\left(\frac{P_D}{P_I}\right)^{L-N+1}}{B(N, L-N+1)}B(N+n, L-N+1-n)\left(\frac{P_D}{P_I}\right)^{N+n-L-1} \\ &= \frac{\Gamma(n+N)\Gamma(L-N+1-n)\left(\frac{P_D}{P_I}\right)^n}{\Gamma(N)\Gamma(L-N+1)} \end{aligned} \quad (4.86)$$

and is infinite when $n \geq L - N + 1$.

The expression (4.86) is equivalent to [66, eq. (21)] when the desired user is subject to Rayleigh fading, i.e. when the parameter $D$ in [66, eq. (21)] is equal to zero. For $n = 1$, expression (4.86) reduces to [65, eq. (14)].

From (4.77), the expression (4.83) for $N = 1$ can be simplified to

$$\begin{aligned} E\left((\gamma^{oc})^n\right) &= \frac{\Gamma(n+1)\Gamma(L-n)\left(1-\rho^2\right)^{L+1}}{\Gamma(L)}\left(\frac{P_D}{P_I}\right)^n \sum_{j=0}^{\infty}\frac{(n+1)_j}{j!}\left(\rho^2\right)^j \sum_{k=0}^{\infty}\frac{(L-n)_k}{k!}\left(\rho^2\right)^k \\ &= \frac{\Gamma(n+1)\Gamma(L-n)\left(1-\rho^2\right)^{L+1}}{\Gamma(L)}\left(\frac{P_D}{P_I}\right)^n \left(1-\rho^2\right)^{-(n+1)}\left(1-\rho^2\right)^{-(L-n)} \\ &= \frac{\Gamma(n+1)\Gamma(L-n)}{\Gamma(L)}\left(\frac{P_D}{P_I}\right)^n \qquad \text{for } N=1 \end{aligned} \tag{4.87}$$

Note that for $\rho = 0$, the expression in (4.83) can also be simplified to expression (4.87). Therefore, the $n$th moment of $\gamma^{oc}$ for $\rho = 0$ or $N = 1$ can be simplified to

$$E\left((\gamma^{oc})^n\right) = \frac{\Gamma(n+1)\Gamma(L-n)}{\Gamma(L)}\left(\frac{P_D}{P_I}\right)^n \qquad \text{for } N=1 \text{ or } \rho=0 \tag{4.88}$$

which is equivalent to the expression of the $n$th moment of SIR in the case of perfect channel estimation in (4.86) when there is only one antenna at the receiver ($N = 1$). For $n = 1$, (4.88) becomes

$$E(\gamma^{oc}) = \frac{P_D}{P_I(L-1)} \qquad \text{for } N=1 \text{ or } \rho=0 \tag{4.89}$$

Therefore, from (4.89), we observe that as $\rho$ goes to zero, the average SIR falls to the level attained when there is only one antenna, regardless of the actual number of antennas, $N$. Moreover, for $N = 1$ the average SIR is independent of the value of $\rho$.

### 4.3.2 Outage Probability

From (4.73), the outage probability when $|\rho| < 1$ can be written as

$$\begin{aligned} P_{out} &= \int_0^{\gamma_0} f_{\gamma^{oc}}(\gamma^{oc}) d\gamma^{oc} \\ &= \left(1-\rho^2\right)^{L-N+2} \left(\frac{P_D}{P_I}\right)^L \sum_{j=0}^{\infty}\sum_{k=0}^{\infty} \frac{(L-N+2)_{j+k}(N)_j(L-N+1)_k \rho^{2(j+k)} \left(\frac{P_D}{P_I}\right)^k}{(L+1)_{j+k} j!k! B(j+1,k+L)} \\ &\quad \times \int_0^{\gamma_0} \frac{(\gamma^{oc})^j}{\left(\frac{P_D}{P_I}+\gamma^{oc}\right)^{j+k+L+1}} d\gamma^{oc} \end{aligned} \tag{4.90}$$

From (A.5), the integral term in (4.90) can be written in terms of the incomplete beta function:

$$\int_0^{\gamma_0} \frac{(\gamma^{oc})^j}{\left(\frac{P_D}{P_I}+\gamma^{oc}\right)^{j+k+L+1}} d\gamma^{oc} = \frac{B_{\frac{\gamma_0}{\frac{P_D}{P_I}+\gamma_0}}(j+1,k+L)}{\left(\frac{P_D}{P_I}\right)^{k+L}} \tag{4.91}$$

By substituting (4.91) in (4.90), the outage probability when $|\rho| < 1$ can be simplified to

$$\begin{aligned} P_{out} &= \left(1-\rho^2\right)^{L-N+2} \sum_{j=0}^{\infty}\sum_{k=0}^{\infty} \frac{(L-N+2)_{j+k}(N)_j(L-N+1)_k \rho^{2(j+k)}}{(L+1)_{j+k} j!k! B(j+1,k+L)} B_{\frac{\gamma_0}{\frac{P_D}{P_I}+\gamma_0}}(j+1,k+L) \\ &= \left(1-\rho^2\right)^{L-N+2} \sum_{j=0}^{\infty}\sum_{k=0}^{\infty} \frac{(L-N+2)_{j+k}(N)_j(L-N+1)_k \rho^{2(j+k)}}{(L+1)_{j+k} j!k!} I_{\frac{\gamma_0}{\frac{P_D}{P_I}+\gamma_0}}(j+1,k+L) \end{aligned} \tag{4.92}$$

where the regularized incomplete beta function $I_w(a,b)$ is defined in (A.6).

From (A.3) and (A.5), we see that for real $p$ and $q$ the $B(p,q)$ and $B_w(p,q)$ are real and non-negative, and $B_w(p,q)$ is always less than or equal to $B(p,q)$ for $0 \le w \le 1$. Hence, from (A.6), $0 \le I_w(p,q) \le 1$ for $0 \le w \le 1$ when $p$ and $q$ are real. Therefore, the infinite summation in (4.92) is upper bounded by

$$UB_{P_{out}} = \left(1-\rho^2\right)^{L-N+2} \sum_{j=0}^{\infty}\sum_{k=0}^{\infty} \frac{(L-N+2)_{j+k}(N)_j(L-N+1)_k}{(L+1)_{j+k}} \frac{(\rho^2)^j}{j!} \frac{(\rho^2)^k}{k!} \tag{4.93}$$

Each term in (4.92) is less than or equal to the corresponding term in (4.93). The expression (4.93) is equal to (4.83) when $n = 0$. We showed in the last section that (4.83) is convergent for $|\rho| < 1$. So, (4.93) is convergent when $|\rho| < 1$, and thus the outage probability expression in (4.92) is convergent as well for $|\rho| < 1$. Note that (4.93) is actually equal to one since from (4.83) for $n = 0$ we have $E\left((\gamma^{oc})^0\right) = E(1) = 1$. Moreover, since from (A.3), (A.5) and (A.6), $I_1(a, b) = 1$ $\forall\, a, b$, the expression (4.93) is equal to the outage probability when $\gamma_0 \to \infty$ which is equal to one as well.

When $|\rho| = 1$, from (4.75), (A.5) and (A.6), the outage probability can be expressed as

$$\begin{aligned} P_{out} &= \frac{\left(\frac{P_D}{P_I}\right)^{L-N+1}}{B(N, L-N+1)} \int_0^{\gamma_0} \frac{(\gamma^{oc})^{N-1}}{\left(\frac{P_D}{P_I} + \gamma^{oc}\right)^{L+1}} d\gamma^{oc} \\ &= \frac{\left(\frac{P_D}{P_I}\right)^{L-N+1}}{B(N, L-N+1)} B_{\frac{\gamma_0}{\frac{P_D}{P_I}+\gamma_0}}(N, L-N+1) \left(\frac{P_D}{P_I}\right)^{N-L-1} \\ &= I_{\frac{\gamma_0}{\frac{P_D}{P_I}+\gamma_0}}(N, L-N+1) \end{aligned} \tag{4.94}$$

It can be shown by using [98, eq. (26.5.24)] that the expression (4.94) is equivalent to the outage probability expression in [67, eq. (9)].

For $N = 1$, from (4.79), the outage probability expression can be simplified to

$$P_{out} = L\left(\frac{P_D}{P_I}\right)^L \int_0^{\gamma_0} \frac{1}{\left(\frac{P_D}{P_I} + \gamma^{oc}\right)^{L+1}} d\gamma^{oc} = 1 - \left(\frac{\frac{P_D}{P_I}}{\frac{P_D}{P_I} + \gamma_0}\right)^L \qquad \text{for } N = 1 \tag{4.95}$$

Note that from (A.6), the integral term in (4.95) can also be expressed in terms of the regularized incomplete beta function:

$$P_{out} = LB_{\frac{\gamma_0}{\frac{P_D}{P_I}+\gamma_0}}(1, L) = \frac{1}{B(1, L)} B_{\frac{\gamma_0}{\frac{P_D}{P_I}+\gamma_0}}(1, L) = I_{\frac{\gamma_0}{\frac{P_D}{P_I}+\gamma_0}}(1, L) \qquad \text{for } N = 1 \tag{4.96}$$

For $\rho = 0$, expression (4.92) can also be simplified to (4.96). Therefore, from (4.95) and (4.96),

the outage probability expression for $N = 1$ or $\rho = 0$ can be written as

$$P_{out} = 1 - \left( \frac{\frac{P_D}{P_I}}{\frac{P_D}{P_I} + \gamma_0} \right)^L = I_{\frac{\gamma_0}{\frac{P_D}{P_I}+\gamma_0}}(1, L) \qquad \text{for } N = 1 \text{ or } \rho = 0 \tag{4.97}$$

The result in (4.97) is equivalent to the expression of outage probability in the case of perfect channel estimation in (4.94) when $N = 1$, as expected.

### 4.3.3 Average Bit Error Probability

Similar to Subsection 3.2.2, if we assume that the interference in (4.2) conditioned on $\boldsymbol{u}$ and $\boldsymbol{h}_j$'s is complex Gaussian, then the BEP conditioned on $\boldsymbol{u}$, $\boldsymbol{h}$ and $\boldsymbol{h}_j$'s for binary DPSK and binary NCFSK is a function only of $\gamma$ defined in (4.3), and can be expressed as

$$P_b\left(E|\boldsymbol{u}, \boldsymbol{h}, \boldsymbol{h}_1, \ldots, \boldsymbol{h}_L\right) = P_b\left(E|\gamma\right) = \frac{1}{2}\text{exp}\left(-\alpha\gamma\right) \tag{4.98}$$

where

$$\alpha = \begin{cases} 1, & \text{for binary DPSK} \\ \frac{1}{2}, & \text{for binary NCFSK} \end{cases} \tag{4.99}$$

The average BEP can be obtained by averaging the conditional BEP in (4.98) over the PDF of SIR. Therefore, from (4.74) and (4.98), the average BEP when $|\rho| < 1$ can be written as

$$\begin{aligned} P_b(E) &= \int_0^\infty P_b(E|\gamma^{oc}) f_{\gamma^{oc}}(\gamma^{oc}) d\gamma^{oc} \\ &= L\left(1-\rho^2\right)^{L-N+2} \left(\frac{P_D}{P_I}\right)^L \sum_{j=0}^{\infty}\sum_{k=0}^{\infty} \rho^{2(j+k)} \frac{(L-N+2)_{j+k}(N)_j(L-N+1)_k \left(\frac{P_D}{P_I}\right)^k}{(1)_j(L)_k j!k!} \\ &\quad \times \int_0^\infty \frac{(\gamma^{oc})^j \text{exp}(-\alpha\gamma^{oc})}{2\left(\frac{P_D}{P_I}+\gamma^{oc}\right)^{j+k+L+1}} d\gamma^{oc} \end{aligned} \tag{4.100}$$

From (A.7) and (A.2), the expression of the average BEP for binary DPSK and binary NCFSK in (4.100) when $|\rho| < 1$ can be simplified to

$$\begin{aligned} P_b(E) &= L\left(1-\rho^2\right)^{L-N+2}\sum_{j=0}^{\infty}\sum_{k=0}^{\infty}\frac{\rho^{2(j+k)}(L-N+2)_{j+k}}{2(L)_k j!k!}(N)_j(L-N+1)_k \\ &\quad \times U\left(j+1, 1-k-L, \frac{\alpha P_D}{P_I}\right) \end{aligned} \tag{4.101}$$

From (A.7), for real $a$, $b$ and $x$ the $U(a,b,x)$ is real and nonnegative. Moreover, $0 \le \exp(-xt) \le 1$ for real nonnegative $x$ when $t \ge 0$. Therefore, from (A.3) and (A.4), for real $a$, $b$ and $x$ we have

$$\begin{aligned} 0 \le U(a,b,x) &= \frac{1}{\Gamma(a)}\int_0^{\infty}\frac{t^{a-1}\exp(-xt)}{(1+t)^{1+a-b}}dt \\ &\le \frac{1}{\Gamma(a)}\int_0^{\infty}\frac{t^{a-1}}{(1+t)^{1+a-b}}dt \\ &= \frac{1}{\Gamma(a)}B(a,1-b) \quad \text{for } a>0 \text{ and } b<1 \\ &= \frac{\Gamma(1-b)}{\Gamma(a-b+1)} \quad \text{for } a>0 \text{ and } b<1 \end{aligned} \tag{4.102}$$

From (4.102), we get $0 \le U\left(j+1, 1-k-L, \frac{\alpha P_D}{P_I}\right) \le \frac{\Gamma(k+L)}{\Gamma(j+k+L+1)}$, and hence, from (A.2), the expression (4.101) is upper bounded by

$$UB_{P_b(E)} = \left(1-\rho^2\right)^{L-N+2}\sum_{j=0}^{\infty}\sum_{k=0}^{\infty}\frac{(L-N+2)_{j+k}}{2(L+1)_{j+k}}(N)_j(L-N+1)_k\frac{(\rho^2)^j}{j!}\frac{(\rho^2)^k}{k!} \tag{4.103}$$

From (4.93) and (4.103), note that $UB_{P_b(E)} = \frac{1}{2}UB_{P_{out}}$. We showed in the last section that $UB_{P_{out}}$ is convergent for $|\rho| < 1$. Therefore, (4.103) is convergent when $|\rho| < 1$, and hence the average BEP expression in (4.101) is also convergent for $|\rho| < 1$.

When $|\rho| = 1$, from (4.75) and (4.98), the average BEP for binary DPSK and binary NCFSK

can be expressed as

$$\begin{aligned} P_b(E) &= \frac{\left(\frac{P_D}{P_I}\right)^{L-N+1}}{B(N, L-N+1)} \int_0^\infty \frac{(\gamma^{oc})^{N-1} \exp(-\alpha\gamma^{oc})}{2\left(\frac{P_D}{P_I}+\gamma^{oc}\right)^{L+1}} d\gamma^{oc} \\ &= \frac{\Gamma(L+1)}{2\Gamma(L-N+1)} U\left(N, N-L, \frac{\alpha P_D}{P_I}\right) \end{aligned} \tag{4.104}$$

### 4.3.4 Numerical Results

In this section, we present a set of numerical results for several performance measures of OC in the presence of channel estimation errors. These results are obtained for an interference-limited system over flat Rayleigh fading channels with multiple equal power interferers. We consider different numbers of receive antennas $N$ and interfering users $L$ when the power of the desired user to the power of an interfering user is $P_D/P_I = 10$. It is apparent from (4.5) that when the channel estimation error variance decreases, the correlation between the exact and estimate channels increases. Therefore, to find the effect of channel estimation errors, the performance of OC is examined for different correlation coefficients in this section.

In Figs. 4.1 and 4.2, we verify the analytical expression derived for the PDF of SIR in (4.66). The PDF of the output SIR is plotted by both the analytical expression and Monte Carlo simulation for $\rho = 0.8$, $N = 6$ and $L = 6$ in Fig. 4.1, and for $\rho = 0.8$, $N = 8$ and $L = 8$ in Fig. 4.2. The number of samples used by the simulations is 100000 in Fig. 4.1 and 200000 in Fig. 4.2. It is clear that the theoretical results match the simulation ones.

Figs. 4.3 and 4.4 show the effect of correlation coefficient on the PDF of SIR. The PDF's are plotted in Fig. 4.3 for $N = 6$ and $L = 6$, and in Fig. 4.4 for $N = 2$ and $L = 6$ by using expressions (4.66) and (4.75) for different correlation coefficients. We can see in both figures that SIR has a better chance to take on larger values as the correlation between the exact and estimated channels increases. However, it is evident that for larger values of SIR the gap between different PDF curves in Fig. 4.4 (for $N = 2$) is smaller in comparison with the PDF curves in Fig. 4.3 (for $N = 6$). Therefore, the PDF of SIR is more sensitive to channel estimation error when there are

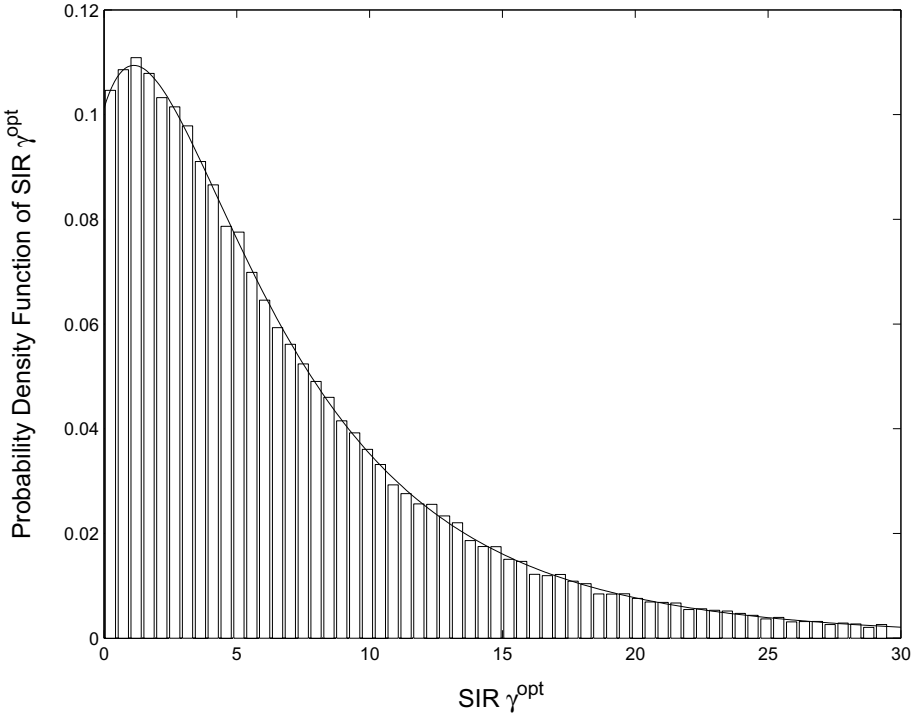


Figure 4.1: Probability density function of the output SIR for $\rho = 0.8$, $N = 6$ and $L = 6$ by using both analytical and simulation results.

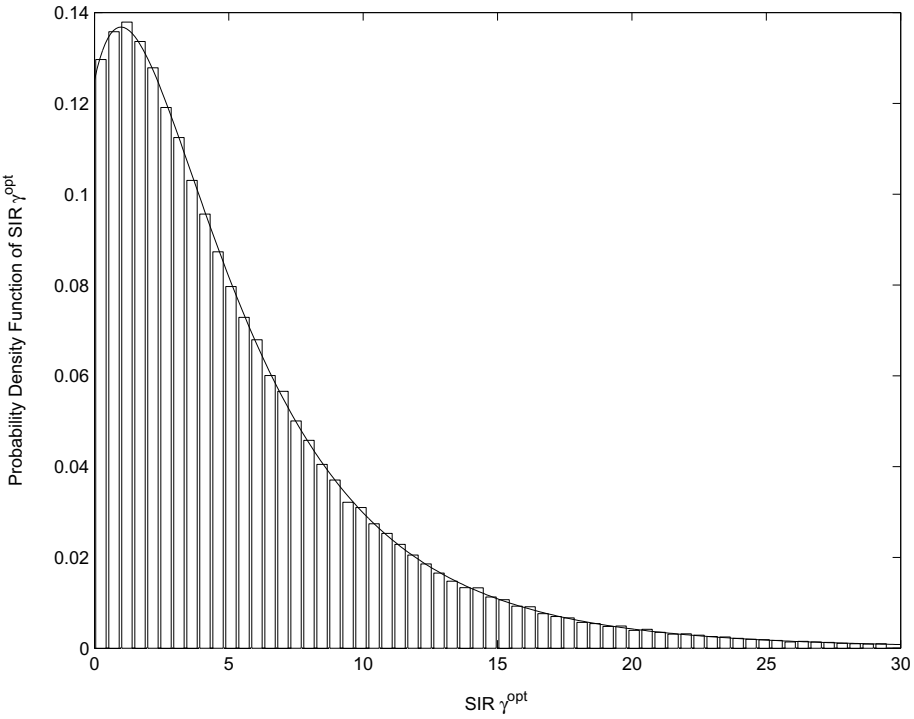


Figure 4.2: Probability density function of the output SIR for $\rho = 0.8$, $N = 8$ and $L = 8$ by using both analytical and simulation results.

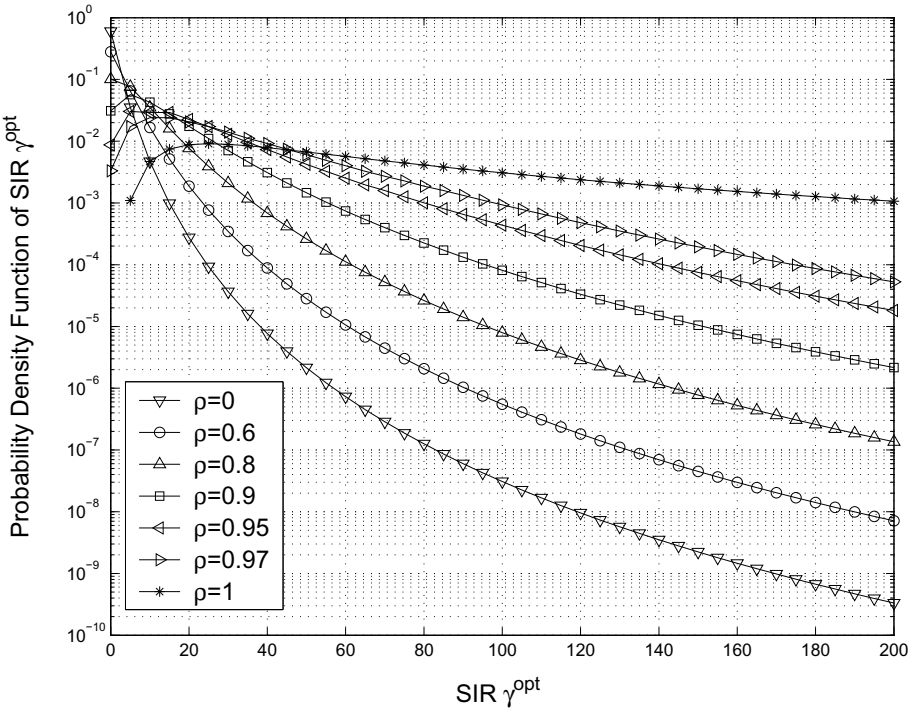


Figure 4.3: Effect of the correlation coefficient on the probability density function of the output SIR for $N = 6$ and $L = 6$.

more antennas at the receiver.

In Fig. 4.5 and 4.6, the PDF of SIR is shown for several correlation coefficients when $L = 8$. The curves are plotted for $N = 8$ in Fig. 4.5 and for $N = 2$ in Fig. 4.6 by using the expressions in (4.66) and (4.75). The PDF curves again shift to the right as the correlation coefficient increases. For larger values of SIR, the gap between different PDF curves in Fig. 4.5 (for $N = 8$) is also larger in comparison with the curves in Fig. 4.6 (for $N = 2$), which shows again as the number of receive antenna increases the performance of OC becomes more sensitive to channel estimation error.

The average SIR is plotted versus the square of the correlation coefficient in Fig. 4.7 for different numbers of antennas, $N$, by both theory (expressions (4.84) and (4.86) for $n = 1$) and simulation when $L = 6$. We can see that except for $N = 1$, the average SIR increases as the correlation coefficient increases, and this performance improvement is more significant with a larger number of antennas at the receiver. For instance, as $\rho^2$ increases from 0.9 to 1, the average

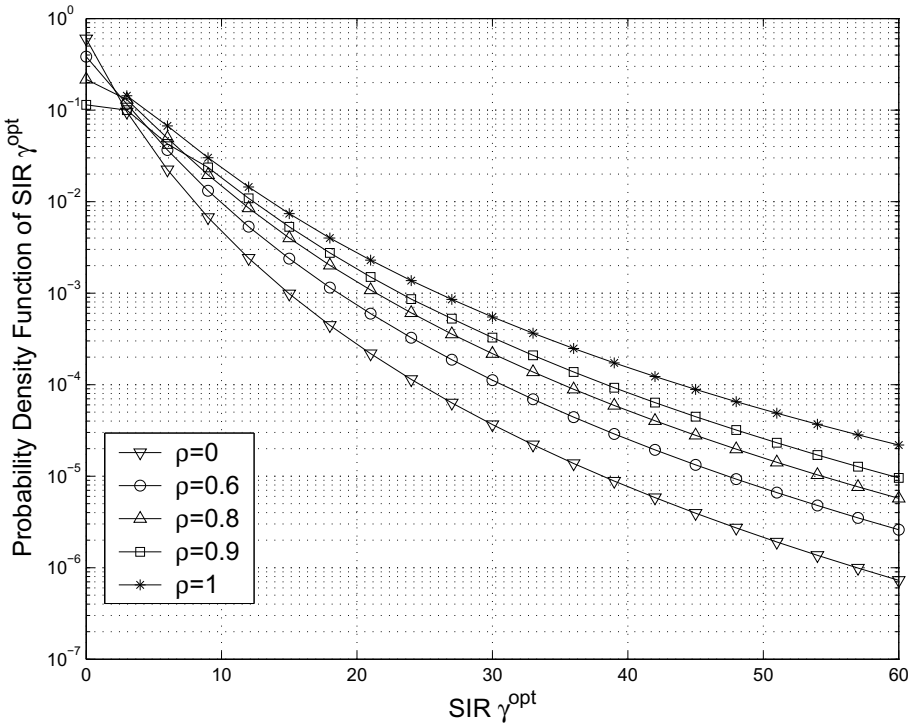


Figure 4.4: Effect of the correlation coefficient on the probability density function of the output SIR for $N = 2$ and $L = 6$.

SIR increases from 18.76 to 50 for $N = 5$, while it only improves from 4.53 to 5 in the case of $N = 2$. The theoretical results in Fig. 4.7 match precisely Monte Carlo simulations, which verifies the derived expression in (4.84) for $n = 1$.

Fig. 4.8 shows the outage probability for threshold $\gamma_0 = 5$ dB against the square of the correlation coefficient with $N$ as the parameter by using both analytical expressions (expressions (4.92) and (4.94)) and simulation when $L = 6$. We observe again that performance improvement due to the increase of the correlation coefficient is more considerable when there is a larger number of antennas. For example, as $\rho^2$ increases from 0.9 to 1, the outage probability decreases only from $0.4876$ to $0.4428$ when $N = 2$, whereas it decreases significantly from $5.01 \times 10^{-2}$ to $3.84 \times 10^{-3}$ for $N = 5$. The analytical and simulation results in Fig. 4.8 match exactly as well, which verifies the analytical expression derived in (4.92).

In Figs. 4.9 and 4.10, the outage probability of OC is plotted versus the SIR threshold $\gamma_0$ for various correlation coefficients. The curves are plotted for $N = 6$ and $L = 6$ in Fig. 4.9,

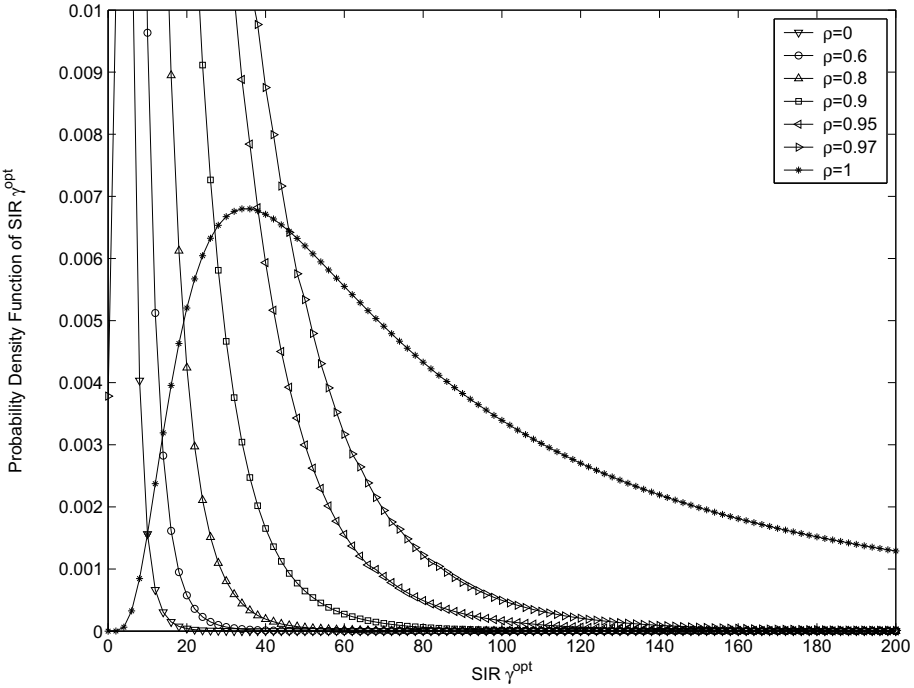


Figure 4.5: Effect of the correlation coefficient on the probability density function of the output SIR for $N = 8$ and $L = 8$.

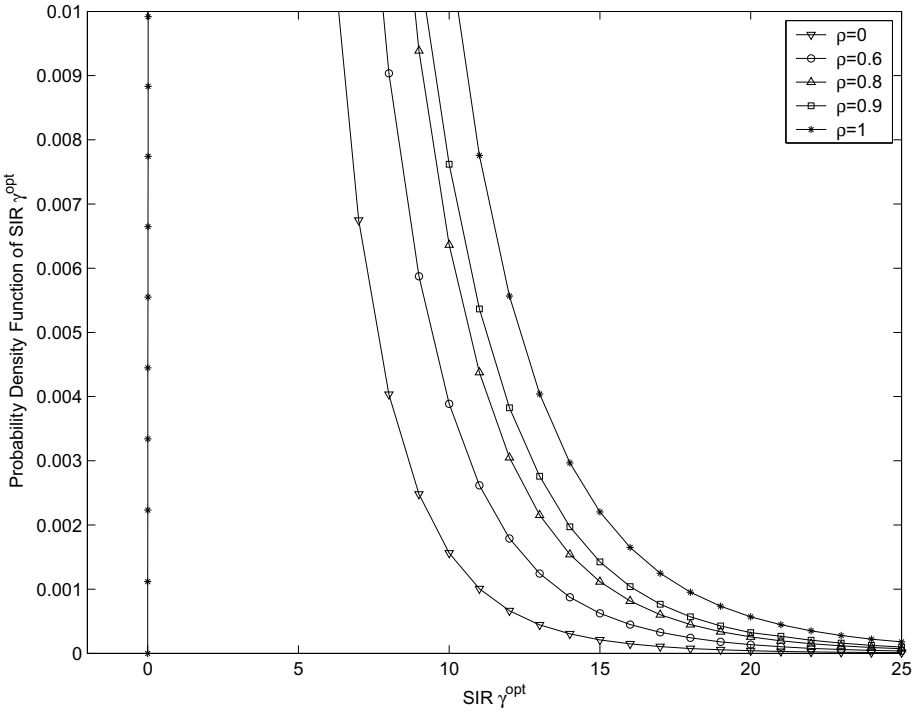


Figure 4.6: Effect of the correlation coefficient on the probability density function of the output SIR for $N = 2$ and $L = 8$.

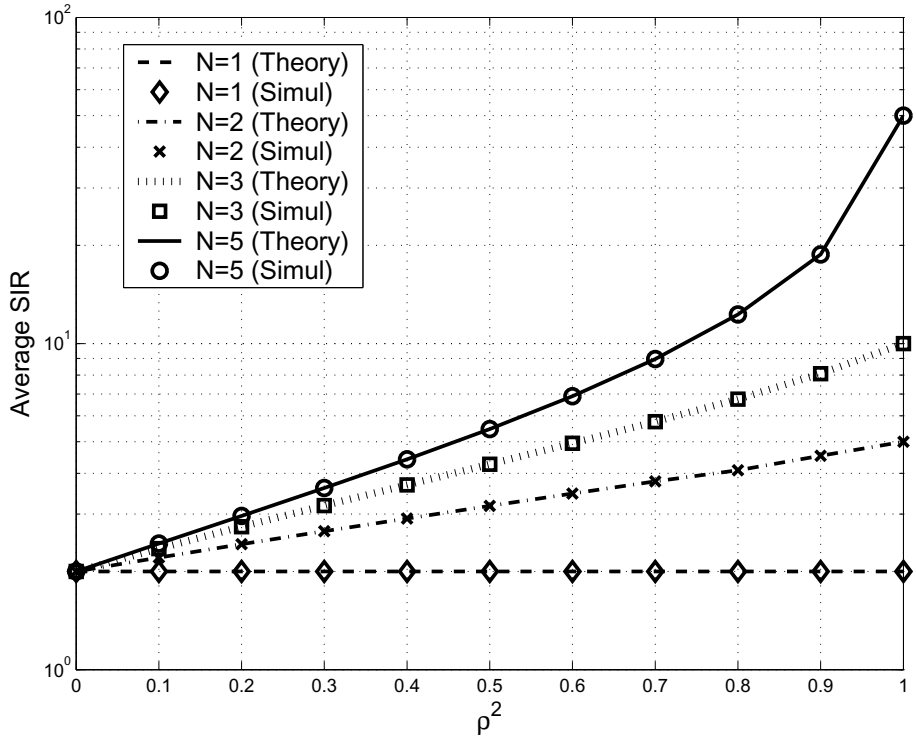


Figure 4.7: Average SIR versus the square of the correlation coefficient for different numbers of antennas when $L = 6$.

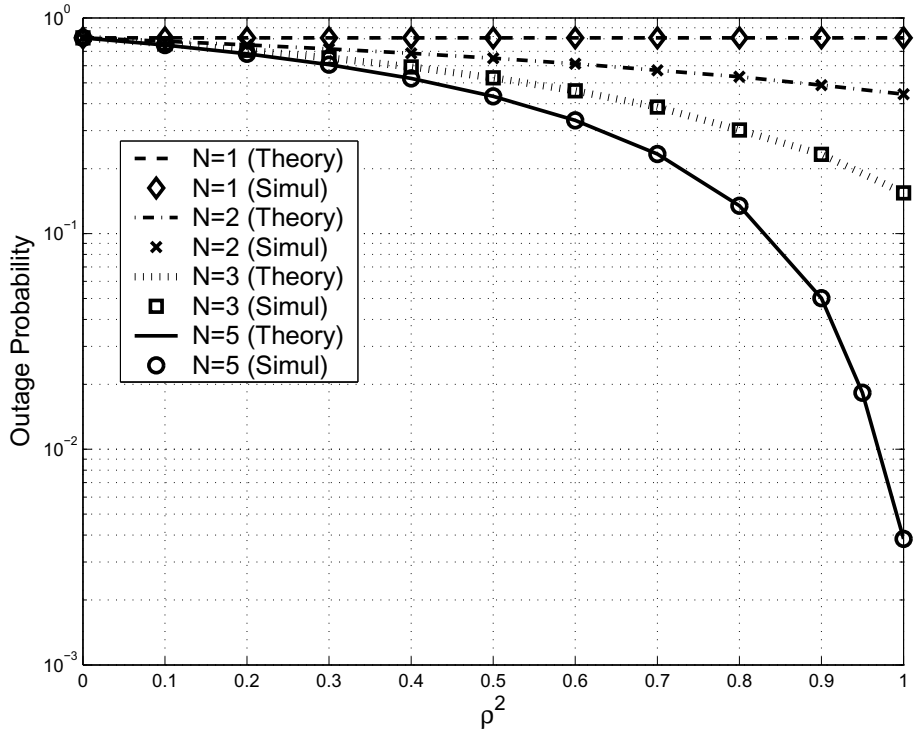


Figure 4.8: Outage probability versus the square of the correlation coefficient for different numbers of antennas when $\gamma_0 = 5$ dB and $L = 6$.

and for $N = 3$ and $L = 6$ in Fig. 4.10 by using the analytical expressions in (4.92) and (4.94). It is apparent that for a given SIR threshold, increasing the correlation coefficient reduces the outage probability. We can see that increasing the correlation coefficient does not lower the outage probability for $N = 3$ in Fig. 4.10 compared with the case of $N = 6$ in Fig. 4.9. For instance, for threshold $\gamma_0 = 5$ dB, as $\rho$ increases from 0.9 to 1, the outage probability decreases from 0.148 to $1.92 \times 10^{-4}$ for $N = 6$, while it only decreases from 0.286 to 0.154 in the case of $N = 3$. As an another example, for the outage probability $P_{out} = 7 \times 10^{-2}$, when $\rho$ increases from 0.9 to 1, SIR threshold changes $10.2$ dB, while the improvement is only $2.8$ dB for $N = 3$. Therefore, we again see that with more antennas at the receiver the performance improvement due to better channel estimation is more significant.

The theoretical and simulation results for the average BEP are plotted versus the square of the correlation coefficient in Fig. 4.11 for DPSK signals and for different number of antennas, $N$, when $L = 6$. For theoretical results, the expressions (4.101) and (4.104) are used with $\alpha = 1$. The curves show that the decrease of the average BEP due to the increase of the correlation coefficient is more substantial with a larger $N$. For instance, as $\rho^2$ increases from 0.9 to 1, the analytical result of the average BEP decreases dramatically from $5.3 \times 10^{-3}$ to $3.5 \times 10^{-4}$ for $N = 5$, while it only decreases from $6.9 \times 10^{-2}$ to $5.55 \times 10^{-2}$ when $N = 2$. Although the theoretical results for the average BEP are derived under the Gaussian distributed interference assumption, we can see a very good match between the theory and simulation from the figure.

In Fig. 4.12, the effect of thermal noise on the performance of the system is examined by using Monte Carlo simulation when the power of noise is $0.5P_I$, $\rho = 0.8$, $N = 3$ and $L = 6$. We can see that our analytical result in interference-limited systems is very close to the result for the systems with low power thermal noise.

Note that analytical expressions in (4.66), (4.84), (4.92), and (4.101) contain infinite summations. To evaluate these expressions, we have to generate a sufficient number of terms in the summations. The number of terms is incremented until the last term is smaller than a threshold. We observe that fortunately not too many terms are needed for convergence and calculation of

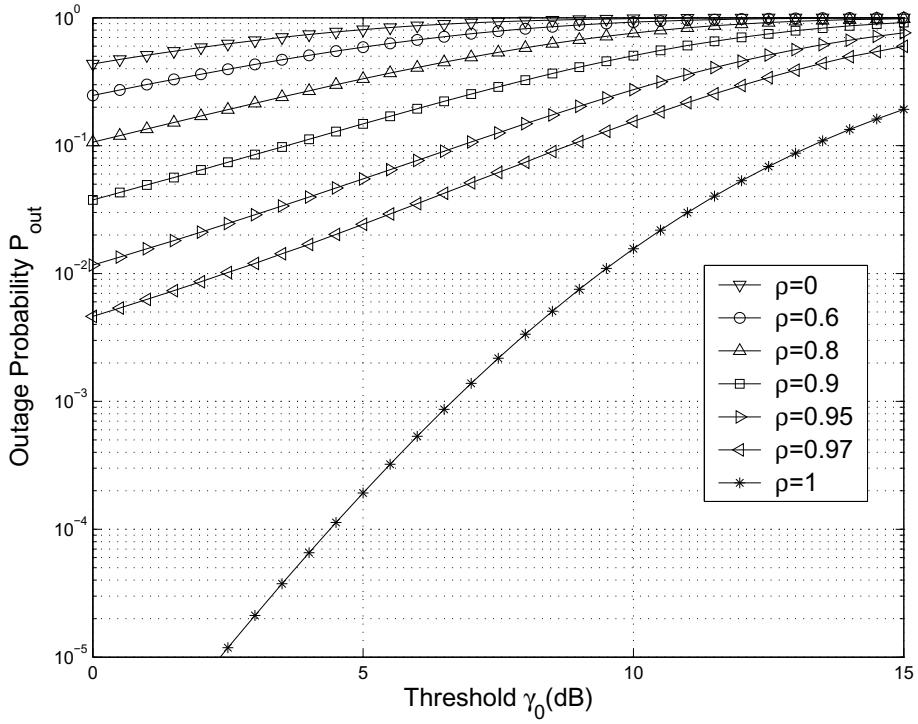


Figure 4.9: Outage probability versus the threshold $\gamma_0$ with the correlation coefficient as the parameter when $N = 6$ and $L = 6$.

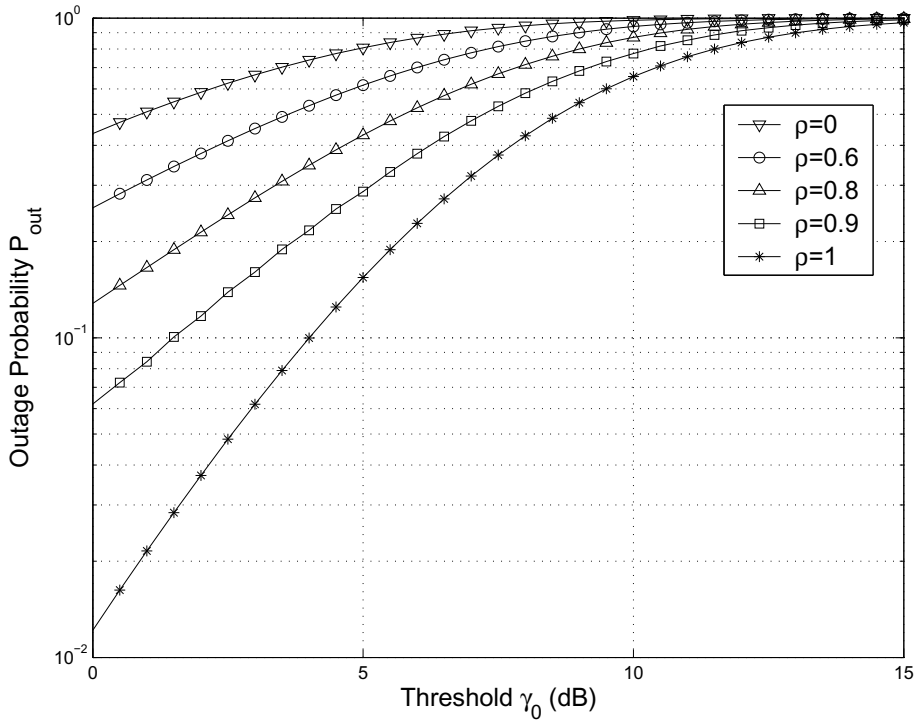


Figure 4.10: Outage probability versus the threshold $\gamma_0$ with the correlation coefficient as the parameter when $N = 3$ and $L = 6$.

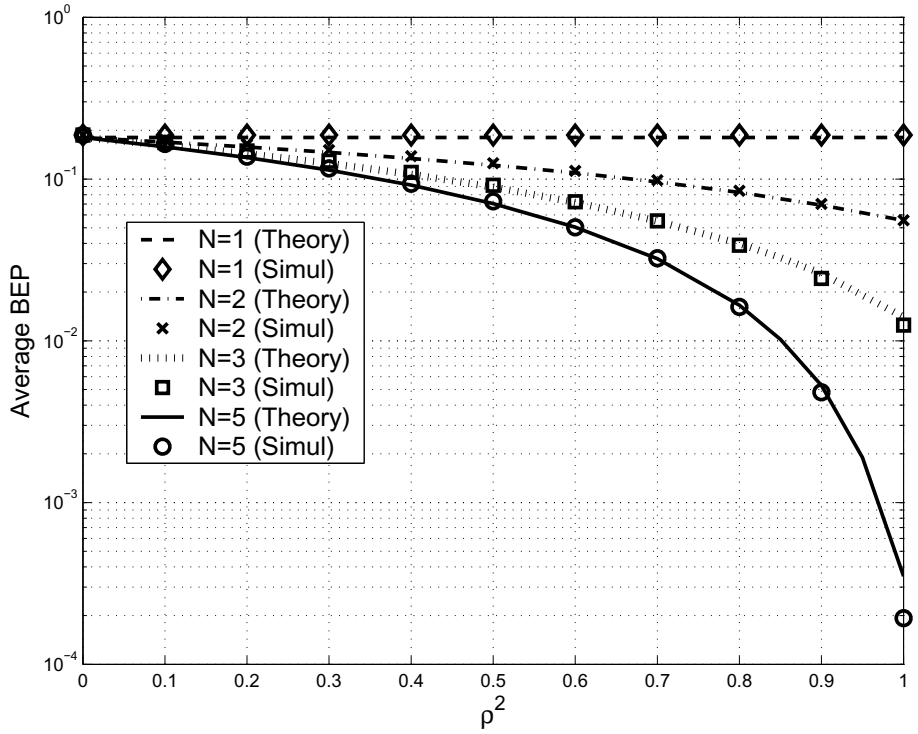


Figure 4.11: Average BEP versus the square of the correlation coefficient for different numbers of antennas when $L = 6$.

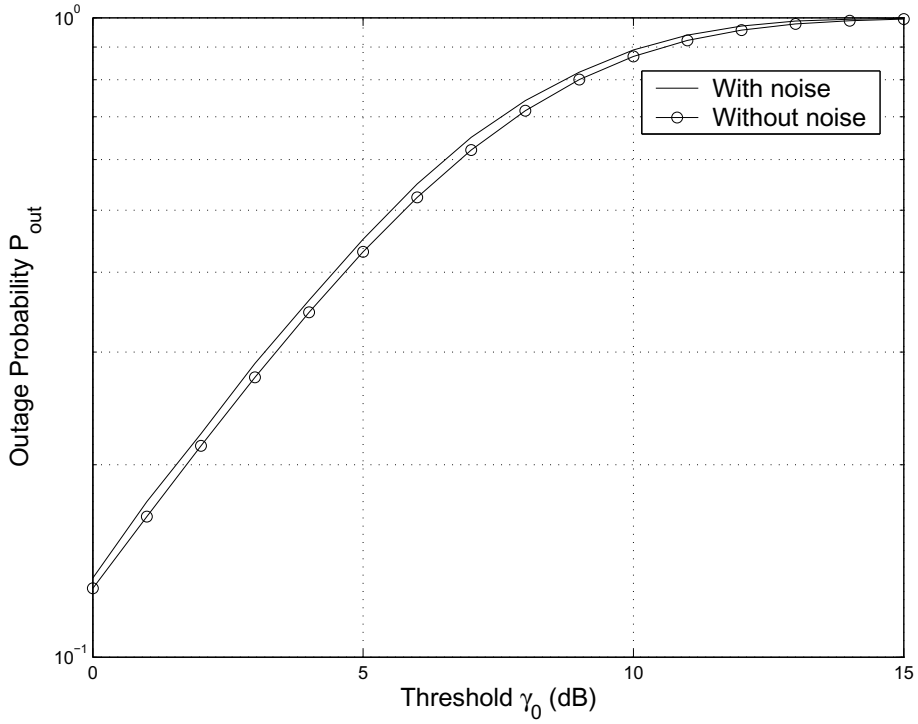


Figure 4.12: Outage probability versus the threshold $\gamma_0$ with and without noise for $\rho = 0.8$, $N = 3$ and $L = 6$ when the power of noise is $0.5P_I$.

these expressions numerically in MATLAB. Therefore, although these expressions contain infinite summations, they can be evaluated with finite complexity. For example, to compute the average SIR in Fig. 4.7 for $N = 5$, $L = 6$ and $\rho^2 = 0.5$, only about $150$ terms are needed to calculate the average SIR expression in (4.84) such that the last term in (4.84) is less than $10^{-4}$. As another example, note from Fig. 4.9 that for $N = 6$, $L = 6$, $\rho = 0.97$, and threshold $\gamma_0 = 2.5$ dB, the outage probability is about $10^{-2}$. Therefore, to evaluate the outage probability for this case by Monte Carlo simulation, at least $10^4$ samples of SIR should be simulated (to observe at least 100 SIR samples less than the given threshold). However, we find that to compute the theoretical expression of the outage probability in (4.92) for this case numerically only $200$ terms are adequate such that the last term in (4.92) is less than $10^{-6}$, which shows how efficient the analytical expressions are in comparison with the Monte Carlo simulations. Therefore, the derived theoretical expressions are very efficient alternatives to time-consuming Monte Carlo simulations in performance evaluation.

## 4.4 Statistical Analysis in Rician/Rayleigh Fading Channels

The statistical analysis in Section 4.2 is performed for the case when the channel of the desired user as well as the channels of interfering users are subject to Rayleigh fading. In this section, we generalize the results of Section 4.2 to a Rician/Rayleigh fading environment where the desired user is subject to Rician fading while the interferers experience Rayleigh fading.

The assumption of Rayleigh fading for both the desired and interfering users is reasonable for macro-cellular (medium to large cell) systems since the distance between the mobile station and the base station is large enough that the line-of-sight (LOS) component can be ignored for the desired user. For micro-cellular systems, especially for urban and indoor micro-cellular system configurations, the interferers from distant co-channel cells can be characterized by Rayleigh distributions as well since it is unlikely that a LOS exists between a co-channel interferer and the desired user's base station. However, since the cell size is smaller in these systems, the desired user and the base station are not far enough apart to ignore the LOS component [101], [102], and Rayleigh

fading may not be a good model for the channel between the desired user and the base station. Therefore, the desired user experiences Rician fading implying the presence of a LOS within the micro-cell while the interferers are subject to Rayleigh fading indicating the absence of a LOS between co-channel cells of a micro-cellular system. This model describes the Rician/Rayleigh fading environment explained in [103], [104].

The analysis in this section is valid for interference-limited systems with Gaussian distributed channel estimation errors. We assume that the interferers have equal power, and the number of interferers exceeds or is equal to the number of antennas. Using multivariate statistical analysis, we derive an exact closed-form expression for the PDF of the output SIR. The theoretical result is verified by Monte Carlo simulations.

### 4.4.1 System Model

We consider again the uplink (mobile to base station) of a wireless communication system in the presence of $L$ interferers. The receiver is equipped with $N$ antenna elements, and $N \leq L$. The system is assumed to be interference limited, and all the interferers are received with the same average power. The $N \times 1$ baseband received signal vector $\boldsymbol{r}$ is given by

$$\boldsymbol{r} = \sqrt{P_D}\boldsymbol{h}d + \sum_{j=1}^{L} \sqrt{P_I}\boldsymbol{h}_j d_j \tag{4.105}$$

where $d$ and $d_j$ are independent symbols with zero mean and unit variance for the desired and the $j$th interfering users, respectively. The complex Gaussian distributed vectors $\boldsymbol{h}$ and $\boldsymbol{h}_j$ correspond to the flat Rician and Rayleigh fading channels for the desired user and the $j$th interferer, respectively, and are mutually independent. We indicate the mean vector of the desired channel by $\boldsymbol{m}$ representing the LOS vector. It is assumed that the receiver antennas are far enough apart, so the fading coefficients at different antennas are independent. Therefore, $\boldsymbol{h} \sim CN_N(\boldsymbol{m}, 2\boldsymbol{I_N})$ and $\boldsymbol{h}_j \sim CN_N(\boldsymbol{0}, 2\boldsymbol{I_N})$ where $CN_p(\boldsymbol{\eta}, \boldsymbol{\Phi})$ denotes a complex multivariate normal distribution for a $p$-dimensional random vector with mean $\boldsymbol{\eta}$ and covariance matrix $\boldsymbol{\Phi}$, and $\boldsymbol{I}_N$ is an $N \times N$ identity

matrix. Received signal powers $P_D$ and $P_I$ correspond to the desired and the interfering users, respectively.

Similar to Section 4.1, we assume that channel estimation error vectors are circularly symmetric Gaussian distributed. In other words, similar to (4.8) we have

$$\boldsymbol{e} \sim CN_N\left(\mathbf{0}, 2\left(1-\rho^2\right)\boldsymbol{I_N}\right) \text{ and } \boldsymbol{e}_j \sim CN_N\left(\mathbf{0}, 2\left(1-\rho^2\right)\boldsymbol{I_N}\right). \tag{4.106}$$

where $\boldsymbol{e}$ and $\boldsymbol{e}_j$ are the channel estimation error vectors of the desired user and the $j$th interferer, respectively, and $\rho$ is the correlation coefficient between the true and estimated channels.

Now, from (4.106), the channel estimate vectors are distributed as

$$\hat{\boldsymbol{h}} \sim CN_N(\boldsymbol{m}, 2\rho^2\boldsymbol{I}_N) \text{ and } \hat{\boldsymbol{h}}_j \sim CN_N(\mathbf{0}, 2\rho^2\boldsymbol{I}_N) \tag{4.107}$$

where $\hat{\boldsymbol{h}}$ and $\hat{\boldsymbol{h}}_j$ denote the estimated channel vectors of the desired user and the $j$th interferer, respectively.

In this section, we assume that $\rho \neq 0$, and to simplify the following analysis without loss of generality, we define

$$\boldsymbol{s} = \frac{\hat{\boldsymbol{h}}}{\rho} \text{ and } \boldsymbol{s}_j = \frac{\hat{\boldsymbol{h}}_j}{\rho} \tag{4.108}$$

Note that from (4.107) and (4.108), vectors $\boldsymbol{s}$ and $\boldsymbol{s}_j$'s are distributed as

$$\boldsymbol{s} \sim CN_N\left(\frac{\boldsymbol{m}}{\rho}, 2\boldsymbol{I}_N\right) \text{ and } \boldsymbol{s}_j \sim CN_N(\mathbf{0}, 2\boldsymbol{I}_N) \tag{4.109}$$

As mentioned in Section 4.1, the normalized OC vector based on $\boldsymbol{s}$ and $\boldsymbol{s}_j$'s can be written as

$$\boldsymbol{u}^{oc} = \frac{\boldsymbol{R}^{-1}\boldsymbol{s}}{\left\|\boldsymbol{R}^{-1}\boldsymbol{s}\right\|} \tag{4.110}$$

where $\|.\|$ denotes the norm of a vector, and the matrix $\boldsymbol{R}$ in (4.110) is again defined as

$$\boldsymbol{R} = \sum_{j=1}^{L} \boldsymbol{s}_j \boldsymbol{s}_j^H \tag{4.111}$$

and similar to Section 4.1, the $SIR\ \gamma^{oc}$ at the output of the optimum combiner can be written as

$$\gamma^{oc} = \frac{P_D \boldsymbol{s}^H \boldsymbol{R}^{-1} \boldsymbol{h}\boldsymbol{h}^H \boldsymbol{R}^{-1} \boldsymbol{s}}{P_I \boldsymbol{s}^H \boldsymbol{R}^{-1} \left( \sum_{j=1}^{L} \boldsymbol{h}_j \boldsymbol{h}_j^H \right) \boldsymbol{R}^{-1} \boldsymbol{s}} \tag{4.112}$$

### 4.4.2 Statistical Analysis

In order to derive the PDF of $\gamma^{oc}$, similar to Section 4.2 first we obtain the PDF of $\gamma^{oc}$ conditioned on the channel estimates.

To get the conditional distribution of SIR, we use Corollary 4.1 mentioned in Section 4.2. The results of that Corollary is still valid in this section because Corollary 4.1 (or Theorem 4.1 from which Corollary 4.1 is derived) is based on the assumption that channel estimation errors of the desired user and interfering user are circularly symmetric Gaussian distributed, and we know from (4.106) that channel estimation errors in this section are circularly symmetric Gaussian distributed, like channel estimation errors in (4.8) in Section 4.2.

As demonstrated in Corollary 4.1, the PDF of $\gamma^{oc}$ conditioned on $\boldsymbol{s}, \boldsymbol{s}_1, ..., \boldsymbol{s}_L$ for $|\rho| < 1$ can be written as

$$\begin{aligned} f_{\gamma^{oc}}(\gamma^{oc}|\boldsymbol{s}, \boldsymbol{s}_1, ..., \boldsymbol{s}_L) = & e^{-\left(\frac{\lambda_1^{oc}+\lambda_2^{oc}}{2}\right)} \\ & \times \sum_{j=0}^{\infty} \sum_{k=0}^{\infty} \frac{\left(\frac{P_D}{P_I}\right)^{k+L} (\gamma^{oc})^j}{\left(\frac{P_D}{P_I} + \gamma^{oc}\right)^{j+k+L+1}} \frac{(\lambda_1^{oc})^j (\lambda_2^{oc})^k}{2^{j+k} B(1+j, L+k) j! k!} \end{aligned} \tag{4.113}$$

where non-centrality parameters $\lambda_1^{oc}$ and $\lambda_2^{oc}$ are defined as

$$\lambda_1^{oc} = \frac{\rho^2}{1-\rho^2} \frac{\left(\boldsymbol{s}^H \boldsymbol{R}^{-1} \boldsymbol{s}\right)^2}{\boldsymbol{s}^H \boldsymbol{R}^{-2} \boldsymbol{s}}, \tag{4.114}$$

and

$$\lambda_2^{oc} = \frac{\rho^2}{1-\rho^2} \frac{\boldsymbol{s}^H \boldsymbol{R}^{-1} \boldsymbol{s}}{\boldsymbol{s}^H \boldsymbol{R}^{-2} \boldsymbol{s}} \tag{4.115}$$

Now, we obtain the PDF of $\gamma^{oc}$ from the conditional PDF found in (4.113). In order to find $f_{\gamma^{oc}}(\gamma^{oc})$, similar to Section 4.2 first we express non-centrality parameters $\lambda_1^{oc}$ and $\lambda_2^{oc}$ in terms of random variables with well-known distributions.

Note that the matrix $\boldsymbol{R}$ in (4.111) depends only on $\boldsymbol{s}_j$'s, the interfering users' fading channels, and does not depend on $\boldsymbol{s}$, the desired user's channel. Moreover, in this section similar to Section 4.2 , it is assumed that the interferers are subject to Rayleigh fading, i.e. $\boldsymbol{s}_j \sim CN_N(\boldsymbol{0}, 2\boldsymbol{I}_N)$. Therefore, $\boldsymbol{R}$ in (4.111) has the same distribution as $\boldsymbol{R}$ in (4.12) since in both cases the interferers experience Rayleigh fading. So, similar to Section 4.2, matrix $\boldsymbol{R}$ in (4.111) has a complex Wishart distribution with $L$ degrees of freedom and covariance matrix $2\boldsymbol{I}_N$ denoted by

$$\boldsymbol{R} \sim CW_N(L, 2\boldsymbol{I}_N) \tag{4.116}$$

Now, similar to Corollary 4.2 in Section (4.2), we can use Theorem 4.2 (which was presented for complex Wishart distributions) to derive the following result.

**Lemma 4.5** *Non-centrality parameters $\lambda_2^{oc}$ and $\lambda_1^{oc}$ in (4.115) and (4.114) can be written as*

$$\lambda_2^{oc} = \frac{\rho^2}{1-\rho^2} xy \tag{4.117}$$

*and*

$$\lambda_1^{oc} = \frac{\rho^2}{1-\rho^2} xz \tag{4.118}$$

*where $x$, $y$ and $z$ are independent random variables, and*

$$x \sim \textit{beta}(L-N+2, N-1), \tag{4.119}$$

$$y \sim \chi^2_{2(L-N+1)} \tag{4.120}$$

*and*

$$z \sim \chi^2_{2N}\left(\frac{\boldsymbol{m}^H\boldsymbol{m}}{\rho^2}\right) \tag{4.121}$$

*where $\chi^2_\nu(\delta)$ denotes a noncentral chi-square distribution with $\nu$ degrees of freedom and noncentrality parameter $\delta$ [97].*

*Proof:* The proof of this Lemma is similar to that of Corollary 4.2 in Section (4.2). Since the vector $\boldsymbol{s}$ and the matrix $\boldsymbol{R}$ are independent, and $\boldsymbol{R} \sim CW_N(L, 2\boldsymbol{I}_N)$, the random variables $\lambda_2^{oc}$ and $\lambda_1^{oc}$ in (4.115) and (4.114) conditioned on $\boldsymbol{s}$, according to (4.35) and (4.36) in Theorem 4.2, can be written as

$$\lambda_2^{oc}|\boldsymbol{s} = \frac{\rho^2}{1-\rho^2}(x|\boldsymbol{s})(y|\boldsymbol{s}) \tag{4.122}$$

and

$$\lambda_1^{oc}|\boldsymbol{s} = \frac{\rho^2}{1-\rho^2}\boldsymbol{s}^H\boldsymbol{s}(x|\boldsymbol{s}) \tag{4.123}$$

where $x|\boldsymbol{s}$ and $y|\boldsymbol{s}$ are independent random variables and from (4.37) are distributed as

$$x|\boldsymbol{s} \sim \text{beta}(L-N+2, N-1) \;\text{ and }\; y|\boldsymbol{s} \sim \chi^2_{2(L-N+1)} \tag{4.124}$$

Now, from (4.122) and (4.123), we get

$$\lambda_2^{oc} = \frac{\rho^2}{1-\rho^2} xy \tag{4.125}$$

and

$$\lambda_1^{oc} = \frac{\rho^2}{1-\rho^2} \boldsymbol{s}^H \boldsymbol{s} x \tag{4.126}$$

From (4.124), the PDF's of $x|\boldsymbol{s}$ and $y|\boldsymbol{s}$ are not functions of $\boldsymbol{s}$, and hence, random variables $x$ and $y$ are independent of $\boldsymbol{s}$. Therefore, from (4.124), $x$ and $y$ are distributed as

$$x \sim \text{beta}(L-N+2, N-1) \text{ and } y \sim \chi^2_{2(L-N+1)} \tag{4.127}$$

as defined in (4.53) and (4.54). Random variables $x$ and $y$ are independent since the joint distribution of $x$ and $y$ can be written as $f_{xy}(x,y) = \int f_{xy}(x,y|\boldsymbol{s}) f_{\boldsymbol{s}}(\boldsymbol{s}) d\boldsymbol{s} = \int f_x(x|\boldsymbol{s}) f_y(y|\boldsymbol{s}) f_{\boldsymbol{s}}(\boldsymbol{s}) d\boldsymbol{s} = \int f_x(x) f_y(y) f_{\boldsymbol{s}}(\boldsymbol{s}) d\boldsymbol{s} = f_x(x) f_y(y) \int f_{\boldsymbol{s}}(\boldsymbol{s}) d\boldsymbol{s} = f_x(x) f_y(y)$.

By defining random variable $z$ as

$$z = \boldsymbol{s}^H \boldsymbol{s} \tag{4.128}$$

non-centrality parameter $\lambda_1^{oc}$ in (4.126) can be written as

$$\lambda_1^{oc} = \frac{\rho^2}{1-\rho^2} xz \tag{4.129}$$

To find the distribution of $z$ in (4.128), we use the property that if a $p$-dimensional real random vector $\boldsymbol{g}$ has a multivariate normal distribution of $N_p(\boldsymbol{\eta}, \boldsymbol{I}_p)$, then $\boldsymbol{g}^H \boldsymbol{g} \sim \chi^2_p(\boldsymbol{\eta}^H \boldsymbol{\eta})$ [91]. Now, since from (4.109) $\boldsymbol{s} \sim CN_N\left(\frac{\boldsymbol{m}}{\rho}, 2\boldsymbol{I}_N\right)$, each complex element of vector $\boldsymbol{s}$ consists of two independent unit variance Gaussian random variables (the real part and the imaginary part), and hence, random variable $z$ in (4.128) is distributed as

$$z \sim \chi^2_{2N}\left(\frac{\boldsymbol{m}^H \boldsymbol{m}}{\rho^2}\right) \tag{4.130}$$

as defined in (4.121). Note that since random variables $x$ and $y$ are independent from $\boldsymbol{s}$, they are also independent from $z$ in (4.128). □

**Corollary 4.4** *The conditional PDF in (4.113) can be expressed in terms of random variables $x$, $y$ and $z$ in (4.119), (4.120) and (4.121) as*

$$\begin{aligned} f_{\gamma^{oc}}(\gamma^{oc}|x,y,z) &= e^{-\frac{\rho^2(xz+xy)}{2(1-\rho^2)}} \sum_{j=0}^{\infty}\sum_{k=0}^{\infty} \frac{\left(\frac{P_D}{P_I}\right)^{k+L}(\gamma^{oc})^j}{\left(\frac{P_D}{P_I}+\gamma^{oc}\right)^{j+k+L+1} 2^{j+k}B(1+j,L+k)j!k!} \\ &\quad \times \left(\frac{\rho^2}{1-\rho^2}\right)^{j+k} x^{j+k}z^j y^k \end{aligned} \tag{4.131}$$

*Proof:* The expression (4.131) can be directly derived by substituting (4.117) and (4.118) in (4.113). □

**Theorem 4.4** *The PDF of $\gamma^{oc}$ in (4.112) for $0<|\rho|<1$ can be expressed as*

$$\begin{aligned} f_{\gamma^{oc}}(\gamma^{oc}) &= \frac{L\left(1-\rho^2\right)^{L+1}\left(\frac{P_D}{P_I}\right)^L e^{-\frac{\boldsymbol{m}^H\boldsymbol{m}}{2\rho^2}}}{\left(\frac{P_D}{P_I}+\gamma^{oc}\right)^{L+1}} \\ &\quad \times \sum_{j=0}^{\infty}\sum_{k=0}^{\infty}\sum_{l=0}^{\infty}\sum_{p=0}^{\infty} \frac{(L+1)_{j+k+l+p}(L+1)_{j+k}(L-N+2)_{j+k}(N)_{j+l}}{(L+1)_{j+k+l}(L+1)_{j+k+p}(1)_j(L)_k(N)_l j!k!l!p!} \\ &\quad \times (L-N+1)_k(N-1)_p \left(\frac{\rho^2\gamma^{oc}}{\frac{P_D}{P_I}+\gamma^{oc}}\right)^j \left(\frac{\frac{P_D}{P_I}\rho^2}{\frac{P_D}{P_I}+\gamma^{oc}}\right)^k \left(\frac{(1-\rho^2)\boldsymbol{m}^H\boldsymbol{m}}{2\rho^2}\right)^l \left(\rho^2\right)^p \end{aligned} \tag{4.132}$$

*where the Gamma function $\Gamma(\cdot)$ and the Pochhammer symbol $(a)_j$ are defined in (A.1) and (A.2) in Appendix A, respectively.*

*Proof:* The PDF expression in (4.132) can be derived by integrating the conditional distribution expression in (4.113) over the distributions of independent random variables $x$, $y$ and $z$ in (4.119), (4.120) and (4.121). □

Similar to the PDF expression (4.66) in Section 4.2, the PDF expression in (4.132) can also be stated in terms of hypergeometric series, and is convergent when $0<|\rho|<1$.

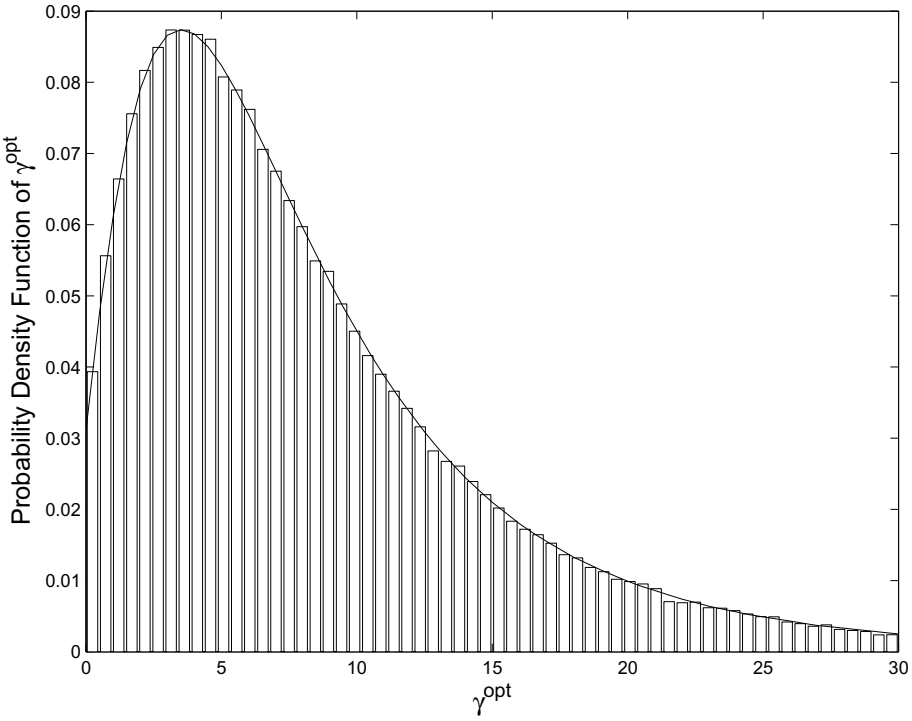


Figure 4.13: Probability density function of the output SIR for $\rho = 0.6$, $N = 3$, $L = 6$ and $\boldsymbol{m} = \sqrt{2} \times \mathbf{1}_3$ by using both analytical and simulation results.

For $\boldsymbol{m} = \mathbf{0}$, i.e. when the desired user is subject to Rayleigh fading, the expression in (4.132) reduces to the PDF expression in (4.66), as expected.

### 4.4.3 Numerical Results

In this section, a set of numerical results is presented when $N = 3$, $L = 6$ and $P_D/P_I = 10$. We assume that $\boldsymbol{m} = \sqrt{2} \times \mathbf{1}_3$ which corresponds to the Rician factor of unity [105] since the variance of each complex element of $\boldsymbol{h}$ is equal to 2, and $\mathbf{1}_3$ denotes a $3 \times 1$ vector of ones.

In Fig. 4.13, we verify the theoretical expression (4.132) derived for the PDF of SIR. The PDF of the output SIR is shown for $\rho = 0.6$ by using both the analytical expression and Monte Carlo simulation of 200,000 samples. We can see that the theoretical result matches the simulated one.

Fig. 4.14 shows the PDF curves for several correlation coefficients by analytical expression (4.132). For $\rho = 1$, i.e. when channel estimates are error-free, we use the PDF expression in [66, eq. (16)] with the parameter $D$ equal to $D = \frac{\boldsymbol{m}^H \boldsymbol{m}}{2}$. Although the theoretical expression in (4.132)

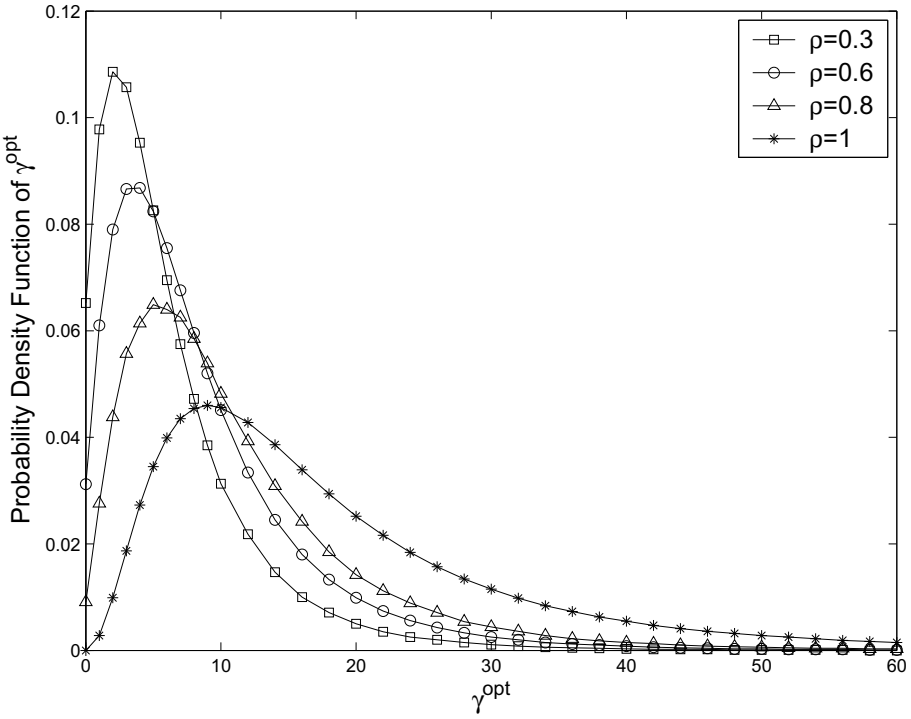


Figure 4.14: Effect of the correlation coefficient on the probability density function of the output SIR for $N = 3$, $L = 6$ and $\boldsymbol{m} = \sqrt{2} \times \mathbf{1}_3$.

contains infinite summations, fortunately not too many terms are needed to converge, and hence, the expression can be evaluated with finite complexity. For example, for $\rho = 0.3$ we observed that almost 20,000 terms are needed on average to calculate (4.132) numerically. It is clear from Fig. 4.14 that the SIR has a higher probability of taking on larger values as the correlation coefficient increases.

As mentioned before, the PDF of SIR can be used to investigate other measures of performance such as the outage probability, i.e. the probability that the SIR is less than or equal to a given threshold. For example, from Fig. 4.14, we can find that as the correlation between the exact and estimated channels increases, the outage probability decreases since the PDF curves shift to the right.

## 4.5 Performance Comparison of MRC with OC

In this section, we compare the performance of MRC and OC over Rayleigh fading channels with imperfect channel estimates. We use the expressions derived for the performance of MRC and OC in this chapter and the last chapter to compare the performance of these two combining techniques.

We present a set of numerical results for the comparison of MRC with OC when the number of interferers is $L = 6$, and $P_D/P_I = 10$. In Figs. 4.15 and 4.16 MRC and OC are compared by using the analytical results derived for the outage probability and the average BEP for DPSK signals. As we can see, for $N = 1$ both combiners have the same performance as expected, and for $N = 2$ OC has a better performance than MRC for almost all $\rho$. But as $N$ increases, there are some ranges of $\rho$ where MRC outperforms OC. From Fig. 4.15, the outage probability of MRC is less than OC's for $N = 3$ when $\rho^2 < 0.39$, for $N = 4$ when $\rho^2 < 0.60$, and for $N = 5$ when $\rho^2 < 0.76$. It is also evident from Fig. 4.16 that MRC surpasses OC in terms of BEP in some cases. The average BEP of MRC is less than OC's for $N = 3$ when $\rho^2 < 0.57$, for $N = 4$ when $\rho^2 < 0.73$, and for $N = 5$ when $\rho^2 < 0.84$. Thus, in contrast to the error-free channel estimation case, MRC can surpass OC especially for small values of $\rho$. Moreover, as $N$ increases, there is a larger range of $\rho$ where MRC outperforms OC.

Therefore, we observe that MRC can have a better performance than OC especially when the correlation between the true and estimated channels is low. This fact can be justified by the following intuitive explanation: The MRC vector depends only on the channel estimate vector of the desired user while the OC vector is a function of both the desired user's channel estimate vector and interfering users' channel estimate vectors. Therefore, when the channel estimator at the receiver performs poorly, MRC can outperform OC.

## 4.6 Summary

In this chapter, we investigated the performance of OC in the presence of circularly symmetric Gaussian distributed channel estimation errors with multiple equal-power interferers. The analysis

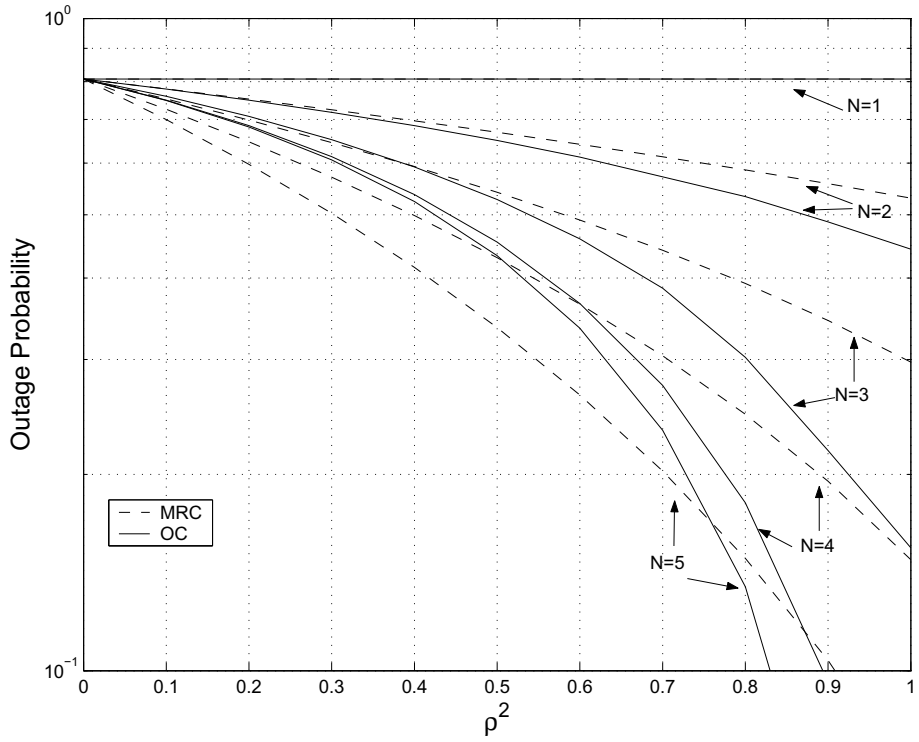


Figure 4.15: Analytical outage probability of MRC and OC versus the square of correlation coefficient for different numbers of antennas when $\gamma_0 = 5$ dB and $L = 6$ .

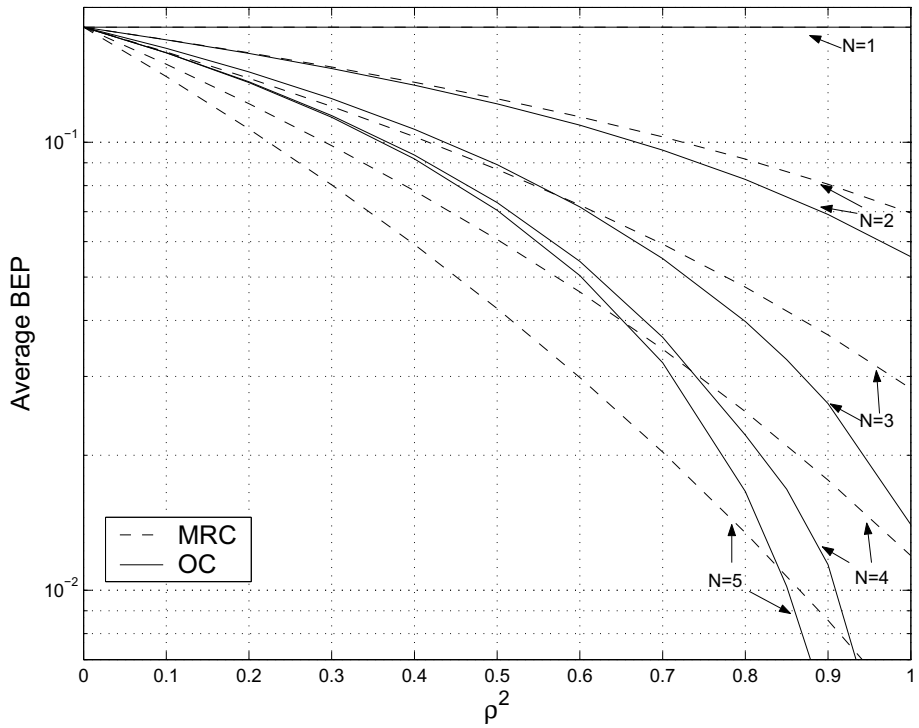


Figure 4.16: Analytical average BEP of MRC and OC versus the square of correlation coefficient for DPSK signals and $N = 1, \ldots, 5$ when $L = 6$.

is performed over flat Rayleigh fading channels when the system is interference-limited and the number of interferers is no less than the number of antennas. We derived an exact closed-form expression for the PDF of the output SIR by using multivariate statistical analysis. Then, we utilized this PDF expression to derive analytical expressions for some important measures of performance such as the moments of SIR, the outage probability and the average bit error probability for binary differential phase-shift keying and non-coherent frequency-shift keying modulations. The analytical results were verified by Monte Carlo simulations. These expressions are useful tools for performance analysis instead of time-consuming Monte Carlo simulations. We quantified the performance improvement as the correlation between the exact and estimated channels increases and showed that this improvement is more substantial when there is a larger number of antennas at the receiver.

We also examined the distribution of the SIR at the output of the optimum combiner for a Rician/Rayleigh fading environment in the presence of circularly symmetric Gaussian distributed channel estimation errors. We quantified the effect of the correlation coefficient between the exact and estimated channels on the PDF of SIR and derived an exact closed-form expression for the PDF of SIR. The analytical expression was verified by Monte Carlo simulations.

Finally, we compared the performance of MRC and OC in the presence of channel estimation errors with multiple interferers over Rayleigh fading channels when the system is interference-limited. We discovered that in the presence of channel estimation errors MRC can outperform OC, especially for small values of the correlation coefficient. Moreover, as the number of antennas increases there is a larger range of correlation coefficients over which MRC outperforms OC.

## 4.7 List of Publications

The material of this chapter can be found in the following papers:

- A. A. Basri and T. J. Lim, "Optimum combining with channel estimation errors in the presence of multiple interferers in flat Rayleigh fading," to appear in *IEEE Trans. Commun.*

- A. A. Basri and T. J. Lim, "Performance of maximal ratio and optimum combining with channel estimation errors and multiple interferers in Rayleigh fading channels," in *Proc. IEEE Veh. Technol. Conf. (VTC-2006 Fall)*, pp. 1345-1349, Sep. 2006.

- A. A. Basri and T. J. Lim, "Optimum combining in Rician/Rayleigh fading environment with channel estimation errors," in *Proc. IEEE 23rd Biennial Symposium on Commun.*, pp. 274-278, May - Jun. 2006.

- A. A. Basri and T. J. Lim, "Performance of optimum combining with imperfect channel estimates," in *Proc. IEEE Wireless Commun. & Networking Conf. (WCNC 2006)*, vol. 3, pp. 1338-1343, Apr. 2006.

- A. A. Basri and T. J. Lim, "Output SIR distribution of optimum combining in Rayleigh fading channels with channel estimation errors," in *Proc. IEEE Int'l Conf. Wireless and Mobile Computing, Networking and Comms. (WiMob'2005)*, vol. 1, pp. 15-22, Aug. 2005.

# Chapter 5

# Conclusions

In the first section of Chapter 2, we derived the structure of ML receiver for binary orthogonal signals in the presence of Gaussian-distributed channel estimation error and additive white Gaussian noise. We found that the ML receiver for binary orthogonal signals is a linear combination of a matched filter and envelope detector. The exact average BEP of the proposed receiver is derived for flat Rayleigh fading channels. We compared the performance of the ML receiver for orthogonal modulation with the one for antipodal signalling in the presence of channel estimation error and found the conditions under which orthogonal modulation results in better performance. The performance of the proposed receiver was analyzed in both quasi-static fading and time-varying fading channels.

In the second section of Chapter 2, we derived the ML receiver for QPSK signals in the presence of Gaussian channel estimation error. We found that the ML receiver is a matched filter which is matched to the channel estimate. An exact closed-form expression is derived for the average BEP of the ML receiver of QPSK signals in Rayleigh fading channels. We also analyzed the performance of the ML receiver of QPSK signals for the special case of quasi-static Rayleigh fading channels with an MMSE channel estimator. It was found that in quasi-static Rayleigh fading channels with an MMSE channel estimator, both BPSK and QPSK modulations result in almost the same average BEP for high enough average SNR.

In the first section of Chapter 3, we examined the performance of the maximal ratio combining technique in the uplink of wireless communication systems in the presence of multiple interferers when channel estimates at the receiver are perfect. We derived an exact closed-form expression for the average BEP of BPSK signals over Rayleigh fading channels. In the second section of Chapter 3, the performance of MRC is studied when the channel estimates are subject to Gaussian-distributed channel estimation error. For this case, closed-form expressions for several performance measures, such as the outage probability and average bit-error probability, are derived. We studied the performance improvement of MRC as the correlation between the true and estimated channels increases and found that this improvement is more substantial when there is a larger number of antennas at the receiver.

In Chapter 4, we investigated the effect of imperfect channel estimation on the performance of OC in the uplink of wireless communication systems. We considered space diversity reception in a flat Rayleigh fading channel in the presence of multiple interferers and channel estimation errors. The main contribution of this chapter was applying multivariate statistical analysis to derive an exact closed-form expression for PDF of the output SIR in terms of hypergeometric functions. This PDF expression was then utilized to obtain expressions for the moments of SIR, outage probability and the average bit error probability. We quantified the performance improvement as the correlation between the exact and estimated channels increases and showed that this improvement is more substantial when there is a larger number of antennas at the receiver.

We also examined the distribution of the SIR at the output of the optimum combiner for a Rician/Rayleigh fading environment in the presence of circularly symmetric Gaussian distributed channel estimation errors. We quantified the effect of the correlation coefficient between the exact and estimated channels on the PDF of SIR and derived an exact closed-form expression for the PDF of SIR. The analytical expression was verified by Monte Carlo simulations.

We compared the performance of MRC and OC in the presence of channel estimation errors with multiple interferers over Rayleigh fading channels when the system is interference-limited.

We discovered that in the presence of channel estimation errors MRC can outperform OC, especially for small values of the correlation coefficient. Moreover, as the number of antennas increases there is a larger range of correlation coefficients over which MRC has performance better than OC.

# Appendix A

# Mathematical Functions

1. The Gamma function is defined as [98, eq. (6.1.1)]

$$\Gamma(p) = \int_0^\infty t^{p-1} e^{-t} dt, \qquad (\Re\{p\} > 0) \tag{A.1}$$

where the symbol $\Re$ indicates the real part. For positive integer $p$, we have $\Gamma(p) = (p-1)!$ [98, eq. (6.1.6)].

2. The Pochhammer symbol $(a)_j$ is defined as [98, eq. (6.1.22)]

$$(a)_j = \frac{\Gamma(a+j)}{\Gamma(a)} \tag{A.2}$$

and for positive integers $a$ and $j$ it can be simplified to $(a)_j = \frac{(a+j-1)!}{(a-1)!}$.

3. The beta function $B(p,q)$ is defined as [98, eq. (6.2.1)]

$$B(p,q) = \int_0^1 t^{p-1}(1-t)^{q-1} dt = \int_0^\infty \frac{t^{p-1}}{(1+t)^{p+q}} dt, \qquad (\Re\{p\} > 0, \Re\{q\} > 0) \tag{A.3}$$

The beta function in (A.3) can also be written in terms of Gamma function [98, eq. (6.2.2)]:

$$B(p,q) = \frac{\Gamma(p)\Gamma(q)}{\Gamma(p+q)} \tag{A.4}$$

Therefore, from (A.4), for positive integers $p$ and $q$ we get $B(p,q) = \frac{(p-1)!(q-1)!}{(p+q-1)!}$.

4. The incomplete beta function $B_w(p,q)$ is defined as [98, eq. (6.6.1)]

$$B_w(p,q) = \int_0^w t^{p-1}(1-t)^{q-1}dt = \int_0^{\frac{w}{1-w}} \frac{t^{p-1}}{(1+t)^{p+q}}dt, \qquad 0 \leq w \leq 1 \tag{A.5}$$

5. The regularized incomplete beta function $I_w(p,q)$ is defined as [98, eqs. (6.6.2), (26.5.1)]

$$I_w(p,q) = \frac{B_w(p,q)}{B(p,q)} \tag{A.6}$$

and $B(p,q)$ and $B_w(p,q)$ are defined in (A.3) and (A.5), respectively.

6. The confluent hypergeometric function $U(a,b,x)$, also known as $\Psi(a,b,x)$, defined as [96, eq. (9.211.4)], [98, eq. (13.2.5)]

$$U(a,b,x) = \frac{1}{\Gamma(a)} \int_0^\infty \frac{t^{a-1}\exp(-xt)}{(1+t)^{1+a-b}}dt, \quad (\Re\{x\} > 0, \Re\{a\} > 0) \tag{A.7}$$

where the Gamma function $\Gamma(p)$ is defined in (A.1).

# Bibliography


[1] J. G. Proakis, *Digital Communications,* 4th ed. Boston: McGraw-Hill, 2001.

[2] M. K. Simon, S. M. Hinedi, and W. C. Lindsey, *Digital Communication Techniques: Signal Design and Detection.* Englewood Cliffs, NJ: PTR Prentice Hall, 1995.

[3] S. Stein, "Unified analysis of certain coherent and noncoherent binary communication systems," *IEEE Trans. Inform. Theory*, vol. IT-10, pp. 43-51, Jan. 1964

[4] M. Schwartz, W. R. Bennett, and S. Stein, *Communication Systems and Techniques.* New York: McGraw-Hill, 1966.

[5] M. K. Simon and M. -S. Alouini, "A unified approach to the performance analysis of digital communications over generalized fading channels," *Proc. IEEE*, vol. 86, pp. 1860-1877, Sept. 1998.

[6] M. K. Simon and M. -S. Alouini, *Digital Communication Over Fading Channels,* 2nd ed. Hoboken, New Jersey: Wiley-Interscience, 2005.

[7] A. Viterbi, "Optimum detection and signal selection for partially coherent binary communication," *IEEE Trans. Inf. Theory*, vol. IT-11, no. 2, pp. 239-246, Apr. 1965.

[8] S. M. Kay, *Fundamentals of Statistical Signal Processing: Estimation Theory.* Englewood Cliffs, NJ: PTR Prentice Hall, 1993.

[9] A. Aghamohammadi and H. Meyr, "On the error probability of linearly modulated signals on Rayleigh frequency-flat fading channels," *IEEE Trans. Commun.*, vol. 38, pp. 1966-1970, Nov. 1990.

[10] M. G. Shayesteh and A. Aghamohammadi, "On the error probability of linearly modulated signals on frequency-flat Ricean, Rayleigh, and AWGN channels," *IEEE Trans. Commun.*, vol. 43, pp. 1454-1466, Feb./Mar./Apr. 1995.

[11] J. K. Cavers, "An analysis of pilot symbol assisted modulation for Rayleigh fading channels," *IEEE Trans. Veh. Technol.*, vol. 40, no. 4, pp. 686-693, Nov. 1991.

[12] S. K. Wilson and J. M. Cioffi, "Probability density functions for analyzing multi-amplitude constellations in Rayleigh and Ricean channels," *IEEE Trans. Commun.*, vol. 47, pp. 380-386, Mar. 1999.

[13] X. Tang, M. -S. Alouini and A. J. Goldsmith, "Effect of channel estimation error on M-QAM BER performance in Rayleigh fading," *IEEE Trans. Commun.*, vol. 47, pp. 1856-1864, Dec. 1999.

[14] L. Cao and N. C. Beaulieu, "Exact error-rate analysis of diversity 16-QAM with channel estimation error," *IEEE Trans. Commun.*, vol. 52, pp. 1019-1029, Jun. 2004.

[15] X. Dong and N. C. Beaulieu, "SER of two-dimensional signalings in Rayleigh fading with channel estimation errors," in *Proc. IEEE Int. Conf. on Commun. (ICC)*, vol. 4, pp. 2763-2767, May 2003.

[16] X. Dong and L. Xiao, "Symbol error probability of two-dimensional signaling in Ricean fading with imperfect channel estimation," *IEEE Trans. Veh. Technol.*, vol. 54, pp. 538-549, Mar. 2005.

[17] R. You, H. Li, and Y. Bar-Ness, "Diversity combining with imperfect channel estimation," *IEEE Trans. Commun.*, vol. 53, no. 10, pp. 1655-1662, Oct. 2005.

[18] S. Verdú, *Multiuser Detection.* New York: Cambridge Univ. Press, 1998.

[19] S. Haykin, *Adaptive Filter Theory.*, 4th ed. N.J: Prentice Hall, 2002.

[20] K. S. Gomadam and S. A. Jafar, "Partially coherent detection in rapidly time varying channels," in *Proc. IEEE Wireless Commun. & Networking Conf. (WCNC'2006)*, vol. 4, pp. 2127-2132, Apr. 2006.

[21] K. S. Gomadam and S. A. Jafar, "Modulation and detection for simple receivers in rapidly time varying channels," To appear in *IEEE Trans. Commun.*

[22] K. E. Baddour and N. C. Beaulieu, "Autoregressive modeling for fading channel simulation," *IEEE Trans. Wireless Commun.*, vol. 4, no. 4, pp. 1650-1662, July 2005.

[23] P. Sadeghi, P. Rapajic, R. Kennedy, and T. Abhayapala, "Autoregressive time-varying flat-fading channels: model order and information rate bounds," in *Proc. IEEE Int. Symp. Inform. Theory (ISIT'2006)*, pp. 1061-1065, July 2006.

[24] M. Médard, "The effect upon channel capacity in wireless communication of perfect and imperfect knowledge of the channel," *IEEE Trans. Inform. Theory*, vol. 46, pp. 933-946, May 2000.

[25] M. Médard, I. Abou-Faycal, and U. Madhow, "Adaptive coded modulation without channel feedback for pilot symbol assisted modulation, in *Proc. 38th Annual Allerton Conference on Communication, Control, and Computing*, Oct 2002.

[26] D. G. Brennan. "Linear diversity combining techniques," *Proc. IRE*, vol. 47, pp. 1075-1102, Jun. 1959.

[27] G. L. Stüber, *Principles of Mobile Communication,* 2nd Ed., Boston: Kluwer Academic Publishers, 2001.

[28] L. C. Godara, "Applications of antenna arrays to mobile communications Part I: Performance improvement, feasibility, and system considerations," *Proc. IEEE*, vol. 85, pp. 1031-1060, July 1997.

[29] Y. Song, S. D. Blostein, and J. Cheng, "Outage probability comparisons for diversity systems with cochannel interference in Rayleigh fading," *IEEE Trans. Wireless Commun.*, vol. 4, no.4 , pp. 1279-1284, Jul. 2005.

[30] J. H. Winters, J. Salz, and R. D. Gitlin, "Impact of antenna diversity on the capacity of wireless communication systems," *IEEE Trans. Commun.,* vol. 42, pp. 1740-1751, 1994.

[31] J. Cui and A. U. H. Sheikh, "Outage probability of cellular radio systems using maximal ratio combining in the presence of multiple interferers," *IEEE Trans. Commun.*, vol. 47, pp. 1121-1124, Aug. 1999.

[32] V. A. Aalo and C. Chayawan, "Outage probability of cellular radio systems using maximal ratio combining in Rayleigh fading channel with multiple interferers," *Electron. Lett.*, vol. 36, no. 15, pp. 1314-1315, Jul. 2000.

[33] C. Chayawan and V. A. Aalo, "On the outage probability of optimum combining and maximal ratio combining schemes in an interference-limited Rice fading channel," *IEEE Trans. Commun.*, vol. 50, pp. 532-535, Apr. 2002.

[34] X. W. Cui, Q. T. Zhang, and Z. M. Feng, "Outage performance for maximal ratio combiner in the presence of unequal-power co-channel interferers", *IEEE Commun. Lett.*, vol. 8, no. 5, pp. 289-291, May 2004.

[35] J. M. Romero-Jerez, J. P. Peña Martín, and A. J. Goldsmith, "Outage probability of MRC with arbitrary power cochannel interferers in Nakagami fading," *IEEE Trans. Commun.*, vol. 55, no. 7, pp. 1283-1286, Jul. 2007.

[36] X. Zhang and N. C. Beaulieu, "Outage probability of MRC with equi-power cochannel interferers in correlated Rayleigh fading," *IEEE Commun. Lett.*, vol. 9, no. 7, pp. 577-579, Jul. 2005.

[37] X. Zhang and N. C. Beaulieu, "Outage probability of MRC with unequal-power cochannel interferers in correlated Rayleigh fading ," *IEEE Commun. Lett.*, vol. 10, no. 1, pp. 7-9, Jan. 2006.

[38] X. W. Cui, Q. T. Zhang, and Z. M. Feng, "Outage probability for maximal ratio combining of arbitrarily correlated faded signals corrupted by multiple Rayleigh interferers," *IEEE Trans. Veh. Technol.*, vol. 55, no. 1, pp. 383-387, Jan 2006.

[39] J. Cui, D. D. Falconer, and A . U. H. Sheikh, "Performance evaluation of optimum combining and maximal ratio combining in the presence of co-channel interference and channel correlation for wireless communication systems," *Mobile Networks and Applications*, vol. 2, pp. 315-324, 1997.

[40] V. A. Aalo and J. Zhang, "On the effect of cochannel interference on average error rates in Nakagami-fading channels," *IEEE Commun. Lett.*, vol. 3, no. 5, pp. 136-138, May 1999.

[41] A. Shah and A. M. Haimovich, "Performance analysis of maximal ratio combining and comparison with optimum combining for mobile radio communications with cochannel interference," *IEEE Trans. Veh. Technol.*, vol. 49, pp. 1454-1463, July 2000.

[42] V. A. Aalo and J. Zhang, "Performance analysis of maximal ratio combining in the presence of multiple equal-power cochannel interferers in a Nakagami fading channel," *IEEE Trans. Veh. Technol.*, vol. 50, pp. 497-503, Mar. 2001.

[43] C. Chayawan and V. A. Aalo, "Average error probability of digital cellular radio systems using MRC diversity in the presence of multiple interferers", *IEEE Trans. Wireless Commun.*, vol. 2, pp. 860-864, Sept. 2003.

[44] Y. Ma, T. J. Lim, and S. Pasupathy, "Error probability for coherent and differential PSK over arbitrary Rician fading channels with multiple cochannel interferers," *IEEE Trans. Commun.*, vol. 50, pp. 429-441, Mar. 2002.

[45] X. Zhang and N. C. Beaulieu, "Outage and error rate of cellular systems using MRC in the presence of multiple interferers and correlated rayleigh fading," in *Proc. IEEE Global Telecommun. Conf. (GLOBECOM 2006)*, Nov. 2006.

[46] P. Bello and B. D. Nelin, "Predetection diversity combining with selectively fading channels," *IRE Trans. Commun. Syst.*, vol. COM-10, pp. 32-42, 1962.

[47] J. G. Proakis, "Probabilities of error for adaptive reception of M-phase signals," *IEEE Trans. Commun. Tech.*, vol. COM-16, no. 1, pp. 71-81, Feb. 1968.

[48] M. J. Gans, "The effect of Gaussian error in maximal ratio combiners," *IEEE Trans. Commun. Tech.*, vol. COM-19, no. 4, pp. 492-500, 1971.

[49] B. R. Tomiuk, N. C. Beaulieu, and A. A. Abu-Dayya, "General forms for maximal ratio diversity with weighting errors," *IEEE Trans. Commun.*, vol. 47, no. 4, pp. 488-492, Apr. 1999.

[50] A. Annamalai and C. Tellambura, "Analysis of hybrid selection/maximal-ratio diversity combiners with Gaussian errors," *IEEE Trans. Wireless Commun.*, vol. 1, no. 3, pp. 498-512, Jul. 2002.

[51] R. Annavajjala and L. B. Milstein, "Performance analysis of linear diversity-combining schemes on Rayleigh fading channels with binary signaling and Gaussian weighting errors," *IEEE Trans. Wireless Commun.*, vol. 4, no .5, pp. 2267-2278, Sep. 2005.

[52] Y. Ma, R. Schober, and S. Pasupathy, "Effect of channel estimation errors on MRC diversity in Rician fading channels," *IEEE Trans. Veh. Technol.*, vol. 54, no. 6, pp. 2137-2142, Nov. 2005.

[53] L. Cao and N. C. Beaulieu, "Exact error-rate analysis of diversity 16-QAM with channel estimation error," *IEEE Trans. Commun.*, vol. 52, no .6, pp. 1019-1029, Jun. 2004.

[54] W. M. Gifford, M. Z. Win, and M. Chiani, "Diversity with practical channel estimation," *IEEE Trans. Wireless Commun.*, vol. 4, no .4, pp. 1935-1947, Jul. 2005.

[55] L. Cao and N. C. Beaulieu, "Closed-form BER results for MRC diversity with channel estimation errors in Ricean fading channels," *IEEE Trans. Wireless Commun.*, vol. 4, no .4, pp. 1440-1447, Jul. 2005.

[56] L. Najafizadeh and C. Tellambura, "BER analysis of arbitrary QAM for MRC diversity with imperfect channel estimation in generalized Ricean fading channels," *IEEE Trans. Veh. Technol.*, vol. 55, no. 4, pp. 1239-1248, Jul. 2006.

[57] Y. Ma, R. Schober, and D. Zhang, "Exact BER for M-QAM with MRC and imperfect channel estimation in Rician fading channels," *IEEE Trans. Wireless Commun.*, vol. 6, no .3, pp. 926-936, Mar. 2007.

[58] Y. Ma and J. Jin, "Effect of channel estimation errors on M-QAM with MRC and EGC in Nakagami fading channels," *IEEE Trans. Veh. Technol.*, vol. 56, no. 3, pp. 1239-1250, May 2007.

[59] Y. Akyildiz and B. D. Rao,"Maximum ratio combining performance with imperfect channel estimates," in *Proc. IEEE Int'l Conf. Acoustics, Speech, and Signal Processing (ICASSP '02)*, vol. 3, pp. 2485-2488, May 2002.

[60] Y. Tokgoz and B. D. Rao, "The effect of imperfect channel estimation on the performance of maximum ratio combining in the presence of cochannel interference," *IEEE Trans. Veh. Technol.*, vol. 55, no. 5, pp. 1527-1534, Sep. 2006.

[61] V. Bogachev and I. Kiselev, "Optimum combining of signals in space diversity reception," *Telecommun. Radio Eng.*, vols. 34/35, pp. 83-85, Oct. 1980.

[62] J. H. Winters, "Optimum combining in digital mobile radio with cochannel interference," *IEEE J. Select. Areas Commun.*, vol. SAC-2, pp. 528-539, Jul. 1984.

[63] A. Shah, A. M. Haimovich, M. K. Simon, and M. S. Alouini, "Exact bit-error probability for optimum combining with a Rayleigh fading Gaussian cochannel interferer," *IEEE Trans. Commun.*, vol. 48, pp. 908-912, June 2000.

[64] V. A. Aalo and J. Zhang, "Performance of antenna array systems with optimum combining in a Rayleigh fading environment," *IEEE Commun. Lett.*, vol. 4, pp. 387-389, Dec. 2000.

[65] A. Shah and A. M. Haimovich, "Performance analysis of optimum combining in wireless communications with Rayleigh fading and cochannel interference," *IEEE Trans. Commun.*, vol. 46, pp. 473-479, Apr. 1998.

[66] M. Kang, M.-S. Alouini, and L.Yang, "Outage probability and spectrum efficiency of cellular mobile radio systems with smart antennas," *IEEE Trans. Commun.*, vol. 50, pp. 1871-1877, Dec. 2002.

[67] C. Chayawan and V. A. Aalo, "On the outage probability of optimum combining and maximal ratio combining schemes in an interference-limited Rice fading channel," *IEEE Trans. Commun.*, vol. 50, pp. 532-535, Apr. 2002.

[68] Q. T. Zhang and X. W. Cui, "Outage probability for optimum combining of arbitrarily faded signals in the presence of correlated Rayleigh interferers," *IEEE Trans. Veh. Technol.*, vol. 53, no. 4, pp. 1043-1051, July 2004.

[69] J. H. Winters and J. Salz, "Upper bounds on the bit-error rate of optimum combining in wireless systems," *IEEE Trans. Commun.*, vol. 46, pp. 1619-1624, Dec. 1998.

[70] M. Chiani, M. Z. Win, A. Zanella, R. K. Mallik, and J. H. Winters, "Bounds and approximations for optimum combining of signals in the presence of multiple co-channel interferers and thermal noise," *IEEE Trans. Commun.*, vol. 51, pp. 296-307, Feb. 2003.

[71] M. Chiani, M. Z. Win, A. Zanella, and J. H. Winters, "A Laguerre polynomial-based bound on the symbol error probability for adaptive antennas with optimum combining," *IEEE Trans. Wireless Commun.*, vol. 3, no. 1, pp. 12-16, Jan. 2004.

[72] D. Lao and A. M. Haimovich, A.M., "Exact closed-form performance analysis of optimum combining with multiple cochannel interferers and Rayleigh fading," *IEEE Trans. Commun.* , vol. 51, Issue: 6, pp. 995-1003, June 2003.

[73] M. Chiani, M. Z. Win, A. Zanella, "Error probability for optimum combining of M-ary PSK signals in the presence of interference and noise," *IEEE Trans. Commun.*, vol. 51, Issue: 11, pp. 1949-1957, Nov. 2003.

[74] R. K. Mallik, M. Z. Win, M. Chiani, and A. Zanella, "Bit-error probability for optimum combining of binary signals in the presence of interference and noise," *IEEE Trans. Wireless Commun.*, vol. 3, Issue: 2, pp. 395-407, March 2004.

[75] D. Lao and A. M. Haimovich, "Exact average symbol error probability of optimum combining with arbitrary interference power," *IEEE Commun. Lett.*, vol. 8, no. 4, pp. 226-228, Apr. 2004.

[76] D. Lao and A. M. Haimovich, "Symbol-Error probability and bit-error probability for optimum combining with MPSK modulation," *IEEE Trans. Commun.*, vol. 52, no. 8, pp. 1276-1281, Aug. 2004.

[77] M. Chiani, M. Z. Win, and A. Zanella, "On optimum combining of M-PSK signals with unequal-power interferers and noise," *IEEE Trans. Commun.*, vol. 53, no. 1, pp. 44-47, Jan. 2005.

[78] H. Gao, P. J. Smith, and M. V. Clark, "Theoretical reliability of MMSE linear diversity combining in Rayleigh-fading additive interference channels," *IEEE Trans. Commun.*, vol. 46, pp. 666-672, May 1998.

[79] E. Villier, "Performance analysis of optimum combining with multiple interferers in flat Rayleigh fading," *IEEE Trans. Commun.*, vol. 47, pp. 1503-1510, Oct. 1999.

[80] T. D. Pham and K. G. Balmain, "Multipath performance of adaptive antennas with multiple interferers and correlated fadings," *IEEE Trans. Veh. Technol.*, vol. 48, pp. 342-352, Mar. 1999.

[81] Y. Tokgoz, B.D. Rao, M. Wengler, and B. Judson, "Performance analysis of optimum combining in antenna array systems with multiple interferers in flat Rayleigh fading," *IEEE Trans. Commun.*, vol. 52, Issue: 7, pp. 1047-1050, July 2004.

[82] Y. Akyildiz and B.D. Rao, "Statistical performance analysis of optimum combining with co-channel interferers and flat Rayleigh fading," in *Proc. of Global Telecommunications Conference (GLOBECOM 2001)*, Volume: 6, pp. 3663-3667, Nov. 2001.

[83] J. S. Kwak and J. H. Lee, "Performance analysis of optimum combining for dual-antenna diversity with multiple interferers in a Rayleigh fading channel," *IEEE Commun. Lett.*, vol. 6, no. 12, pp. 541-543, Dec. 2002.

[84] J. S. Kwak and J. H. Lee, "Closed-form expressions of approximate error rates for optimum combining with multiple interferers in a Rayleigh fading channel," *IEEE Trans. Veh. Technol.*, vol. 55, no. 1, pp. 158-166, Jan. 2006.

[85] D. Yue, X. Wang, and F. Xu, "Performance analysis for optimum combining of Rayleigh fading signals with correlated Rayleigh interferers and noise," *IEEE Signal Processing Lett.*, vol. 13, no.5, pp. 269-272, May 2006.

[86] M. R. McKay, A. Zanella, I. B. Collings, and M. Chiani, "Optimum combining of Rician-faded signals: analysis in the presence of interference and noise," in *Proc. IEEE Intl. Conf. on Commun. (ICC'2007)*, June 2007.

[87] A. M. Haimovich, A. Shah, and X. Wu, "Reduced-rank array processing for wireless communications with applications to IS-54/IS-136," *IEEE Trans. Commun.*, vol. 48, pp. 743-747, May 2000.

[88] B. Kecicioglu, M. Torlak, and A. Kavak, "Performance of optimum combining with channel estimation errors," in *Proc. 62nd IEEE Vehicular Technology Conf. (VTC-2005-Fall)*, vol. 4, pp. 2230-2234. Sept. 2005.

[89] A. Narula, M. J. Lopez, M. D. Trott, and G. W. Wornell, "Efficient use of side information in multiple antenna data transmission over fading channels," *IEEE J. Select. Areas Commun.*, vol. 16, pp. 1423-1436, Oct. 1998.

[90] R. J. Muirhead, *Aspects of Multivariate Statistical Theory.* New York: Wiley, 1982.

[91] M. S. Srivastava and C. G. Khatri, *An Introduction to Multivariate Statistics.* New York: Elsevier North Holland, 1979

[92] A. K. Gupta and D. K. Nagar, *Matrix Variate Distributions.* Chapman & Hall/CRC, 2000.

[93] A. Papoulis and S. U. Pillai, *Probability, Random Variables, and Stochastic Processes.* Boston: McGraw-Hill, 2002.

[94] H. M. Srivastava and Per W. Karlsson, *Multiple Gaussian Hypergeometric Series.* E. Horwood; New York: Halsted Press, 1985.

[95] H. Exton, *Multiple hypergeometric functions and applications.* E. Horwood; New York: Halsted Press, 1976.

[96] I. S. Gradshteyn and I. M. Ryzhik, *Table of Integrals, Series, and Products, 5th ed.* Boston: Academic, 1994.

[97] N. L. Johnson, S. Kotz, and N. Balakrishan, *Continuous Univariate Distributions, Volume 2.*, New York: Wiley & Sons, 1994.

[98] M. Abramowitz and I. A. Stegun, *Handbook of Mathematical Functions with Formulas, Graphs, and Mathematical Tables,* 10th printing. New York: Wiley, 1972.

[99] N. R. Goodman, "Statistical analysis based on a certain multivariate complex Gaussian distribution (an introduction)," *Ann. Math. Statist.,* vol. 34, no. 1, pp. 152-177, Mar. 1963.

[100] H. Cramér, *Mathematical Methods of Statistics.* Princeton University Press, Princeton, New Jersey, 1946.

[101] R. J. Bultitude and G. K. Bedal, "Propagation characteristics in microcellular urban mobile radio channels at 910 MHz," *IEEE J. Select. Areas Commun.*, vol. 7, pp. 31-39, Jan. 1989

[102] T. S. Rappaport, "Characterization of UHF multipath radio channels in factory buildings," *IEEE Trans. Antennas Propagat.*, vol. 37, pp. 1058-1069, Aug. 1989.

[103] Y.-D. Yao and A. U. H. Sheikh, "Outage probability analysis for microcell mobile radio systems with cochannel interferers in Rician/Rayleigh fading environment," *Electron. Lett.*, vol. 26, pp. 864-866, June 1990.

[104] Y.-D. Yao and A. U. H. Sheikh, "Investigation into cochannel interference in microcellular mobile radio systems," *IEEE Trans. Veh. Technol.,* vol. 41, pp.114-123, May 1992.

[105] S. Benedetto and E. Biglieri, *Principles of digital transmission: with wireless applications.* New York: Kluwer Academic/Plenum Publishers, 1999.